

11-18-2015

Synthesis And Characterization Of Neo-Confused Porphyrins And Related Systems

Arwa Salem Almejbel
Illinois State University, arwa-3112@hotmail.com

Follow this and additional works at: <https://ir.library.illinoisstate.edu/etd>

 Part of the [Organic Chemistry Commons](#)

Recommended Citation

Almejbel, Arwa Salem, "Synthesis And Characterization Of Neo-Confused Porphyrins And Related Systems" (2015). *Theses and Dissertations*. 486.
<https://ir.library.illinoisstate.edu/etd/486>

This Thesis is brought to you for free and open access by ISU ReD: Research and eData. It has been accepted for inclusion in Theses and Dissertations by an authorized administrator of ISU ReD: Research and eData. For more information, please contact ISUREd@ilstu.edu.

SYNTHESIS AND CHARACTERIZATION OF NEO-CONFUSED PORPHYRINS AND RELATED SYSTEMS

Arwa S. Almejbel

132 Pages

Carbaporphyrins have been the focus of many studies, and a wide variety of related carbaporphyrinoid systems have been reported. N-Confused porphyrins are a class of carbaporphyrins where one pyrrole unit has been inverted. In this work, a newly discovered family of porphyrin isomers where one of the pyrrolic subunits is connected to the meso-bridge in a 1,3-fashion, called neo-confused porphyrins, has been investigated.

Reaction of pyrrole-3-carbaldehydes with acetoxymethylpyrroles **39** and NaH in DMF gave neo-confused dipyrromethanedialdehydes. The resulting dialdehydes underwent an acid catalyzed condensation with a dipyrromethane to give neo-confused phlorins, and following oxidation with FeCl₃ afforded new neo-confused porphyrins. These porphyrinoids differ from previous neo-confused porphyrins in that they do not possess fused benzo- units or electron withdrawing ester substituents. Instead, the neo-confused ring is substituted with a phenyl or bromo group. Reaction of neo-confused porphyrins with nickel(II) or palladium(II) acetate afforded the organometallic complexes. The aromaticity of the neo-confused porphyrins and their derivatives were

assessed by proton NMR spectroscopy and UV-Vis spectroscopy.

KEYWORDS: Carbaporphyrins, N-confused porphyrins, Neo-confused porphyrins.

SYNTHESIS AND CHARACTERIZATION OF NEO-CONFUSED PORPHYRINS
AND RELATED SYSTEMS

ARWA S. ALMEJBEL

A Thesis Submitted in Partial
Fulfillment of the Requirements
for the Degree of

MASTER OF SCIENCE

Department of Chemistry

ILLINOIS STATE UNIVERSITY

2016

© 2016 Arwa S. Almejbel

SYNTHESIS AND CHARACTERIZATION OF NEO-CONFUSED PORPHYRINS
AND RELATED SYSTEMS

ARWA S. ALMEJBEL

COMMITTEE MEMBERS:

Timothy D. Lash, Chair

Shawn R. Hitchcock

Christopher Hamaker

ACKNOWLEDGMENTS

I would first like to acknowledge Saudi Cultural Mission (SACM) for the generous scholarship. I also would like to thank Chemistry Department faculty members and my colleagues for their advice and support, as well as my committee members, Dr. Shawn Hitchcock and Dr. Christopher Hamaker. A special thanks to my awesome research adviser Dr. Timothy Lash for the generous guidance, patience and endless support for the past two years. I would also thank my family and friends for their unwavering love and support.

A. S. A.

CONTENTS

| | Page |
|---|------|
| ACKNOWLEDGMENTS | i |
| CONTENTS | ii |
| TABLES | iii |
| FIGURES | iv |
| SCHEMES | vi |
| CHAPTER | |
| I. PORPHYRINS AND RELATED SYSTEMS | 1 |
| Introduction | 1 |
| Porphyrins as Photosensitizers | 6 |
| Synthesis of Porphyrinoids | 7 |
| Theoretical Studies of N- and Neo-confused Porphyrins | 21 |
| Conclusion | 23 |
| II. RESULTS AND DISCUSSION | 24 |
| Conclusions | 62 |
| III. EXPERIMENTAL | 63 |
| REFERENCES | 88 |
| APPENDIX: Selected NMR spectra | 92 |

TABLES

| Table | Page |
|--|------|
| 1. Thermal rearrangement of vinyl oxime 57 to pyrrole 58 | 47 |

FIGURES

| Figure | Page |
|---|------|
| 1. Porphyrin structure | 2 |
| 2. Ring currents in porphyrins | 4 |
| 3. Structures of heme (left) and chlorophyll (right) | 5 |
| 4. Porphyrin tautomers | 5 |
| 5. Carbaporphyrin, N-confused porphyrin and neo-confused porphyrin | 12 |
| 6. Tetraphenylporphyrin (TPP) (4) and N-Confused Porphyrin (NCP) (17) | 14 |
| 7. N-confused porphyrin (17) and N-fused porphyrin (22) | 15 |
| 8. Neo-confused porphyrins | 17 |
| 9. Metal complexes of neo-confused porphyrins | 20 |
| 10. Structures of neo-confused porphyrin and benzo-neo-confused porphyrin tautomers and their relative energies (kcal/mol) compared to porphyrin and benzoporphyrin, respectively | 22 |
| 11. 500 MHz proton NMR spectrum of bromo neo-confused dipyrromethane 37a | 30 |
| 12. 500 MHz proton NMR spectrum of bromo neo-confused porphyrin 36a | 33 |
| 13. UV-vis spectrum of bromo neo-confused porphyrin 36a in CH ₂ Cl ₂ | 34 |
| 14. Protonation of bromo neo-confused porphyrin 36a | 35 |
| 15. 500 MHz proton NMR spectrum of neo-confused porphyrin dication 36aH₂²⁺ in TFA-CDCl ₃ | 36 |

| | |
|---|----|
| 16. UV-vis spectrum of neo-confused porphyrin 36a in dichloromethane (red line) and 2% TFA-CH ₂ Cl ₂ (blue line) | 37 |
| 17. 500 MHz proton NMR spectrum of nickel(II) complex 53 | 40 |
| 18. UV-vis spectrum of the nickel(II) complex 53 in CH ₂ Cl ₂ | 41 |
| 19. 500 MHz proton NMR spectrum of palladium(II) complex 54 | 43 |
| 20. UV-vis spectrum of the palladium(II) complex 54 in CH ₂ Cl ₂ | 44 |
| 21. 500 MHz proton NMR spectrum of phenyl neo-confused Dipyrrylmethane 37b | 48 |
| 22. 500 MHz proton NMR spectrum of phenyl neo-confused porphyrin 36b | 50 |
| 23. UV-vis spectrum of phenyl neo-confused porphyrin 36b in CH ₂ Cl ₂ | 51 |
| 24. Protonation of phenyl neo-confused porphyrin 36b H ₂ ²⁺ | 52 |
| 25. 500 MHz proton NMR spectrum of phenyl neo-confused porphyrin 36b H ₂ ²⁺ in TFA-CDCl ₃ | 52 |
| 26. UV-vis spectrum of neo-confused porphyrin 36b in dichloromethane (purple line) and 2% TFA-CH ₂ Cl ₂ (green line) | 53 |
| 27. 500 MHz proton NMR spectrum of palladium(II) complex 61 in CDCl ₃ | 55 |
| 28. 500 MHz proton NMR spectrum of nickel(II) complex 62 in CDCl ₃ | 57 |
| 29. 500 MHz proton NMR spectrum of aza neo-confused dipyrromethane 63 in CDCl ₃ | 59 |
| 30. 500 MHz proton NMR spectrum of methyl aza neo-confused dipyrromethane 70 in CDCl ₃ | 61 |

SCHEMES

| Scheme | Page |
|--|------|
| 1. Rothmund method for synthesis of <i>meso</i> -tetraphenylporphyrin | 7 |
| 2. Conversion of chlorin to porphyrin | 8 |
| 3. One-pot synthesis of <i>meso</i> -substituted porphyrins | 9 |
| 4. "2+2" MacDonald condensation reaction | 10 |
| 5. Synthesis of tripyrranes | 11 |
| 6. "3+1" MacDonald condensation reaction | 11 |
| 7. Synthesis of benzocarbaporphyrins | 13 |
| 8. Synthesis of N-fused porphyrins | 16 |
| 9. N-confused corrole and neo-confused corrole (norrole) | 17 |
| 10. Method developed for the synthesis of neo-confused porphyrin esters | 18 |
| 11. Retrosynthetic analysis of neo-confused porphyrins using MacDonald's "2+2" condensation approach | 25 |
| 12. Retrosynthetic analysis of the key intermediary dipyrroledialdehydes | 25 |
| 13. Synthesis of 5-acetoxymethyl-3,4-dimethylpyrrole-2-carbaldehyde 39 | 27 |
| 14. Synthesis of 5-bromo pyrrole-3-carbaldehyde 40a | 28 |
| 15. Synthesis of bromo-neo-confused dipyrrylmethane 37a | 29 |
| 16. Synthesis of bromo neo-confused porphyrin using a "2+2" condensation | 31 |

| | | |
|-----|--|----|
| 17. | Attempted synthesis of neo-fused porphyrin 52 | 38 |
| 18. | Synthesis of nickel(II) neo-confused porphyrin 53 | 39 |
| 19. | Synthesis of the palladium(II) complex of bromo neo-confused Porphyrin 54 | 42 |
| 20. | Proposed synthesis of phenyl neo-confused porphyrin 36b | 45 |
| 21. | Synthesis of 5-phenyl pyrrole-3-carbaldehyde 40b | 45 |
| 22. | Synthesis of phenyl neo-confused dipyrromethanedialehyde 37b | 47 |
| 23. | Synthesis of phenyl neo-confused porphyrin 36b | 49 |
| 24. | Synthesis of palladium(II) complex 61 | 54 |
| 25. | Synthesis of nickel(II) complex 62 | 56 |
| 26. | Attempted synthesis of aza neo-confused porphyrin 64 | 58 |
| 27. | Synthesis of methyl formyl imidazole 69 | 60 |
| 28. | Attempted synthesis of methyl aza neo-confused porphyrin 71 | 61 |

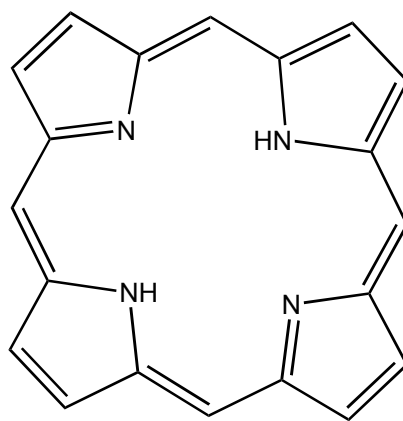
CHAPTER I
PORPHYRINS AND RELATED SYSTEMS

Introduction

The majority of complex animal and plant life that exists on our planet today relies on a class of aromatic heterocycles known as porphyrins. Photosynthesis and respiration are at the heart of what makes life possible. During the Archean period, life on earth was dominated by bacteria and archaea and the atmosphere was devoid of free oxygen. The evolution of oxygenic photosynthesis from cyanobacteria changed the earth and its atmosphere forever. The process involves the oxidation of water to form molecular oxygen which is released into the atmosphere.¹ Eventually the earth's atmosphere changed from anaerobic to aerobic leading to a dramatic increase in biodiversity. Life has since evolved to utilize oxygen, leading to eukaryotic organisms and plants containing chloroplasts for photosynthesis and eventually hemoglobin in the red blood cells for oxygen transportation in vertebrates.¹

Porphyrins are organic molecules that play very important roles in the metabolism of living organisms such as bacteria, animals and plants. The term *Porphyrin* derives from The Greek word *porphura* meaning reddish-purple.² Hematoporphyrin was isolated in 1871 by the German chemist Hoppe-Seyler. When he treated dried blood with concentrated H_2SO_4 (aq), a purple colored compound was formed that was named hematoporphyrin, from a Greek words for blood and purple.^{1,2}

Porphyrins have a characteristic square shape (Figure 1) built up from four pyrrole subunits. The porphyrins are pigments that are either naturally found in living organisms or synthetically formed.¹



1

Figure 1: Porphyrin structure

Porphyrins are highly aromatic due in part to the presence of a π -electron pathway that obeys Hückel's rule of aromaticity, where the number of π electrons is $[4n + 2]$. In

porphyrins, the continuous π electron delocalization pathway involves 18 π electrons ($n = 4$).^{1,2}

The aromatic character of porphyrins can be confirmed by proton NMR spectroscopy. Studies performed over the last fifty years have demonstrated that ^1H NMR spectra are very informative and adequately reflect the structural features of porphyrins. The presence of the extended delocalized π -electron system of the porphyrin macrocycle gives rise to a strong ring current in molecules that have been placed in a magnetic field.

The ring current causes anisotropic shielding of the protons located in the field of its action and together with the diamagnetic component of paired σ -electrons leads to a substantial shift of their signals in the ^1H NMR spectra. It can be stated that the ring current and the aromaticity of porphyrins change in a similar way in response to the analogous changes in the molecular structure of the porphyrin and the medium, which is most clearly seen in comparisons of the spectra of porphyrins and their precursors. Due to the anisotropic effect from the porphyrin ring current, the NMR signals for the deshielded *meso*-protons (protons on the bridging methine carbons) show up at low field (the external protons usually show up near +10 ppm), whereas the signals for the shielded protons on the inner nitrogen atoms show up at very high field (commonly at -4 ppm). Figure 2 illustrates the effects due to the diamagnetic ring current, which results in shielding and deshielding regions.¹

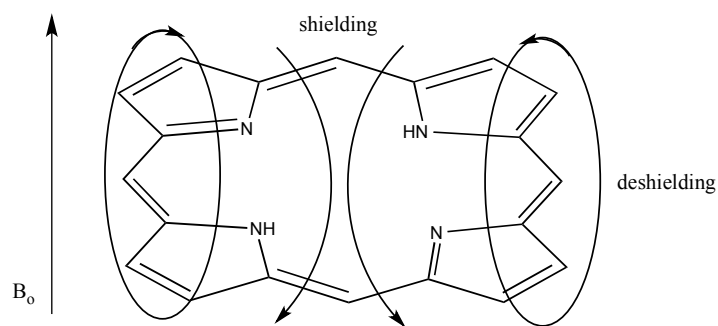


Figure 2: Ring currents in porphyrins

As mentioned above, porphyrins are highly conjugated structures, and have characteristic UV-vis spectra. A strong absorption appears around 400 nm, which is known as the Soret band, and smaller peaks show up between 500 nm to 700 nm that are called Q bands. The Q bands are responsible for the intense red or green color of porphyrins in solutions.¹

The study of porphyrin chemistry includes synthesis, structural characterization and the formation of numerous derivatives. The most common derivatives of porphyrins are metal complexes, in which a metal ion is present in the interior of the cavity. The best known example of a metallic complex in humans and other mammals is the heme group in hemoglobin. In this case, the metal ion in the center is iron(II), and heme gives blood its characteristic red color (Figure 3). In plants, the most important porphyrin derivative is chlorophyll, where the coordinated metal is magnesium (Figure 3). Porphyrins and their derivatives are crucial structures in virtually all living organisms.¹

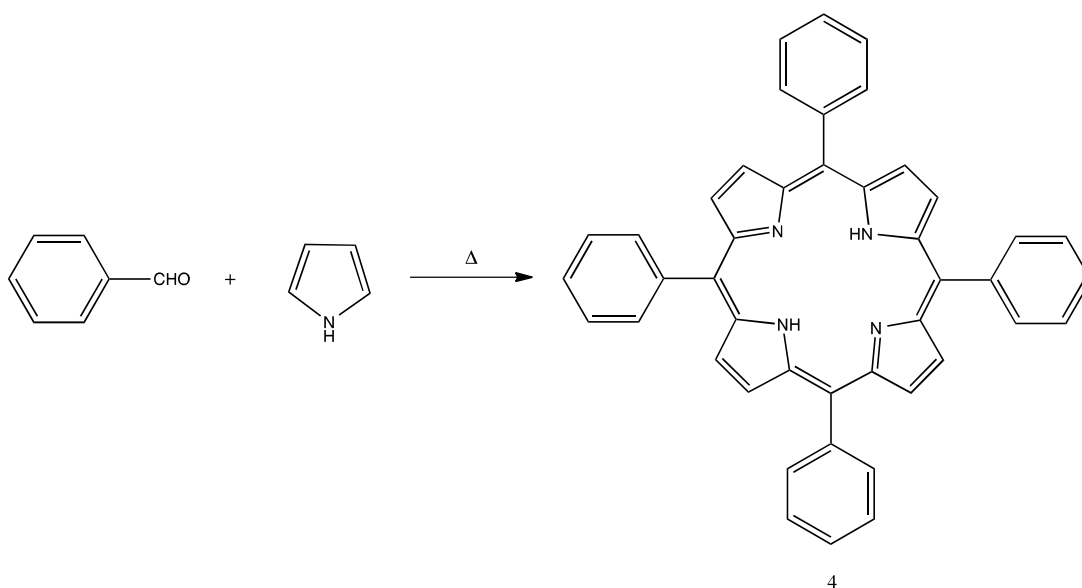
Porphyrins as Photosensitizers

Photosensitisers have the ability to absorb light at a specific wavelength, transforming it into energy, which is transferred to a substrate or molecular oxygen, leading to the production of ROS (Reactive Oxygen Species). Thus, a good photosensitiser should absorb light efficiently, forming a high quantum yield of photosensitiser in the excited triplet state. The excited triplet state should also be relatively stable, increasing the probability of reacting with either oxygen or a suitable substrate. Compounds that have the ability to form excited triplet states generally possess conjugated systems; hence porphyrin type structures have been utilized as photosensitisers.⁵

As noted above, free base porphyrins have a UV/visible spectrum consisting of one intense absorption band, referred to as the Soret band, at 380-430 nm, and four less intense Q bands at higher wavelengths.⁵ The optical properties of different porphyrin derivatives are dependent on the functional groups that are present on the porphyrin core. Porphyrins absorb photons efficiently at wavelengths corresponding to their absorption peaks, leading to high excited triplet state yields, which efficiently produce ROS.⁵

Synthesis of Porphyrinoids

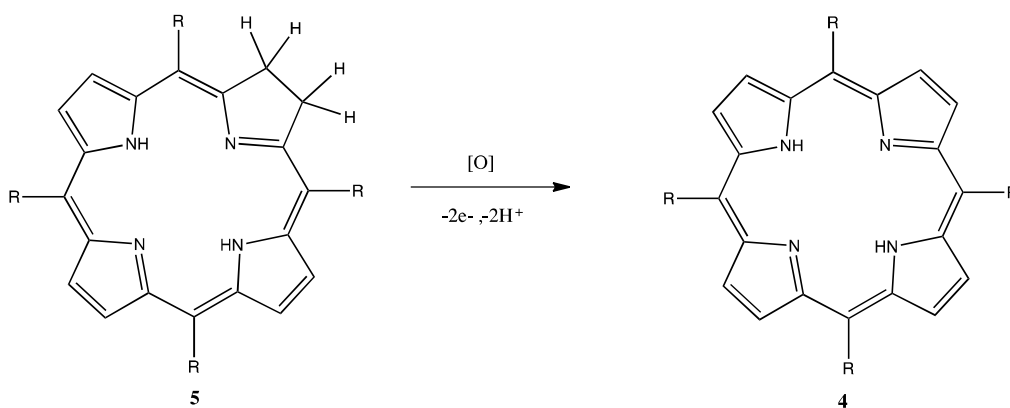
In 1935, Rothemund investigated a route to synthesize symmetrical porphyrins such as tetraphenylporphyrin (TPP) (Scheme 1).⁶ Initially, acetaldehyde and pyrrole were heated with methanol in a sealed vessel at different temperatures and similar studies were performed employing different aldehydes. The porphyrins generated were observed spectroscopically and shown to be contaminated with other porphyrinic substances. One of these was later isolated by column chromatography and shown to



Scheme 1: Rothemund method for synthesis of *meso*-tetraphenylporphyrin.

be the related dihydroporphyrin or chlorin (Scheme 2). The chlorin can be converted to the porphyrin via an oxidation step. A few years later, Rothemund improved the preparation of TPP by changing some of the conditions. In the developed procedure, pyrrole and benzaldehyde were heated in pyridine in a sealed vessel and following

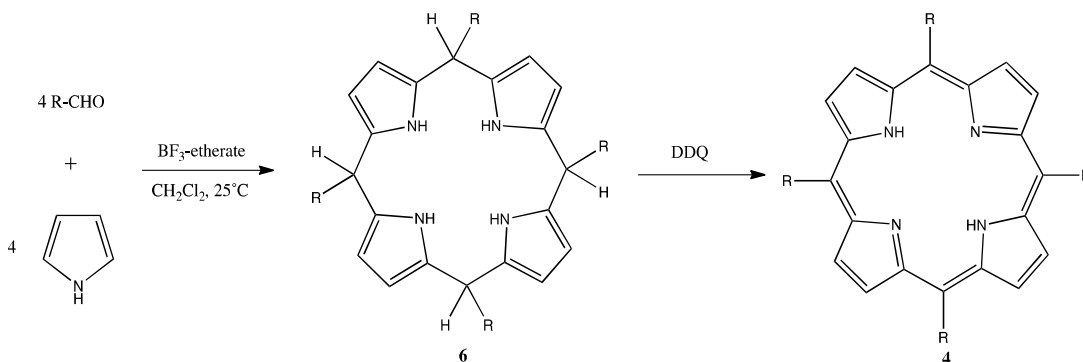
cooling over an 18 h period afforded blue needles in 9% yield.^{6,7} During an investigation of the chlorin isolated by Rothemund, Calvin and coworkers found that addition of zinc acetate to the reaction mixture significantly increased the yield to above 11%. However, this method was time consuming.⁷



Scheme 2: Conversion of chlorin to porphyrin

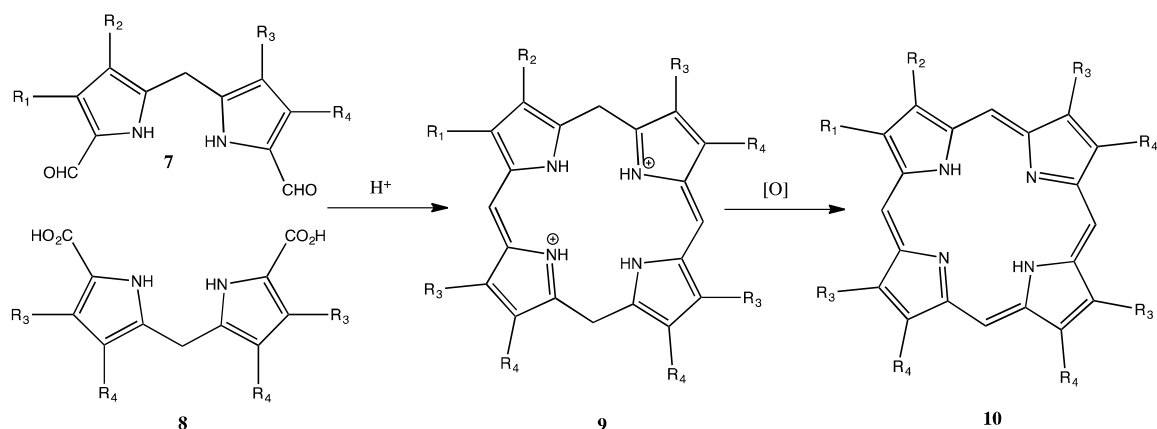
In the later 1960s, Adler, Longo and coworkers reported a greatly improved procedure based on Rothemund's method. They condensed benzaldehyde and pyrrole in acidic solvents at reflux and open to air. The solvents employed in this method were: acetic acid, acetic acid in the presence of metal salts, and benzene containing chloroacetic acid or propionic acid. This alternative route for preparing TPP can give >20% yield.^{7,8} In addition, this method did not require an oxygen free environment and required shorter reaction times. However, both the Rothemund and Adler-Longo methods are only suitable for symmetrical porphyrins.^{6,7,8} Further improvements to the synthesis of tetraphenyl porphyrins were reported by Lindsey *et al.* using milder conditions (Scheme 3). In these reactions, dilute solutions of pyrrole and benzaldehyde in dichloromethane are

reacted at room temperature in the presence of a Lewis acid catalyst such as boron trifluoride etherate. Oxidation, usually with 2,3-dichloro-5,6-dicyano-1,4-benzoquinone (DDQ), furnishes TPP in 40-60% yield.⁹



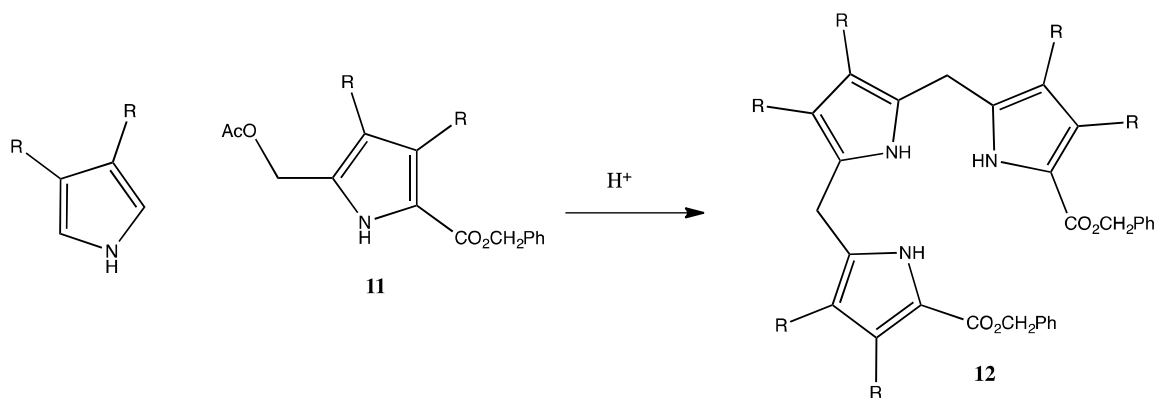
Scheme 3: One-pot synthesis of *meso*-substituted porphyrins

Hans Fischer developed routes to synthesize asymmetrical porphyrins in the 1920s, but these methods required harsh conditions and gave low yields. In 1960, MacDonald published a new method for porphyrin synthesis. A 5,5'-dipyrrylmethane dialdehyde **7** was condensed with α -unsubstituted dipyrromethane **8** in the presence of an acid catalyst to generate a porphodimethene intermediate **9**, and following air oxidation the final porphyrin product **10** was obtained (Scheme 4).^{7,10} The MacDonald reaction has been one of the important methods for synthesizing *meso*-unsubstituted porphyrins. Moreover, a variation on MacDonald's condensation was an important step in the total synthesis of chlorophyll a.⁷

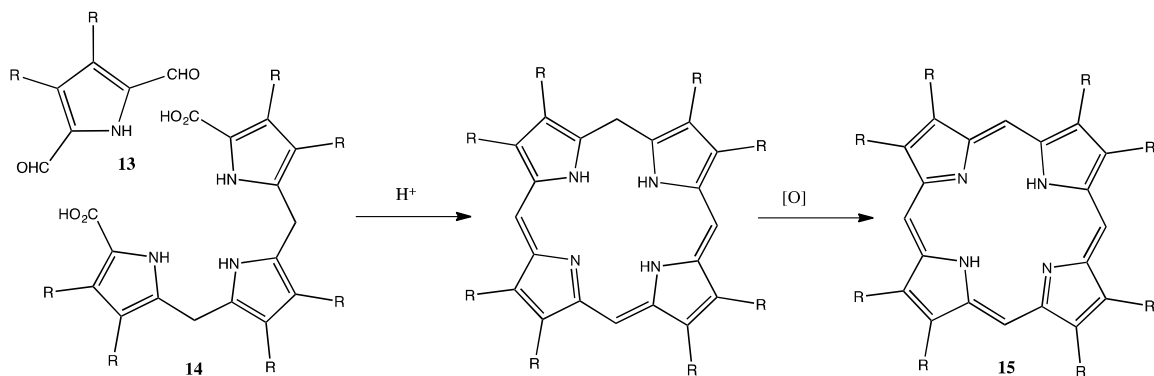


Scheme 4: “2+2” MacDonald condensation reaction

In the mid 1990s, the “3+1” approach was shown to be the method of choice for the synthesis of porphyrin analogues.⁷ The development of a straightforward approach for preparing tripyrranes facilitated the success of this approach.^{7,11} This was accomplished by reacting a 2,5-disubstituted pyrrole with two equivalents of an acetoxymethylpyrrole **11** under acidic conditions to afford protected tripyrrane **12**. The tripyrrolic products are usually prepared as dibenzyl esters **12** (Scheme 5). Hydrogenolysis over palladium-charcoal affords the corresponding dicarboxylic acids **14** and these condense with pyrrole dialdehydes **13** to give, following an oxidation step, the corresponding porphyrins **15** (Scheme 6).¹¹



Scheme 5: Synthesis of tripyrranes



Scheme 6: “3+1” MacDonald condensation reaction

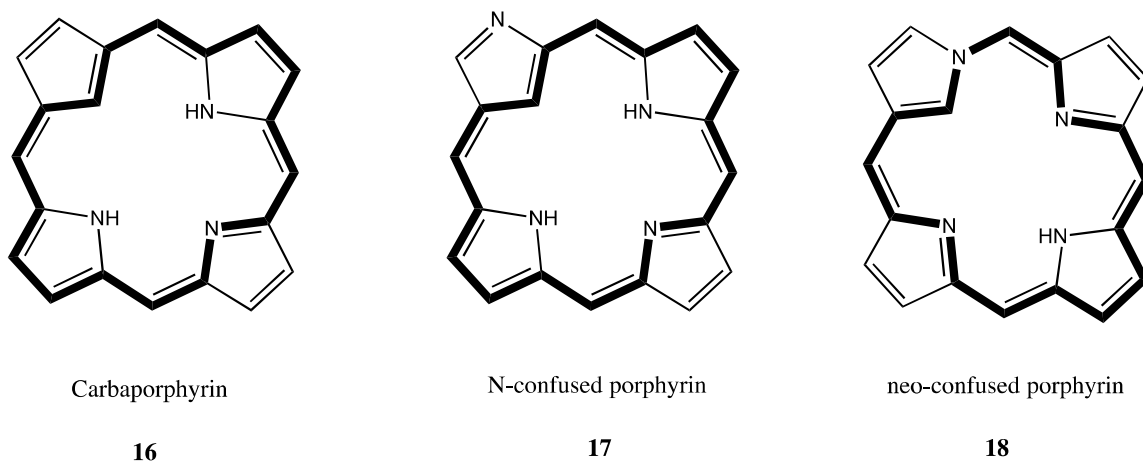
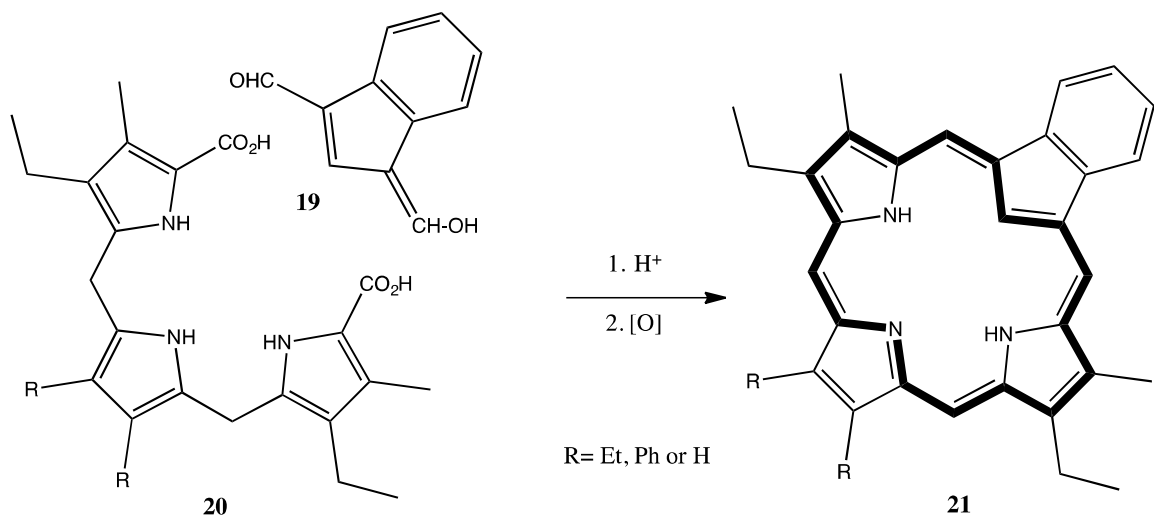


Figure 5: Carbaporphyrin, N-confused porphyrin and neo-confused porphyrin

Carbaporphyrins **16** are porphyrin analogues where one of the internal nitrogens has been replaced with a carbon atom. This class of porphyrin has been widely investigated due to their unusual reactivity such as forming organometallic complexes under mild conditions. Examples of related carbaporphyrinoid systems are N-confused porphyrins **17** and neo-confused porphyrins **18** (Figure 5).^{13,14}

Most of the work that has been carried out on carbaporphyrins has dealt with benzocarbaporphyrins because of the straightforward synthesis of this type of porphyrin analogue. This system can easily be synthesized from indenedicarbaldehyde **19** and tripyrrane **20** in the presence of an acid catalyst, and following oxidation with DDQ the conjugated porphyrinoid **21** is obtained in >40% yield (Scheme 7).¹⁴



Scheme 7: Synthesis of benzocarba porphyrins

N-confused porphyrin (NCP) **17**, an isomer of tetraphenylporphyrin (TPP) **4** (Figure 6), was discovered in 1994. NCP differs from true porphyrins because one of the pyrrole units is inverted so that nitrogen appears on the periphery (Figure 6). Furuta *et al.* (1994)¹⁴ reported that NC-TPP **17** was obtained through the well-known condensation reaction between benzaldehyde and pyrrole, but instead of the usual propionic acid, a mixture of HBr and tert-Butanol/dichloromethane was used. Information about the structure of NC-TPP was ascertained using NMR spectroscopy and single-crystal X-ray diffraction; the results showed that the molecule was less planar than TPP. Furuta *et al.* (1994) hypothesized that the ring distortion was due to repulsion by the three inner hydrogens. Latos-Grazynski and coworkers also reported an independent synthesis of NCP in 1994.¹⁵

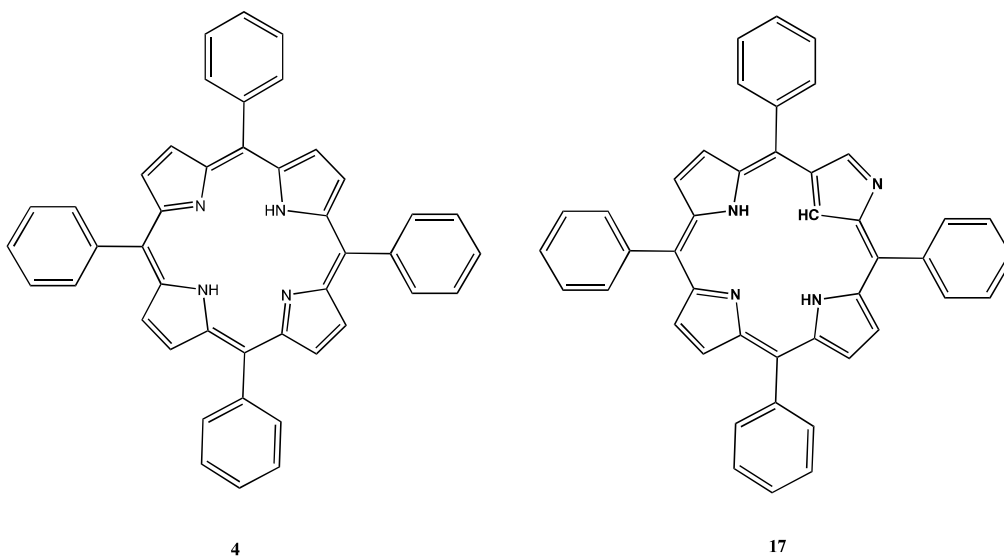
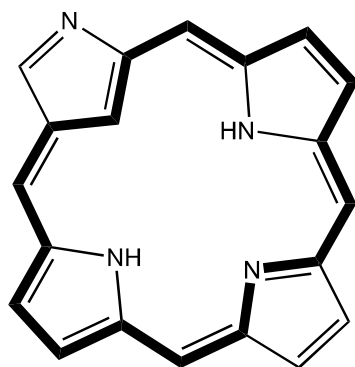


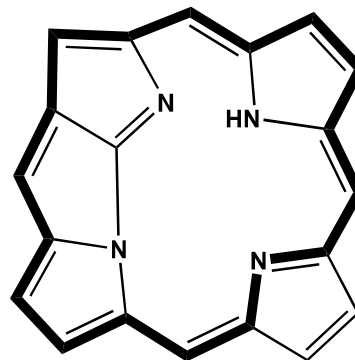
Figure 6: Tetraphenylporphyrin (TPP) (4) and N-Confused Porphyrin (NCP) (17)

Following the discovery of NCPs, hundreds of papers have been published on these unusual porphyrin isomers. In addition, doubly N-confused porphyrins with two inverted pyrrole units have been prepared, as well as expanded N-confused systems. N-Confused porphyrins form coordinated complexes within the porphyrinoid cavity and at the peripheral nitrogen. The NCP core can generate stable organometallic derivatives and may stabilize high oxidation state complexes such as Ag(III) derivatives. The N-confused porphyrins display high reactivity towards electrophilic substitution reactions such as bromination and nitration compared to regular porphyrins. Moreover, NCPs are more flexible than ordinary porphyrins and can exist as an aromatic tautomer or less aromatic form with an external NH.^{14,15}



N-confused porphyrin

17



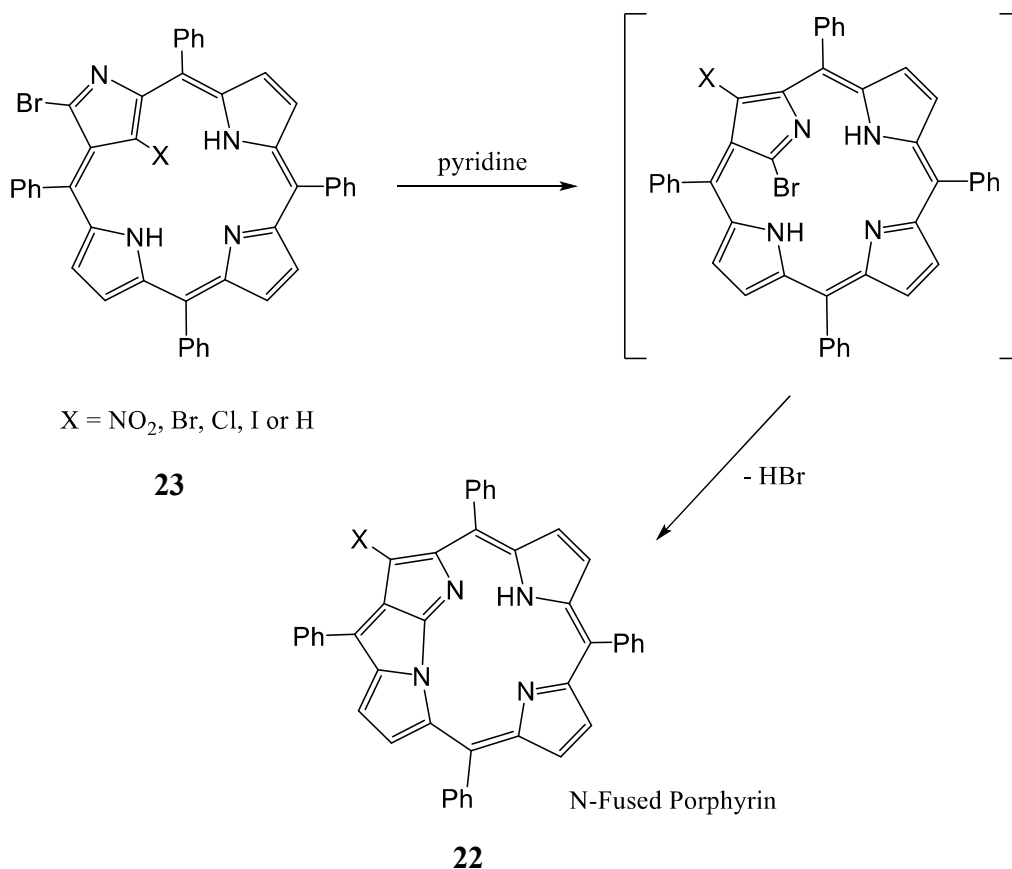
N-Fused porphyrin

22

Figure 7: N-confused porphyrin (**17**) and N-fused porphyrin (**22**)

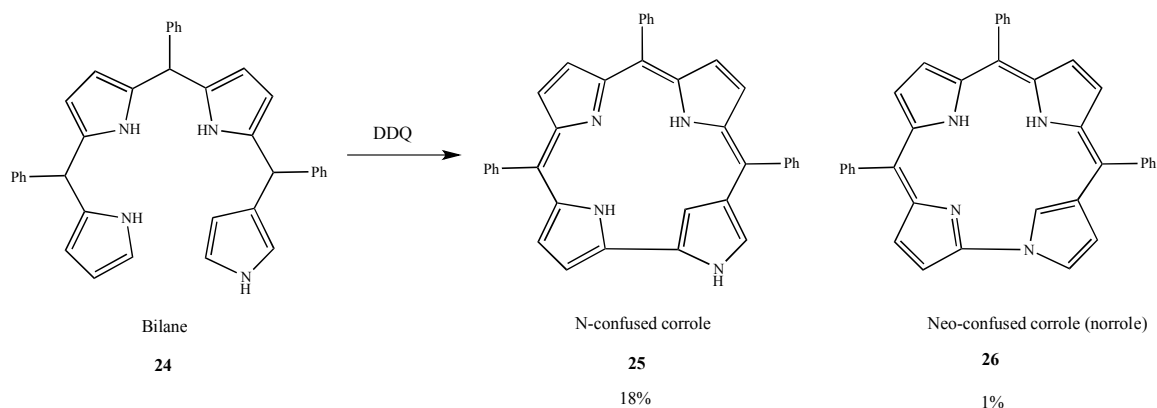
N-Fused porphyrin (NFP) **22** was discovered by Furuta *et al.* (1999) and (2000) (Figure 7). NFP **22** can be made from N-confused porphyrins **17** by several pathways including spontaneous production from a bromo-substituted N-confused tetraarylporphyrin **23** in a pyridine solution (Scheme 8).^{15,16} The formation of NFP **22** involves inversion of the “confused” pyrrole unit, followed by generation of a carbon-nitrogen bond (Scheme 8).¹⁶ X-ray diffraction studies (Furuta *et al.*, 2000) showed that the resulting fused tri-pentacyclic ring at the center is almost planar, although the remaining structure is highly distorted and the aryl units on the periphery tilt from 12.4° to 64.4° from the plane of the center ring.¹⁶ Proton NMR and UV/Vis spectroscopy indicated a) three-centered H bonding in the NFP ring, b) UV-Vis transitions near 360, 500, and 550 nm, and c) weak bands near 650, 700, 850, and 940 nm for a solution in CH₂Cl₂.

Addition of base to the N-fused porphyrin resulted in ring opening to regenerate the NCP system.¹⁶



Scheme 8: Synthesis of N-fused porphyrins

In 2011, Furuta and coworkers oxidized N-confused bilane **24** with DDQ which gave N-confused corrole **25**, with a direct carbon-carbon link between two pyrrole units, in 18% yield. In addition, a minor product with a direct carbon-nitrogen link was isolated in 1% yield, and the new system was named neo-confused corrole or norrole **26** (Scheme 9).¹⁷



Scheme 9: N-confused corrole and neo-confused corrole (norrole)

Recently, a third class of porphyrin isomers was proposed (Figure 8). In this new proposed variation, one of the pyrrole rings is linked to a methine carbon via a nitrogen atom. This new variation was called a neo-confused porphyrin. Neo-confused porphyrins **18** can potentially take on aromatic characteristics due to the presence of a 17-atom 18- π -electron delocalization pathway.¹⁸

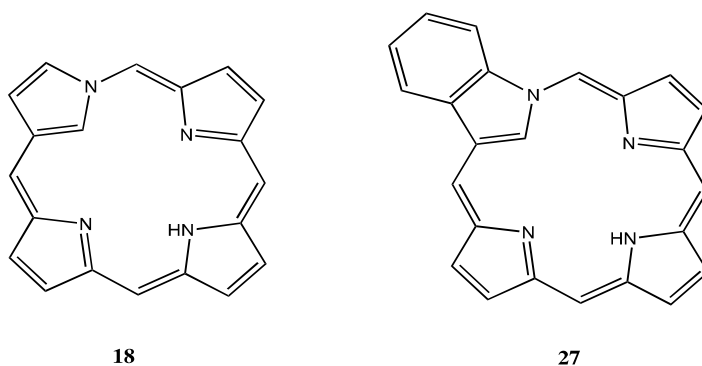
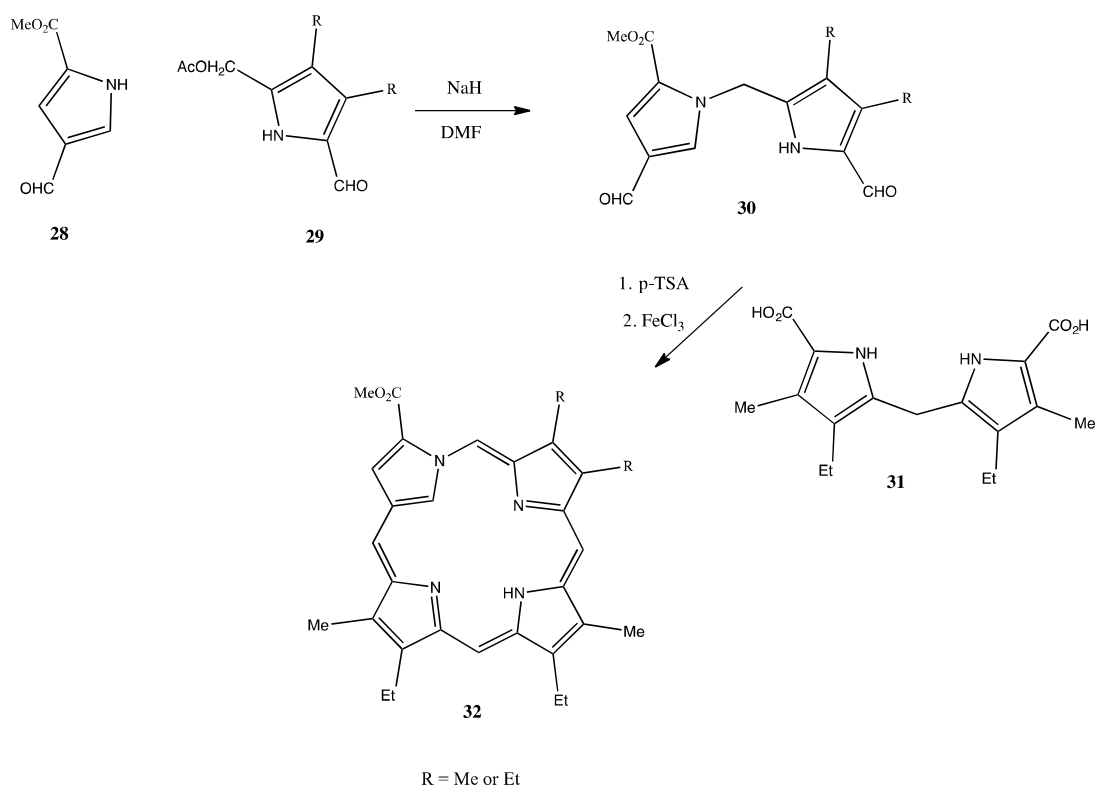


Figure 8: Neo-confused porphyrins

Several examples of this new class of porphyrin analogues were prepared using dipyrrolicdialdehydes as intermediates. The neo-confused porphyrins demonstrated remarkably similar UV-vis spectral profiles to porphyrins. The proton NMR spectra for neo-confused porphyrins demonstrated that they are significantly less aromatic than true porphyrins and carbaporphyrins. The internal CH for benzo-neo-confused porphyrins was observed upfield near -0.5 ppm, but benzocarbaporphyrinsmethine proton show this resonance substantially further upfield near -7 ppm.^{18,19}



Scheme 10: Method developed for the synthesis of neo-confused porphyrin esters

Attempts to synthesize neo-confused porphyrins using a “3 + 1” approach resulted in decomposition of the material under acidic conditions, with no identifiable products. The “2 + 2” method yielded more favorable results, but in the initial study the desired product was only obtained in 25% yield. This was subsequently improved when the oxidation step was carried out with aqueous FeCl₃ instead of DDQ (Scheme 10).¹⁹

In 2014, Lash and coworkers reported an efficient method for the synthesis of neo-confused porphyrins without fused benzo-units. In the synthesis of neo-confused porphyrin **32** described by Lash *et al.* (2014), the intermediate dipyrrolicdialdehydes **30** were formed by reacting pyrrole-3-carbaldehyde **28** with 5-acetoxymethylpyrrole-2-carbaldehyde **29** and sodium hydride in DMF (Scheme 10). The next step involved MacDonald "2+2" condensations of the dialdehydes with dipyrromethanes to produce dihydroporphyrinoids, and finally oxidation with ferric chloride produced neo-confused porphyrins **32**. These molecules reacted with nickel(II) or palladium(II) acetate to give the organometallic derivatives of neo-confused porphyrin **33** and **34** (Figure 9).¹⁹ This study investigated the unique spectral and synthetic properties of this new class of porphyrin isomers. This research forms the groundwork for future investigations into these porphyrin isomers. Neo-confused porphyrins show surprisingly similar characteristics to regular porphyrins, exhibiting significant aromatic character and the ability to form metallo-derivatives. However, far more work will be required to understand how the structural modification due to the neo-confused ring affects the properties of these macrocycles.¹⁹

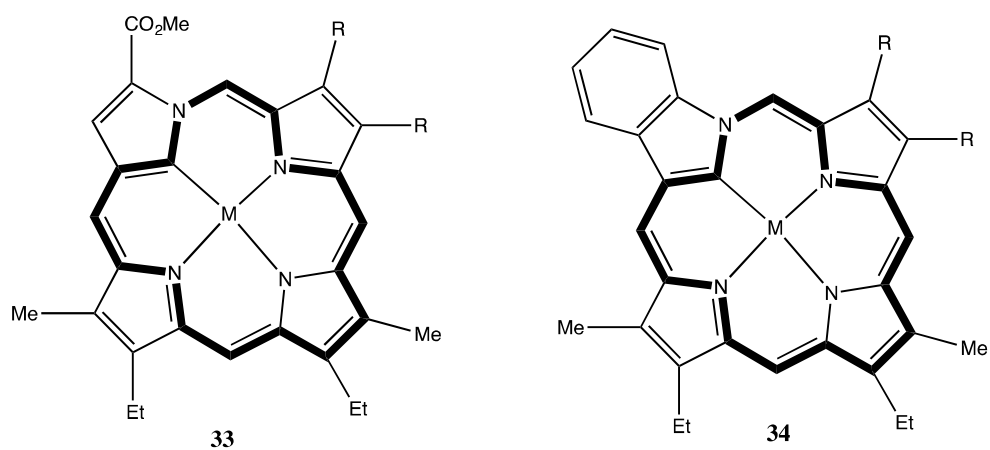
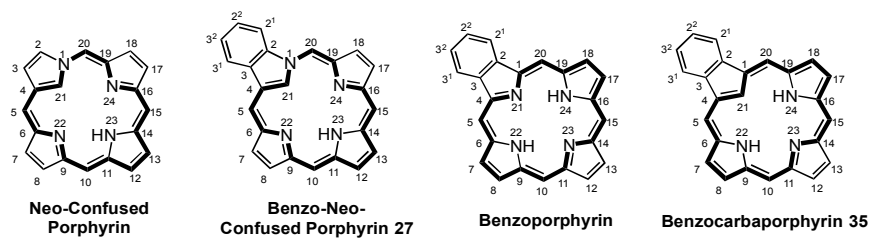


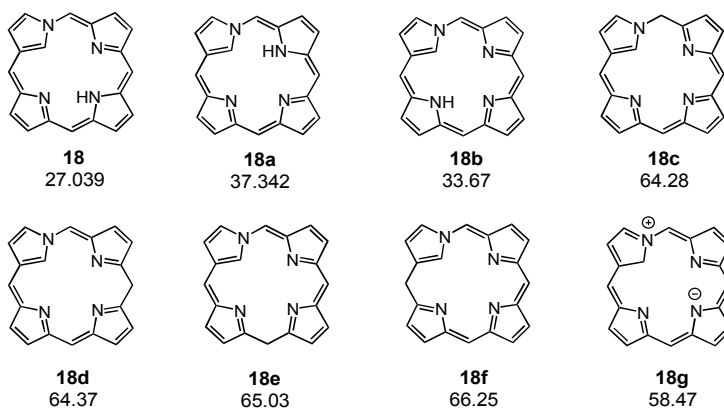
Figure 9: Metal complexes of neo-confused porphyrins

Theoretical Studies of N- and Neo-confused Porphyrins

In order to gain further insights into N-confused and neo-confused porphyrin systems, computational studies have been performed.²⁰In a study by AbuSalim and Lash in 2013, tautomers of N-confused porphyrin, neo-confused porphyrin and regular porphyrins were investigated using standard density functional theory calculations (Figure 10). The neo-confused tautomers differed from one another by the placement of a single hydrogen atom. In N-confused porphyrin, the ring is tilted at an angle of 16.55° relative to the macrocyclic plane, which agrees with previous X-ray structure studies.²⁰In neo-confused tautomers, the structures end up in an almost planar state, because the cavity only has to accommodate one or two hydrogen atoms. Within the study, four tautomers with methylene bridges, which interrupt the conjugation of the macrocycle, were also investigated. These were found to have relative energies of 64.28 to 66.25 kcal mol⁻¹ compared to porphyrins which means that they are not stable enough to isolate.²⁰



Neo-Confused Porphyrin Tautomers



Benzo-Neo-Confused Porphyrin Tautomers

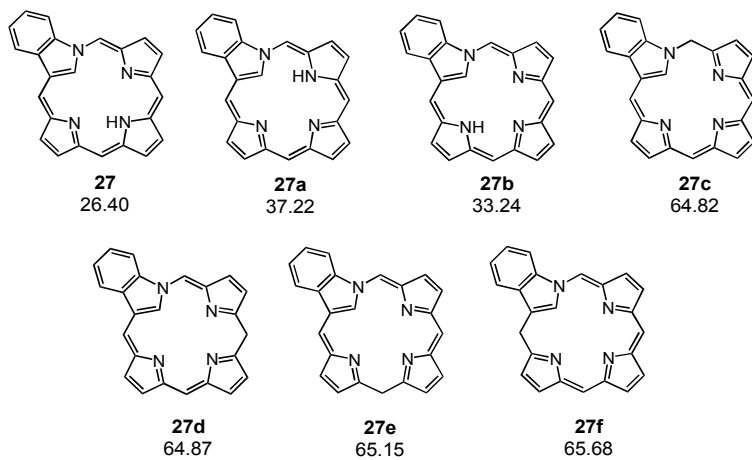


Figure 10: Structures of neo-confused porphyrin and benzo-neo-confused porphyrin tautomers and their relative energies (kcal/mol) compared to porphyrin and benzoporphyrin, respectively

Eight neo-confused porphyrin (neo-CP) and seven benzo-neo-confused porphyrin (B-neo-CP) tautomers were studied. In addition, twelve benzoporphyrin tautomers and twelve benzocarporphyrin tautomers, were used for comparison (Figure 10). It was found that the most stable tautomer of neo-CP was 27.04 kcal mol⁻¹ higher in energy than porphyrin, and the most stable B-neo-CP was 26.40 kcal mol⁻¹ higher than benzoporphyrin. Nucleus independent chemical shifts showed that the fully conjugated neo-CP and B-neo-CP tautomers had a significant amount of diatropic character, but this value is lower than for porphyrins.²⁰ It should also be noted that 18 π electron delocalization pathways that pass through a fused benzene ring are less favorable than alternative delocalization pathways that bypass this unit.²⁰

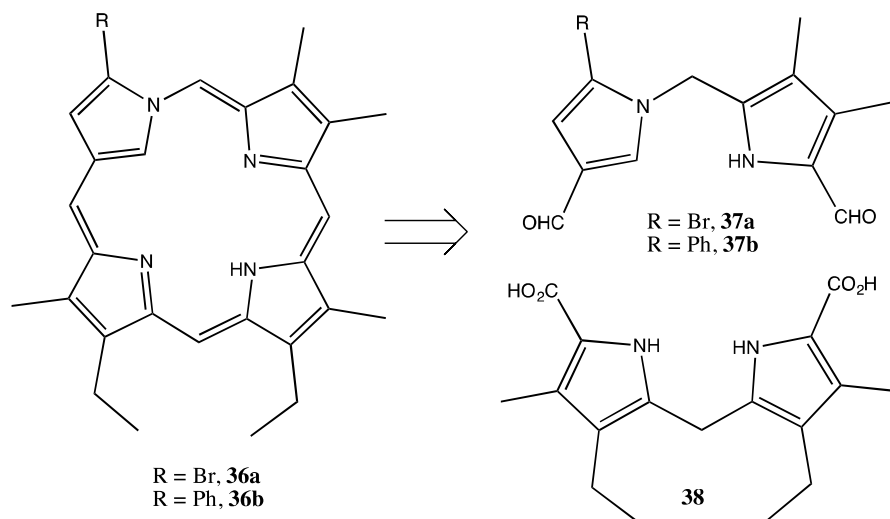
Conclusion

In this thesis, the synthesis of neo-confused porphyrins with bromo- or phenyl-substituents is presented. These new porphyrinoids are the first neo-confused porphyrins to be prepared that lack an ester substituent or a fused benzo- unit. The aromatic properties of these macrocycles have been assessed by proton NMR spectroscopy and organometallic derivatives have been prepared.

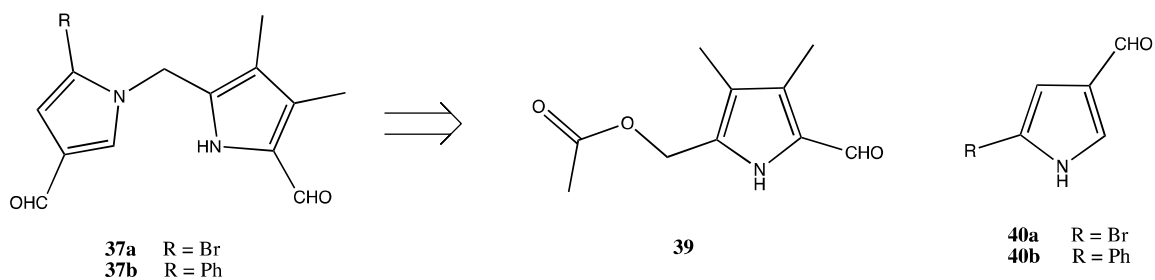
CHAPTER II

RESULTS AND DISCUSSION

A great deal of interest has been directed towards N-confused porphyrins **17** since they were first discovered in 1994.¹⁴ This type of porphyrin analogue is different from true porphyrins **1** because one of the pyrrole subunits is connected via α and β positions, which results in the nitrogen being relocated to the outside of the macrocycle. NCPs are true porphyrin isomers as the only difference is the arrangement of one pyrrole unit. Another type of porphyrin isomer **18** has been proposed where the nitrogen atom of the pyrrole ring is connected to the adjacent *meso*-carbon.¹⁸ However, until recently there had been no literature reports on the system, and it was unclear whether structures of this type would retain overall aromatic character. This type of porphyrin isomer, like N-confused porphyrins, can be considered to be a carbaporphyrinoid system as an internal methine unit has replaced by core nitrogen atom. Lash and coworkers successfully generated a benzo-fused version of this type of porphyrin isomer and named it neo-confused porphyrin.¹⁸ The proton NMR spectra for benzo-fused neo-confused porphyrins showed that they retained diatropic character, although this was somewhat reduced compared to true porphyrins or carbaporphyrins. In this work, bromo and phenyl neo-confused porphyrins have been successfully synthesized. The proton NMR spectra for this type of porphyrin analogue showed that bromo and phenyl neo-confused porphyrins retained diatropic character, although this was significantly reduced compared to true porphyrins.



Scheme 11: Retrosynthetic analysis of neo-confused porphyrins using MacDonald's "2+2" condensation approach

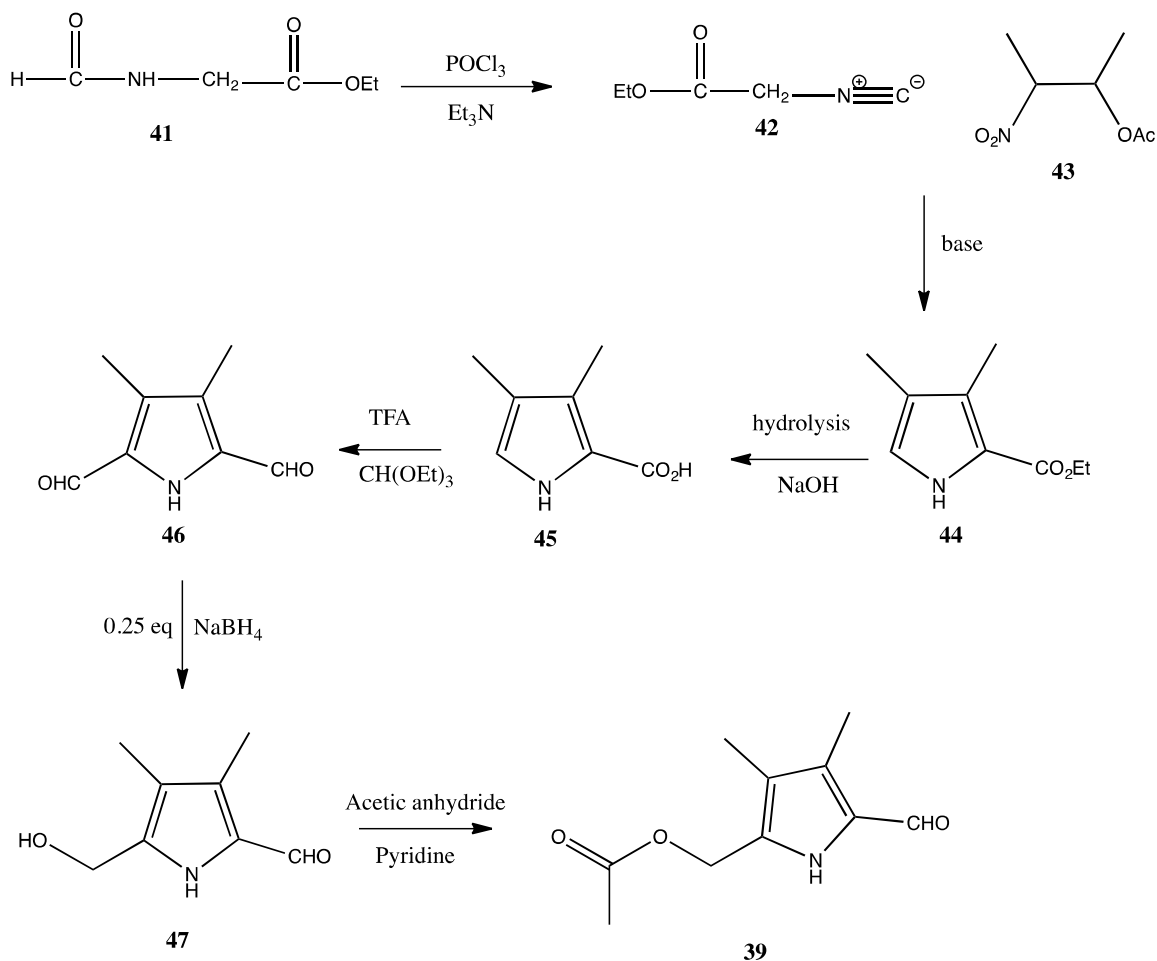


Scheme 12: Retrosynthetic analysis of the key intermediary dipyrroledialdehydes

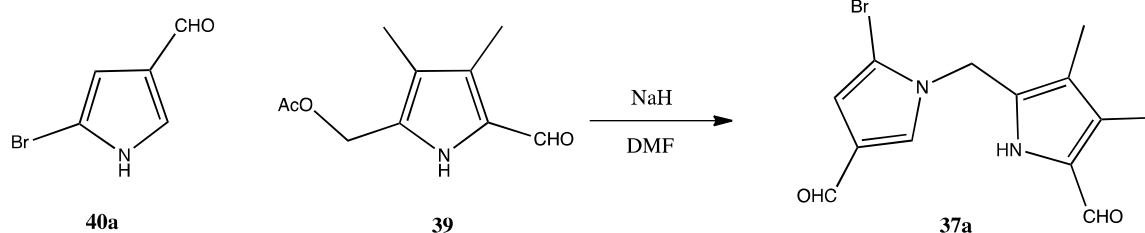
MacDonald's "2+2" approach was selected to prepare this system (Scheme 11). This required three dipyrrolic intermediates, the known dipyrrolymethanedicarboxylic acid **38** and 1,2'-dipyrrolymethane dialdehydes **37a** and **37b**. The synthesis of the key intermediates **37a** and **37b** was crucial for these investigations. It was anticipated that these dialdehydes could be constructed from acetoxymethylpyrrolecarbaldehyde **39** and 3-pyrrole carbaldehydes **40a** and **40b** (Scheme 12).

The synthesis first targeted acetoxymethylpyrrole aldehyde **39**, which was prepared by adapting literature procedures.²¹ *N*-Formylglycine ethyl ester **41** was reacted with freshly distilled phosphorus oxychloride in the presence of triethylamine to afford ethyl isocyanoacetate **42**. Using the Barton- Zard method, ethyl isocyanoacetate **42** was reacted with 3-acetoxy-2-nitro-butane **43** in the presence of tetramethylguanidine to give ethyl 3,4-dimethylpyrrole-2-carboxylate **44** (Scheme 13). Following hydrolysis with sodium hydroxide, 3,4-dimethylpyrrole-2-carboxylic acid **45** was isolated. In order to form dimethylpyrroledicarbaldehyde **46**, carboxylic acid **45** was dissolved in TFA and triethylorthoformate was added slowly to the solution. The reaction appeared to be temperature sensitive, and was controlled using a salt-ice bath. The dialdehyde **46** was isolated as brown solid in 97% yield, which was a significant improvement over the 49% reported in the earlier literature²¹ and the 71% yield reported by Li.^{21, 22} Conversion of the dialdehyde to mono-alcohol **47** required the selective reduction of one aldehyde unit. The mono-alcohol **47** was generated by reducing the dialdehyde **46** with 0.25 equivalents of the mild reducing agent NaBH₄ and afforded 3,4-dimethyl pyrrole-2-carbaldehyde-5-carbinol **47** in 98% yield as a brown solid. The acetylation of mono-alcohol **47** was temperature and time dependent. Pyrrole carbinol **47** was reacted with acetic anhydride

and pyridine at -3°C for 1 h, and this gave the desired
 acetoxyethylpyrrolecarbaldehyde **39** in 85% yield (Scheme 13).



Scheme 13: Synthesis of 5-acetoxyethyl-3,4-dimethylpyrrole-2-carbaldehyde **39**



Scheme 15: Synthesis of bromo-neo-confused dipyrromethane **37a**

Reaction of 5-bromopyrrole-3-carbaldehyde **40a** with sodium hydride in DMF, followed by addition of acetoxymethylpyrrole **39**, gave the neo-confused dipyrromethane **37a** in 65% yield (Scheme 15). Initially, THF was used as a solvent, but gave very low yields. After numerous trials, the best results were obtained when the reaction was carried out at 30° C. However, greatly improved results were obtained when DMF was used as the solvent (Figure 11).²²

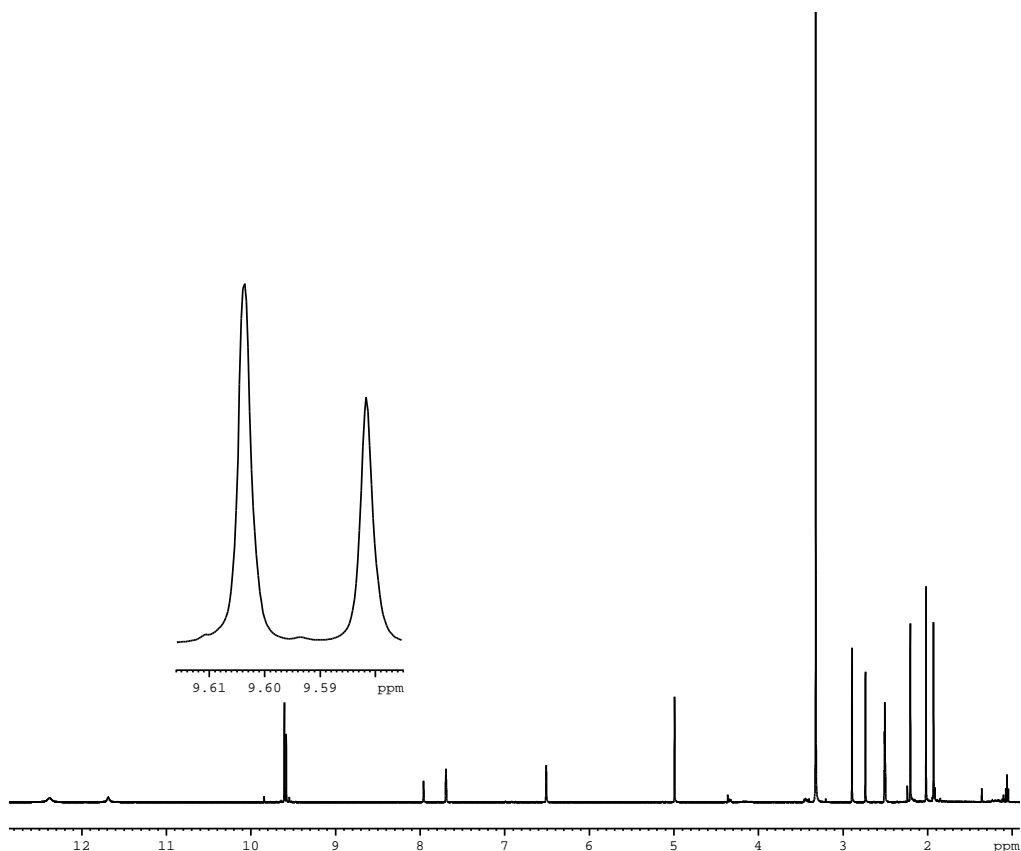
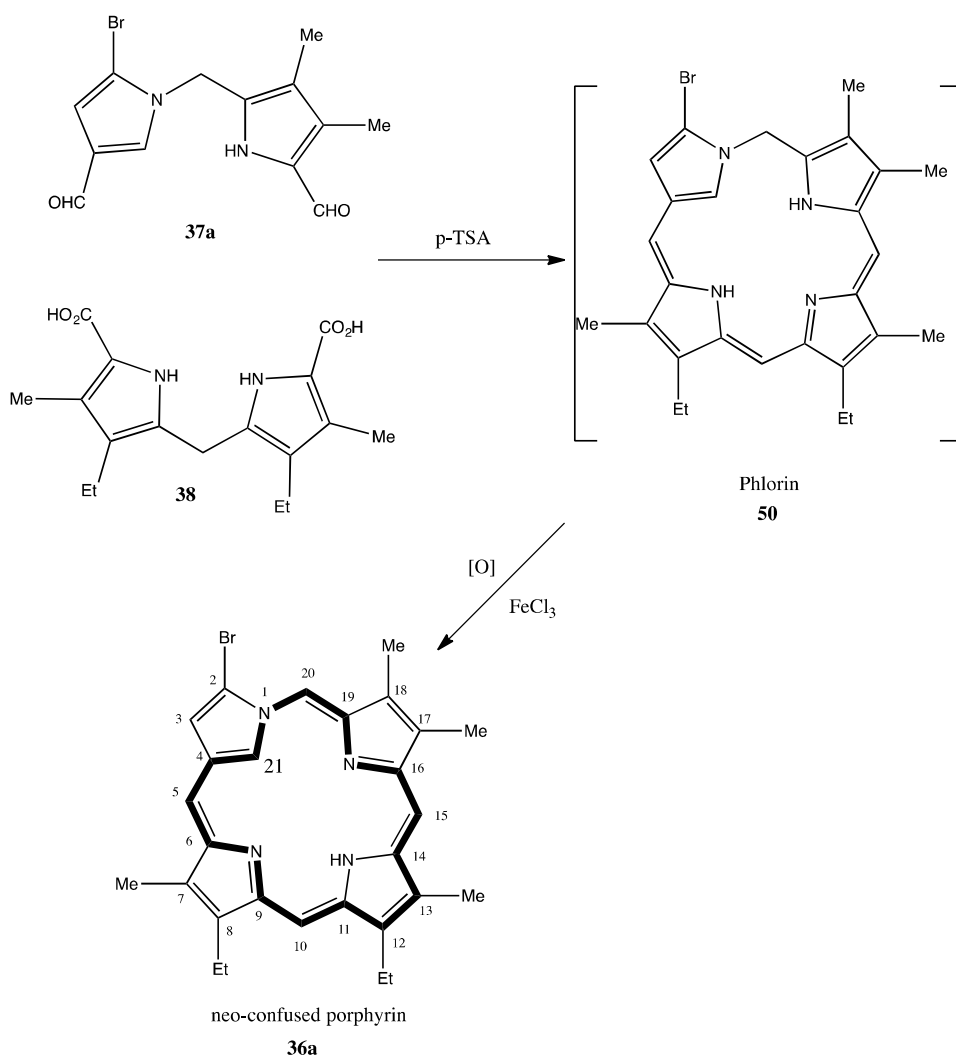


Figure 11: 500 MHz proton NMR spectrum of bromo neo-confused dipyrromethane **37a**

The novel dialdehyde **37a** was carried on through a MacDonald's "2+2" condensation with dipyrromethane **38** in methanol and dichloromethane in the presence of *p*-toluenesulfonic acid at room temperature for 16 h. Before the oxidation process, a bright blue fraction corresponding to phlorin **50** was observed. This phlorin was unstable and exposure to air spontaneously led to the formation of neo-confused porphyrin **36a**. When the reaction mixture was stirred with a 0.2% aqueous ferric chloride solution for 2 hours, neo-confused porphyrin **36a** was generated in 45% yield after purification by

grade 3 alumina column chromatography. However, the bromoporphyrinoid was somewhat unstable. Attempts to recrystallize bromo neo-confused porphyrin **36a** led to decomposition. To further purify bromo neo-confused porphyrin **33a**, a second column was performed (Scheme 16).



Scheme 16: Synthesis of bromo neo-confused porphyrin using a "2+2" condensation

The spectroscopic data for the fully conjugated neo-confused porphyrin **36a** was consistent with an aromatic system. The proton NMR spectrum for **33a** shows a moderate

diatropic ring current, with the *meso* protons being observed as four singlets at 8.20, 8.35, 8.70 and 9.09 ppm (Figure 12). One of the *meso* protons showed a substantial downfield shift compared to the other three protons because the CH is connected to the neo-confused nitrogen. In addition, the external pyrrolic CH gave rise to a doublet at 8.10 ppm due to coupling to the 21-CH. However, the peak for CH-21, which appeared upfield at -1.3 ppm, only showed this interaction as a slight broadening of the resonance. The internal NH was also shifted upfield to -0.02 ppm. The diamagnetic ring current in **36a** appears to be comparable to the benzo-fused neo-confused porphyrin **27**. In the proton NMR spectrum of **27**, the *meso*-protons appeared at 9.09, 9.33, 9.83 and 9.91 ppm, values that are further downfield compared to the corresponding resonances in **36a** with the exception of the CH that is connected to the nitrogen. However, the internal NH and CH for **27** were reported to show up at -0.33 and -0.74 ppm, respectively, values that indicate a slightly reduced diatropic ring current compared to **36a**. Although neo-confused porphyrins do not possess an [18]annulene π delocalization pathway, a 17-atom 18 π electron delocalization pathway which includes the pair of electrons on the neo-confused nitrogen atom appears to be responsible for the aromatic characteristics of this system.¹⁹

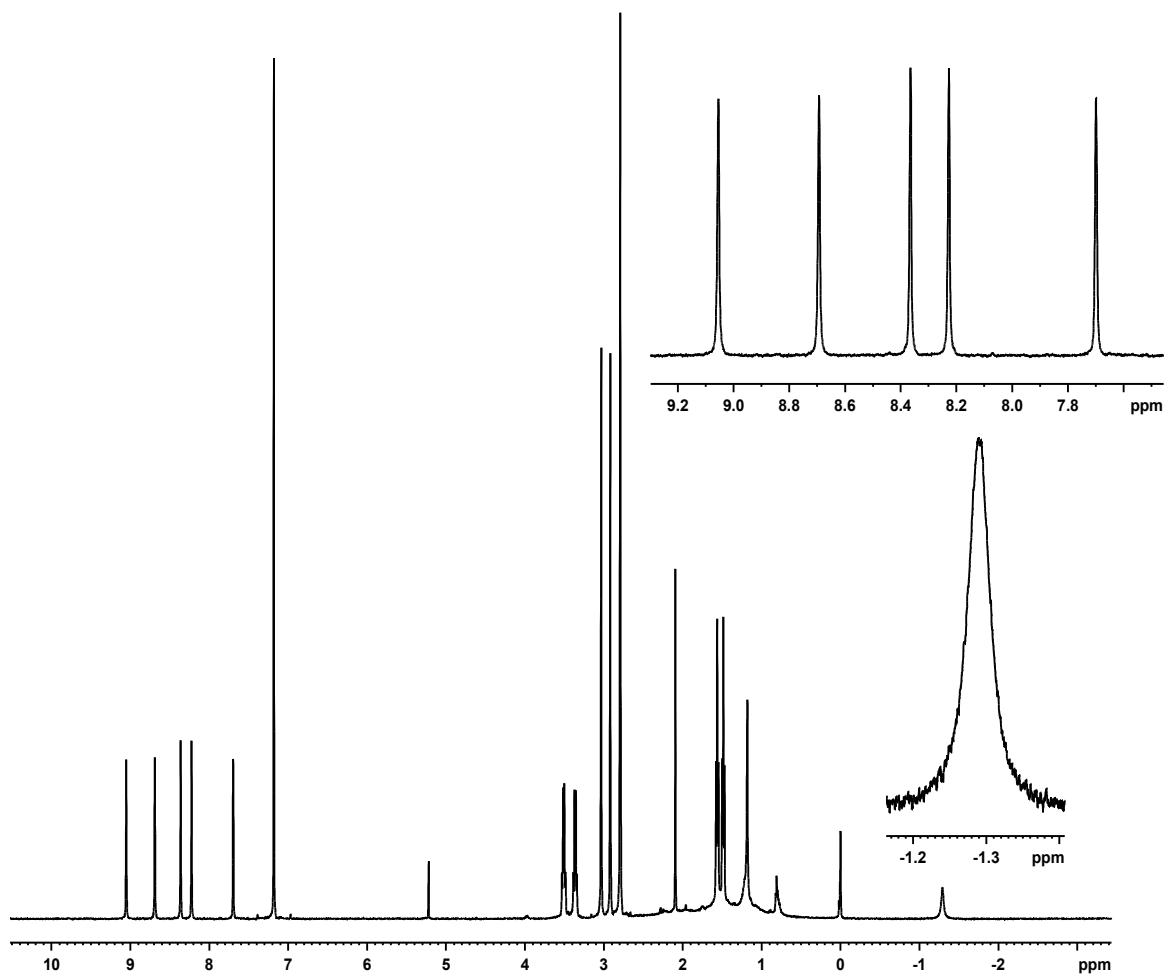


Figure 12: 500 MHz proton NMR spectrum of bromo neo-confused porphyrin **36a**

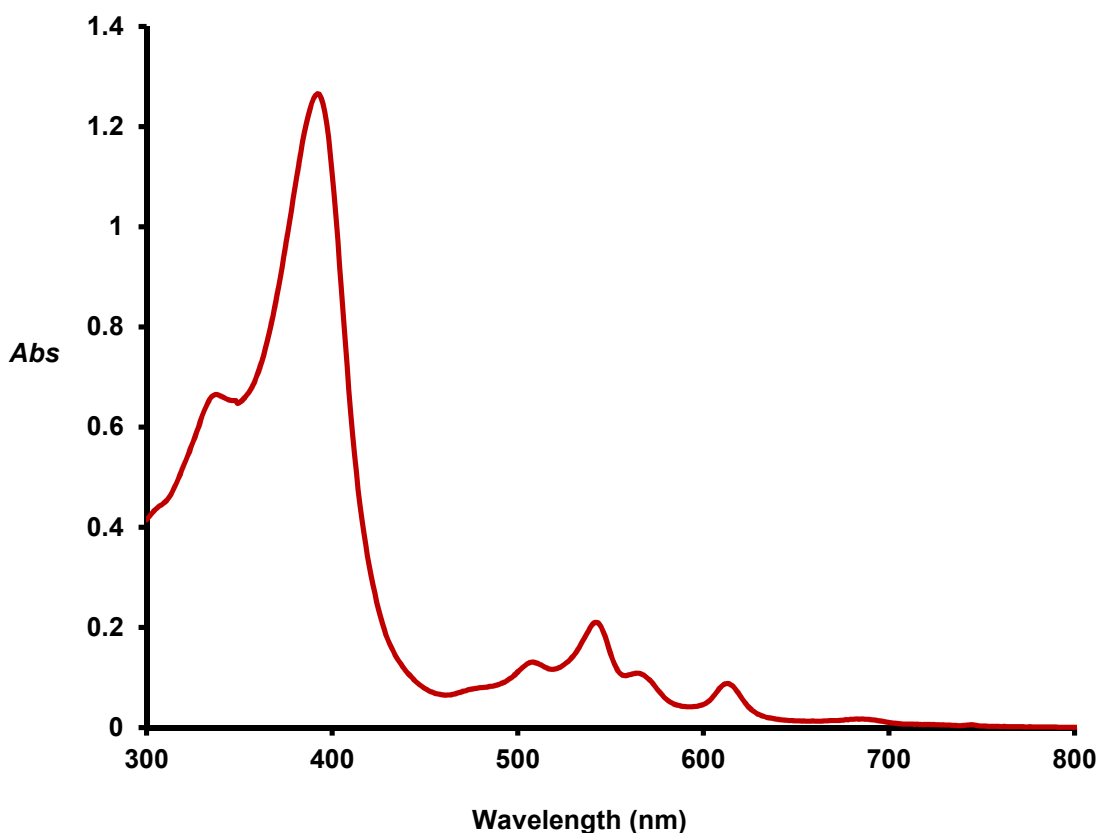


Figure 13: UV-vis spectrum of bromo neo-confused porphyrin **36a** in CH_2Cl_2

The UV-vis spectrum of bromo neo-confused porphyrin **36a** had similar characteristics to true porphyrins. A strong Soret band was present at 392 nm with several Q bands following at higher wavelength values of 508, 542, 564, 613 and 682 nm (Figure 13).

In TFA-CDCl_3 , the corresponding dication $\mathbf{36aH}_2^{2+}$ (Figure 14) showed a significantly enhanced diatropic ring current and the internal CH shifted upfield to -1.96

ppm, while the *meso*-proton resonances moved downfield to give four 1H singlets at 8.92, 9.01, 9.58 and 9.95 ppm (Figure 15).

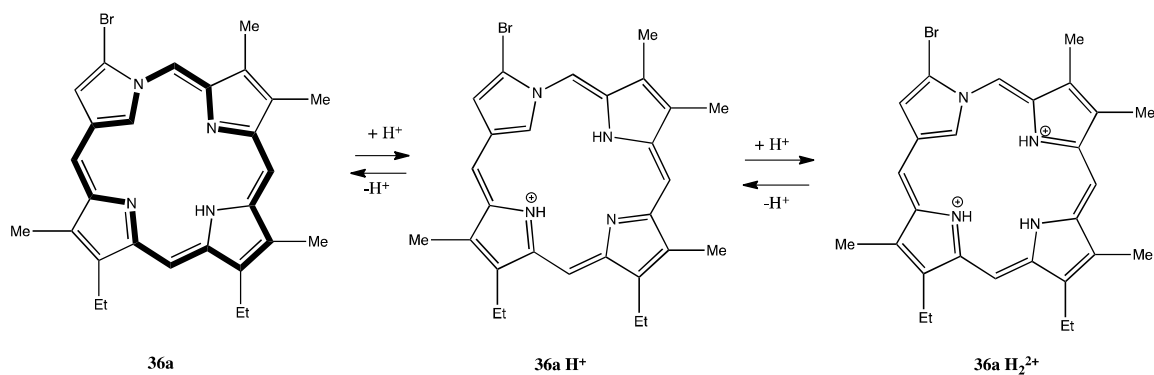


Figure 14: Protonation of bromo neo-confused porphyrin **36a**

Addition of TFA also gave rise to changes in the UV-vis spectrum for **36a**. At higher concentrations of TFA, a new species was generated with a Soret band at 377 nm corresponding to the dication **36aH₂²⁺** (Figure 16).

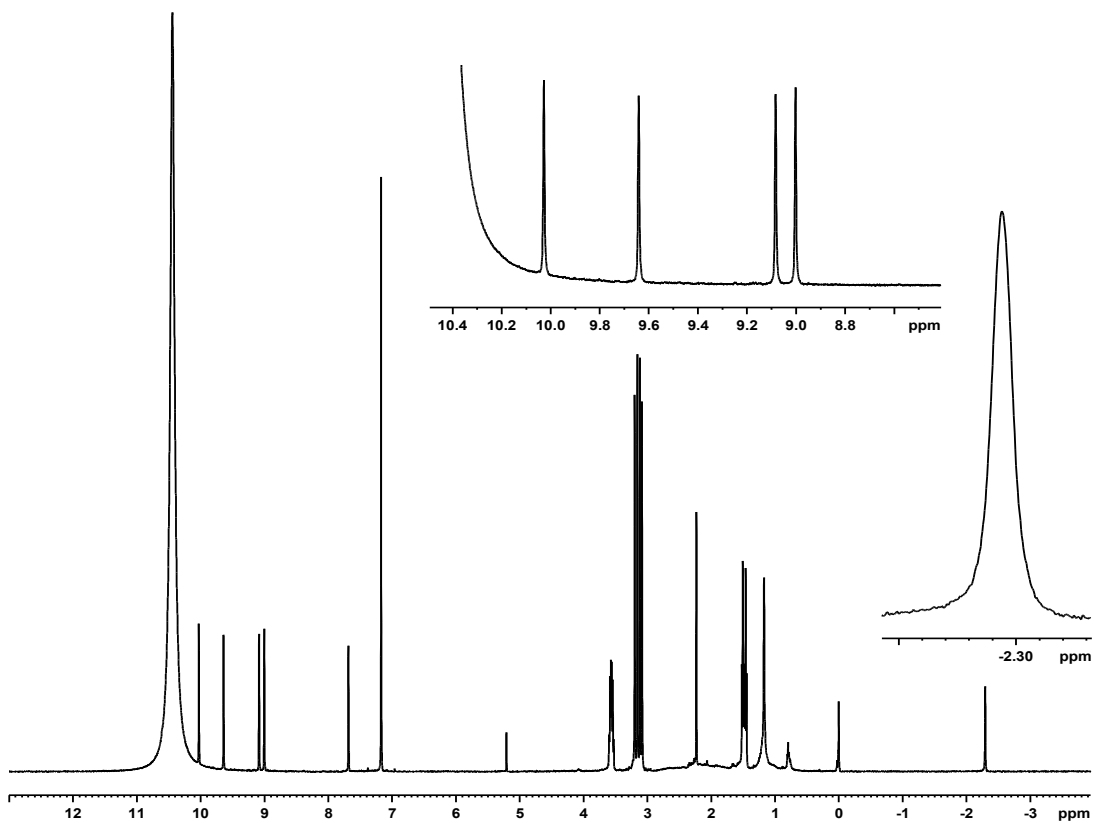


Figure 15: 500 MHz proton NMR spectrum of neo-confused porphyrin dication $36aH_2^{2+}$ in TFA- $CDCl_3$

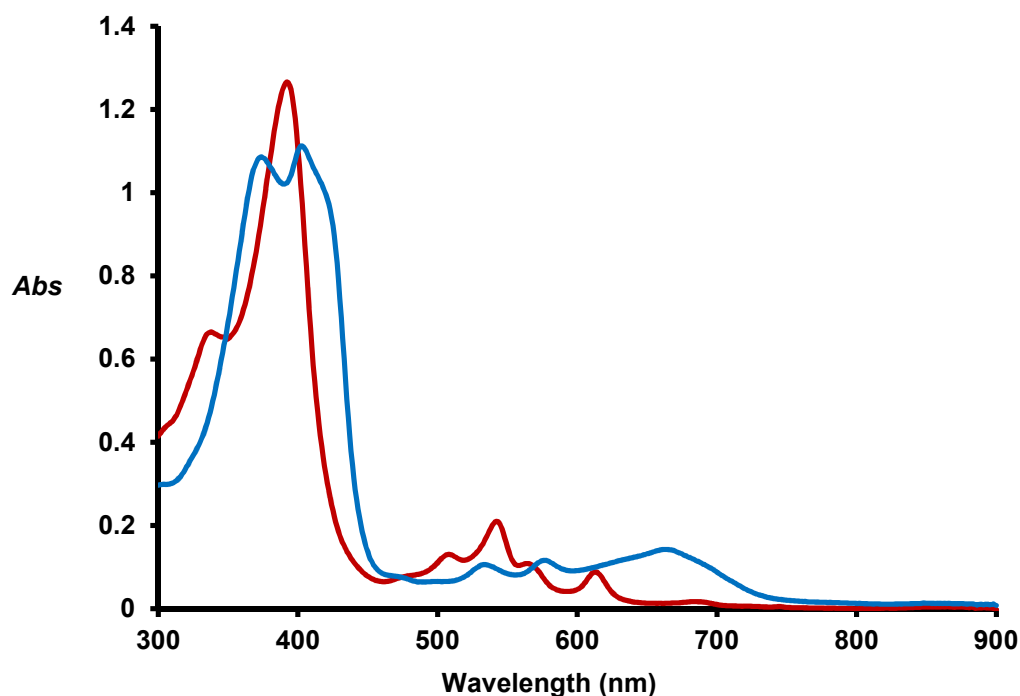
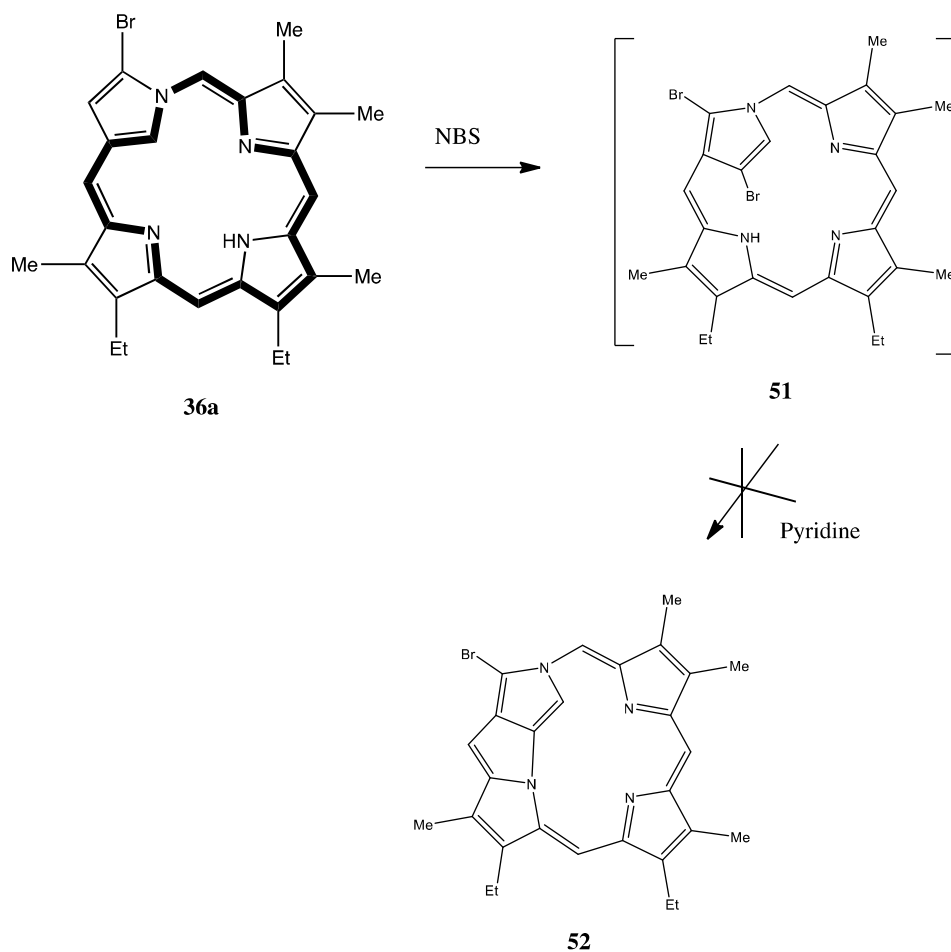


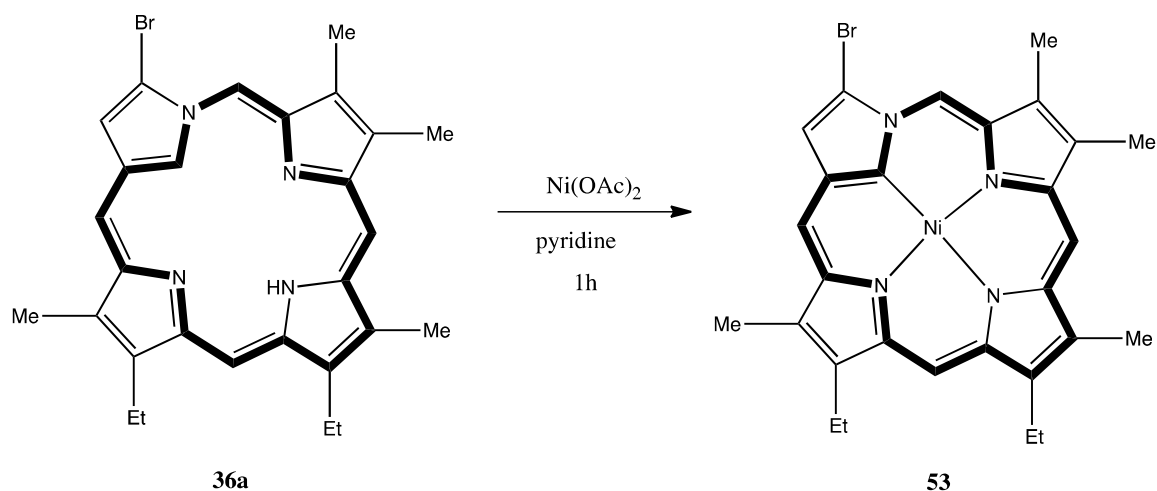
Figure 16: UV-vis spectrum of neo-confused porphyrin **36a** in dichloromethane (red line) and 2% TFA-CH₂Cl₂ (blue line)

The possibility of forming a neo-fused porphyrin **52** from bromo neo-confused porphyrin **36a** was investigated (Scheme 17). A second bromination at the inner carbon seemed to be beneficial for the ring fusing process that leads to N-fused porphyrins and the same strategy was attempted for the neo-confused series. Bromo neo-confused porphyrin **36a** was treated with 1 equivalent of *N*-bromosuccinimide (NBS) for 5 minutes at room temperature, followed by refluxing in pyridine for 12 hr. However, no ring fused products could be identified. Refluxing bromo neo-confused porphyrin **36a** in pyridine

without first treating it with NBS did not lead to decomposition, but gave back the starting material **36a** rather than the desired fused system **52**.¹⁶ This is surprising as **36a** decomposed when recrystallization was attempted and the system appears to be stabilized under these basic conditions. Nevertheless, the formation of neo-fused porphyrin **52** could not be achieved.



Scheme 17: Attempted synthesis of neo-fused porphyrin **52**



Scheme 18: Synthesis of nickel(II) neo-confused porphyrin **53**

Metalation of bromo neo-confused porphyrin **36a** was also investigated. Although bromo neo-confused porphyrin **36a** appeared to be somewhat unstable and decomposed when heated, when pyridine was used as solvent in an attempt to form neo-fused porphyrin **52**, **36a** appeared to be far more stable. Hence, pyridine was used as the solvent for metalation reaction. Reaction of **36a** with nickel(II) acetate in refluxing pyridine afforded the nickel(II) derivative **53** in 60% yield (Scheme 18).

The proton NMR spectrum for **53** showed that the metal complex had similar diatropic character to the free base form of neo-confused porphyrin **36a**, although the *meso*-protons were shifted slightly further downfield. In addition, the external pyrrolic proton showed up as a singlet because there is no longer an internal CH to couple to this unit. As the internal NH and CH units are no longer present, there are no longer any upfield resonances (Figure 17).

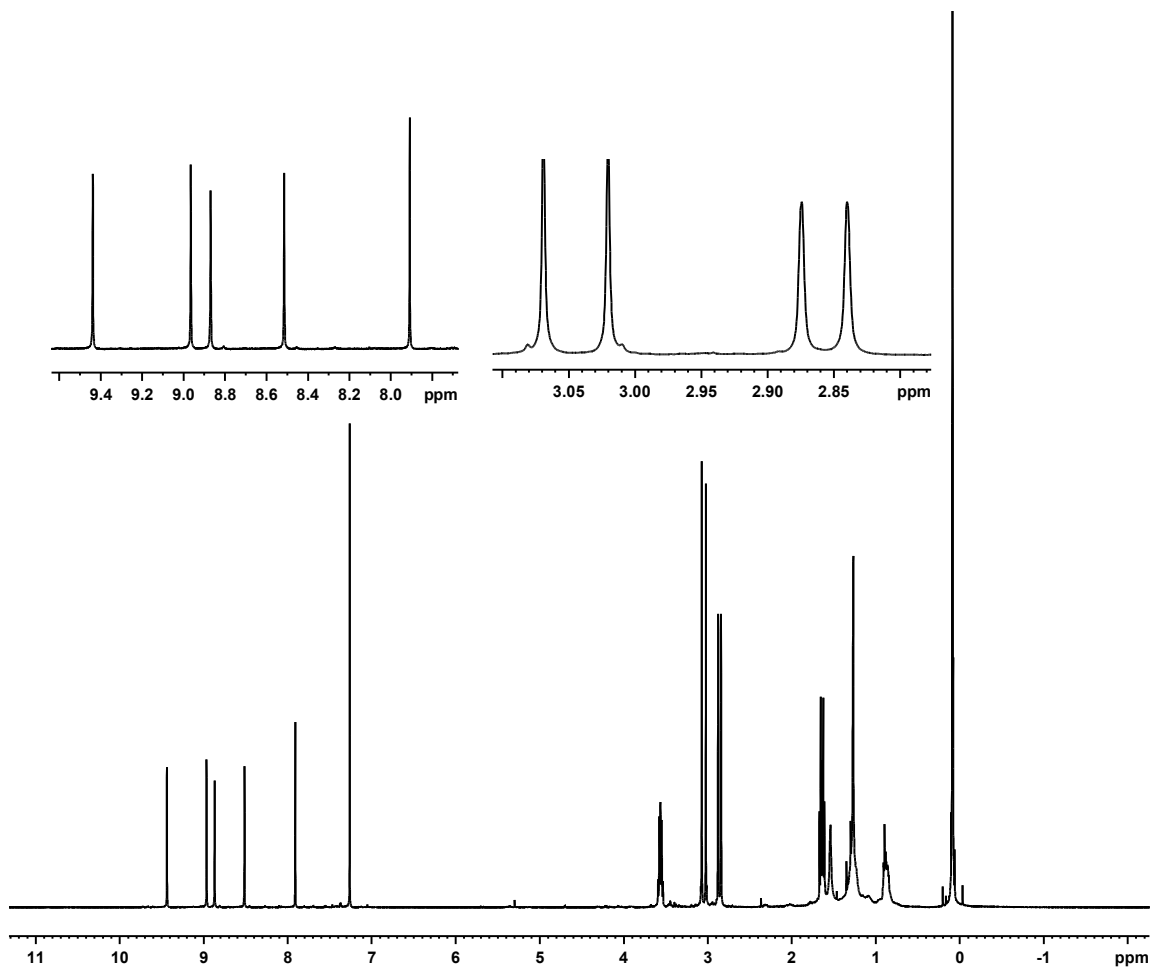


Figure 17: 500 MHz proton NMR spectrum of the nickel(II) complex **53**

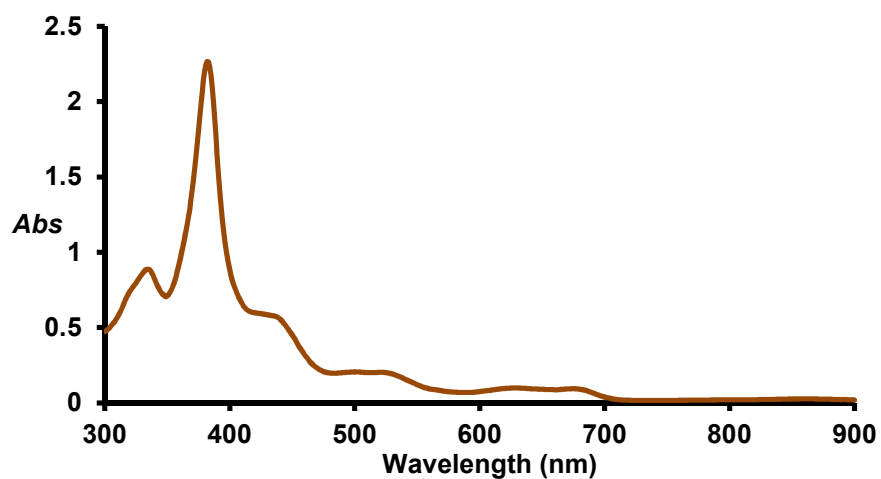
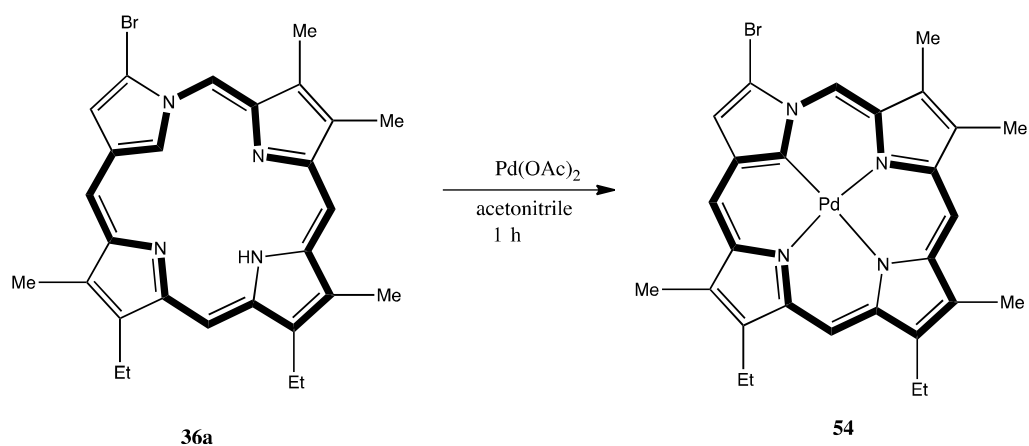


Figure 18: UV-vis spectrum of the nickel(II) complex **53** in CH_2Cl_2

The UV-vis spectrum of the nickel(II) complex of bromo neo-confused porphyrin **53** had similar characteristics to true porphyrins. A strong Soret band was present at 382 nm with several Q bands following at higher wavelengths of 524, 629 and 676 nm (Figure 18).



Scheme 19: Synthesis of the palladium(II) complex **54**

The synthesis of a related palladium(II) complex **54** was also performed. Initial attempts to prepare the palladium complex of bromo neo-confused porphyrin **54** in acetonitrile for 3 hours were unsuccessful. However, when **36a** was reacted with palladium(II) acetate in acetonitrile under reflux for 1 hour, the palladium(II) derivative **54** was isolated as dark green solid in 80% yield (Scheme 19).

The proton NMR spectrum for **54** showed that the palladium complex has slightly increased diamagnetic character compared to bromo neo-confused porphyrin **36a** (Figure 19). The *meso*-protons were observed at 8.63, 8.92, 9.05 and 9.50 ppm, which is shifted slightly downfield compared to the free base **36a**. In addition, the external pyrrolic proton

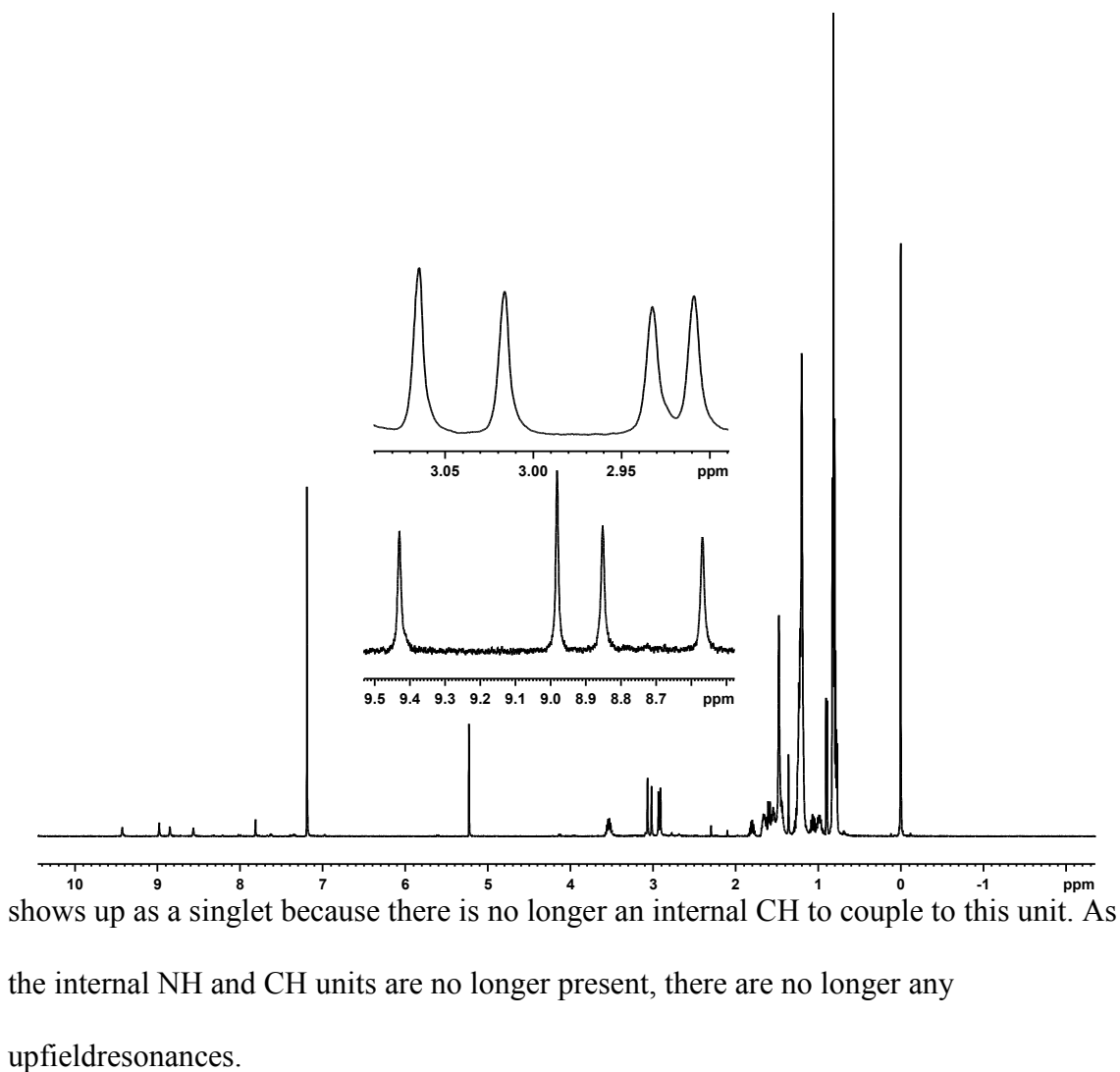


Figure 19: 500 MHz proton NMR spectrum of the palladium(II) complex **54**

The UV-vis spectrum of the palladium(II) complex of bromo neo-confused porphyrin **54** had similar characteristics to true porphyrins. A strong Soret band was present at 370 nm with several Q bands following at higher wavelengths of 500, 531, 602, 646 and 856 nm (Figure 20).

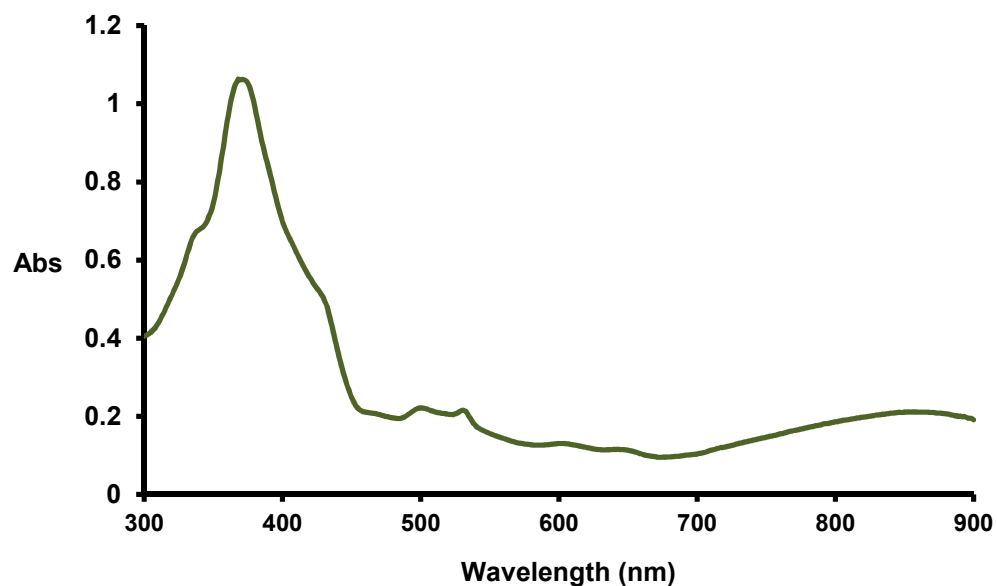
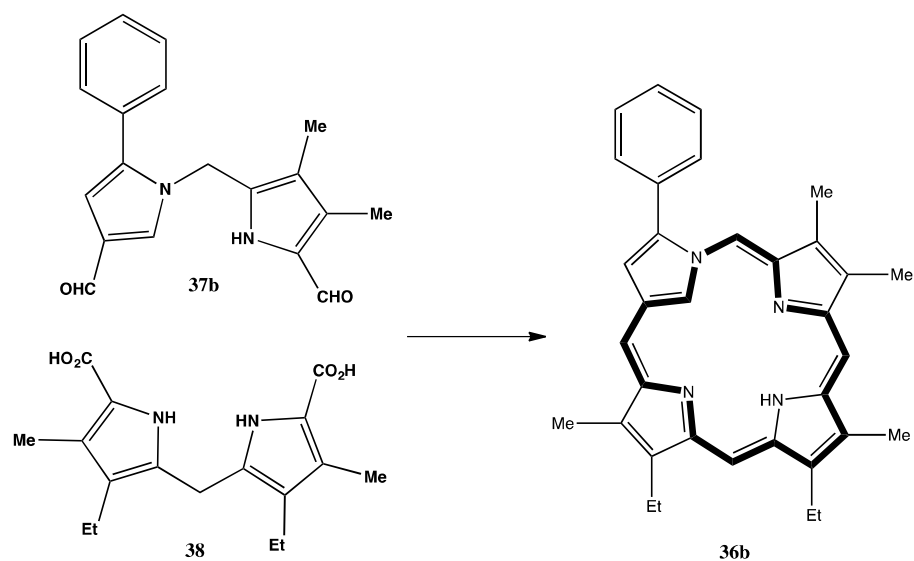
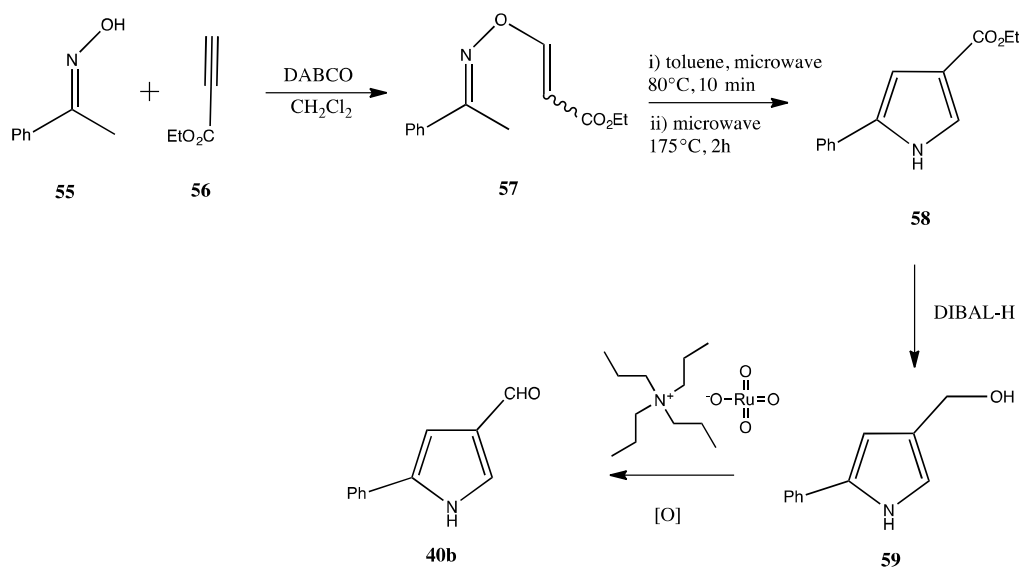


Figure 20: UV-vis spectrum of the palladium(II) complex **54** in CH_2Cl_2

Given the success in synthesizing bromo neo-confused porphyrin **36a**, the synthesis of related phenyl porphyrinoid **36b** was also investigated (Scheme 20).



Scheme 20: Proposed synthesis of phenyl neo-confused porphyrin **36b**

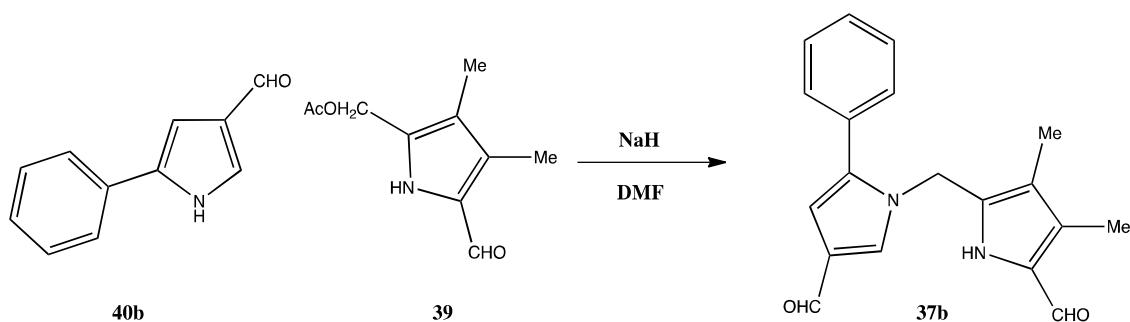


Scheme 21: Synthesis of 5-phenylpyrrole-3-carbaldehyde **40b**

In order to synthesize the phenyl neo-confused porphyrin **36b**, it was first necessary to prepare 5-phenylpyrrole-3-carbaldehyde **40b** from acetophenoneoxime**55** (Scheme 21). Acetophenoneoxime**55** was prepared using a literature procedure.²⁵ Reaction of acetophenoneoxime**55** and 1,4-diazabicyclo[2.2.2]octane (DABCO) with ethyl propiolate**56** in dichloromethane at room temperature afforded the vinyl oxime**57** as a mixture of E:Z-alkene isomers in 85% yield (Scheme 21). It was found that the optimal temperature for the formation of vinyl oxime**57** was 80°C.²⁵ The second stage of the synthesis was directed toward the thermal rearrangement of vinyl oxime**57** to phenyl pyrrole ester **58**. At this stage, higher temperatures were required. In previous research, traditional heating did not afford the desired pyrrole **58**.²⁴ In order to overcome the activation barrier for the conversion of vinyl oxime**57** to pyrrole **58**, vinyl oxime**57** was heated up in toluene to 170°C under microwave irradiation for 45 minutes, which gave the vinyl oxime**57** back. Increasing the temperature to 180°C led to decomposition. However, when the temperature was maintained at 175°C and the heating time increased to 2 h, the desired pyrrole **58** was isolated in 84% yield.

| Entry | Solvent/Conditions | Results |
|-------|-----------------------------------|----------------------------------|
| 1 | Toluene, microwave, 170°C, 45 min | Starting material back 57 |
| 2 | Toluene, microwave, 180°C, 45 min | Decomposition |
| 3 | Toluene, microwave, 175°C, 2h | Phenyl pyrrole ester 58 |

Table 1: Thermal rearrangement of vinyl oxime **57** to pyrrole **58**.



Scheme 22: Synthesis of phenyl neo-confused dipyrrolymethanedialdehyde **37b**

The next step involved the reduction of the ester group in phenyl pyrrole ester **58** to an alcohol **59** using DIBAL-H, followed by oxidation using tetra-*n*-propylammonium perruthenate. This gave the desired phenyl pyrrole aldehyde **40b** in 60% yield. Phenyl pyrrole aldehyde **40b** was then reacted with acetoxy methyl pyrrole aldehyde **39** and sodium hydride in DMF at 30°C to give the dipyrrolymethanedialdehyde **37b** in 60% yield (Scheme 22, Figure 21).

Phenyl neo-confused porphyrin **36b** was prepared from dipyrroledialdehyde **37b** and dicarboxylic acid **38** using MacDonald's "2+2" condensation. Following oxidation with 0.2% aqueous FeCl₃ for 1 h, and purification on an alumina column, the neo-confused porphyrin **36b** was isolated as a purple powder in 40% yield (Scheme 23). Attempts to recrystallize **36b** were successful, but resulted in substantial losses due to the relatively high solubility of this compound. The phenyl substituent on the neo-confused dipyrrylmethane **37b** may be responsible of increasing the stability of the system.

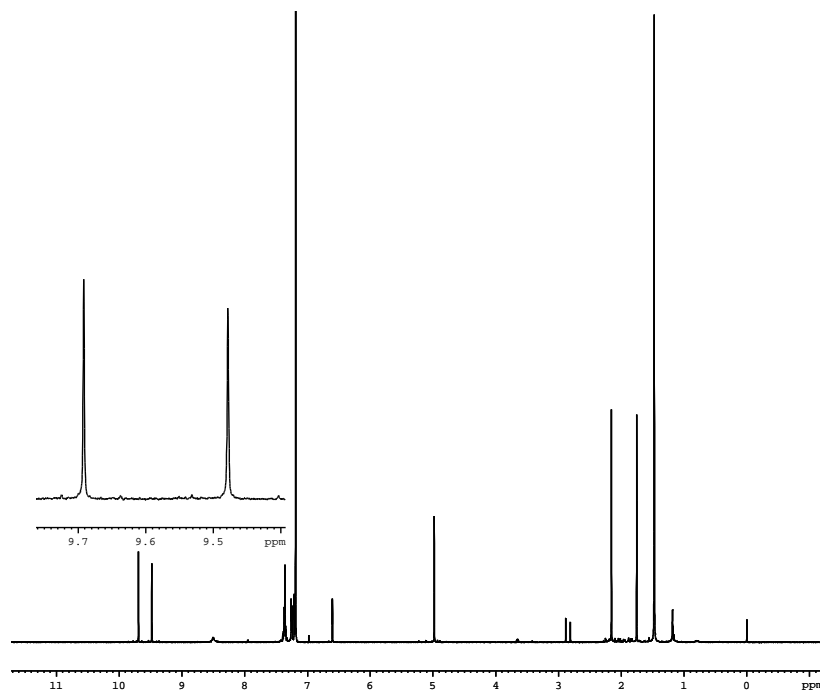
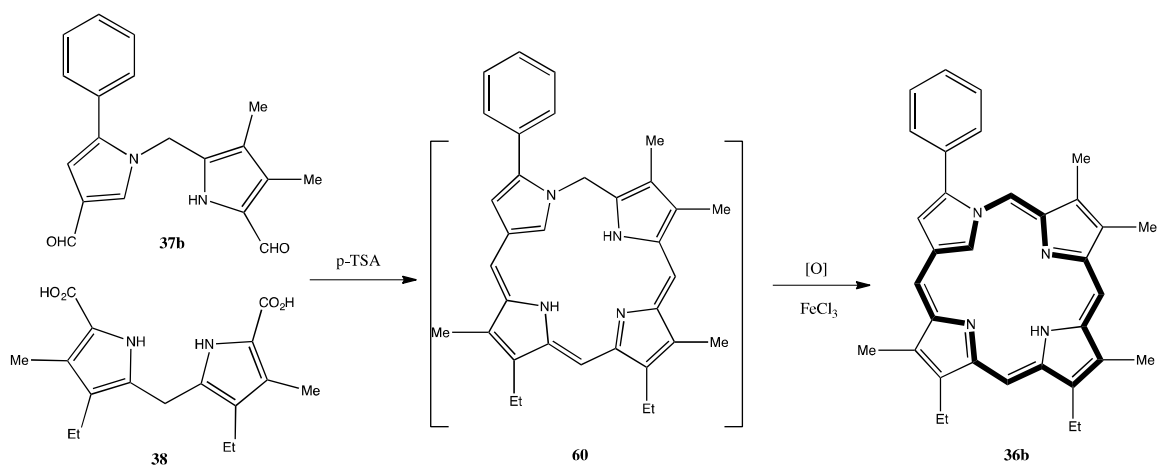


Figure 21: 500 MHz proton NMR spectrum of phenyl neo-confused dipyrrylmethane **37b**



Scheme 23: Synthesis of phenyl neo-confused porphyrin **36b**

The *meso*-protons of **36a** showed up at 8.55, 8.65, 9.12 and 9.41 ppm in the proton NMR spectrum, which was slightly further downfield than had been seen for bromo neo-confused porphyrin **36a**. The external pyrrolic hydrogen was observed at 8.67 ppm. Nevertheless, the internal CH proton gave a peak at 0.057 ppm and the NH showed up at -0.036 ppm, indicating a reduced upfield shift. (Figure 22).

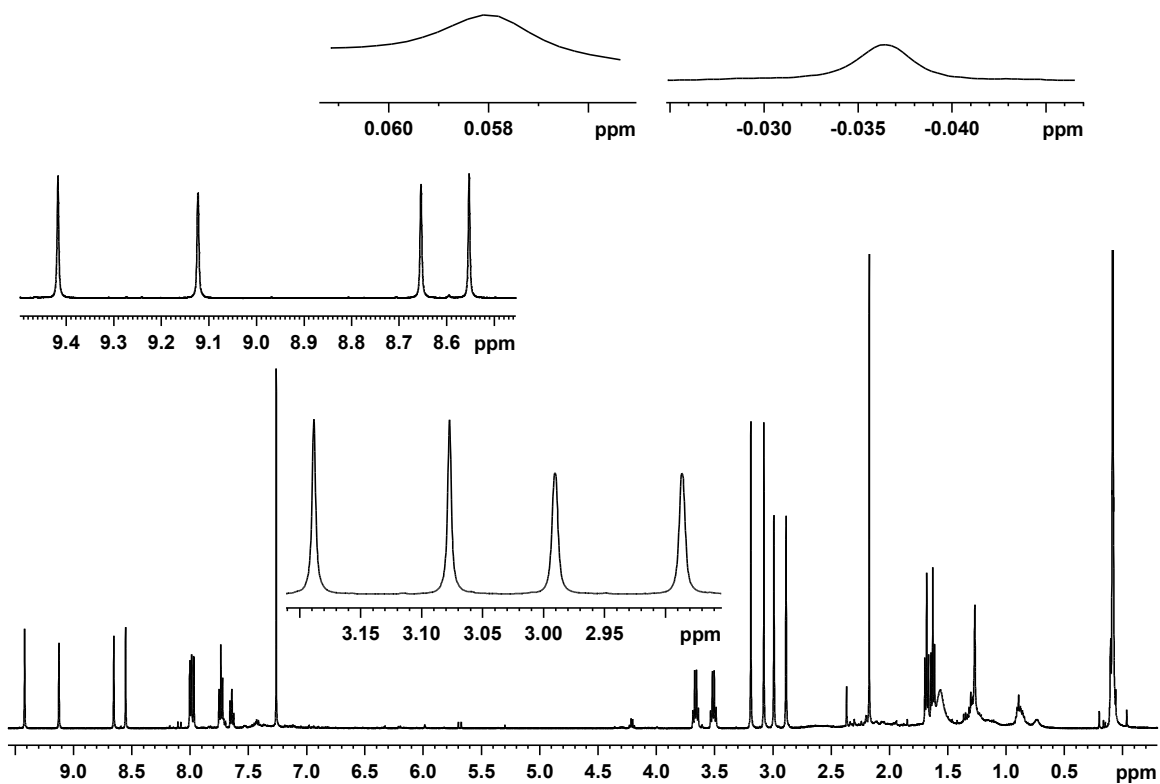


Figure 22: 500 MHz proton NMR spectrum of phenyl neo-confused porphyrin **36b**

The UV-vis spectrum of the phenyl neo-confused porphyrin **36b** had similar characteristics to true porphyrins. A strong Soret band was present at 392 nm with several Q bands following at higher wavelengths of 508, 542, 566, 612 and 682 nm (Figure 23).

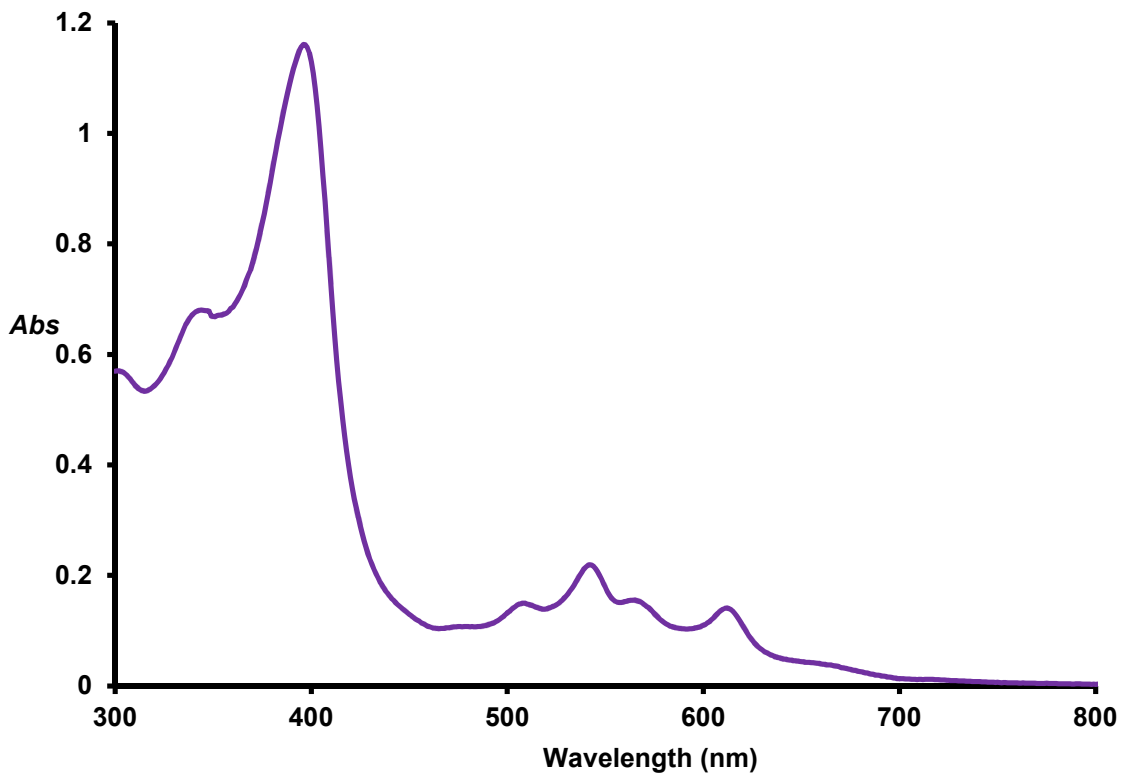


Figure 23: UV-vis spectrum of phenyl neo-confused porphyrin **36b** in CH₂Cl₂

In TFA-CDCl₃, the corresponding dication **36b**H₂²⁺ (Figure 24) showed a substantially enhanced diatropic ring current and the internal CH shifted upfield to -2.79 ppm, while the *meso*-proton resonances moved downfield to give four ¹H singlets at 9.14, 9.22, 9.80 and 9.88 ppm (Figure 25).

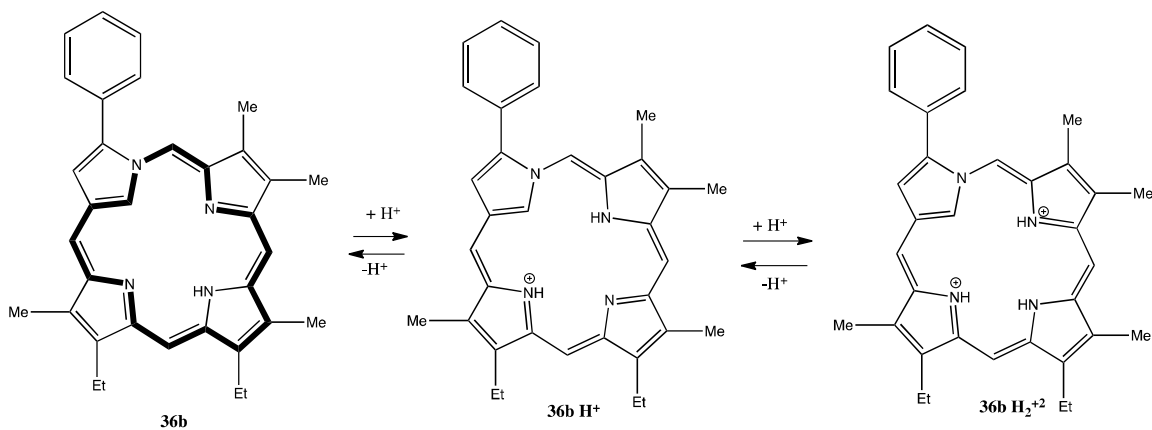


Figure 24: Protonation of phenyl neo-confused porphyrin $36bH_2^{2+}$

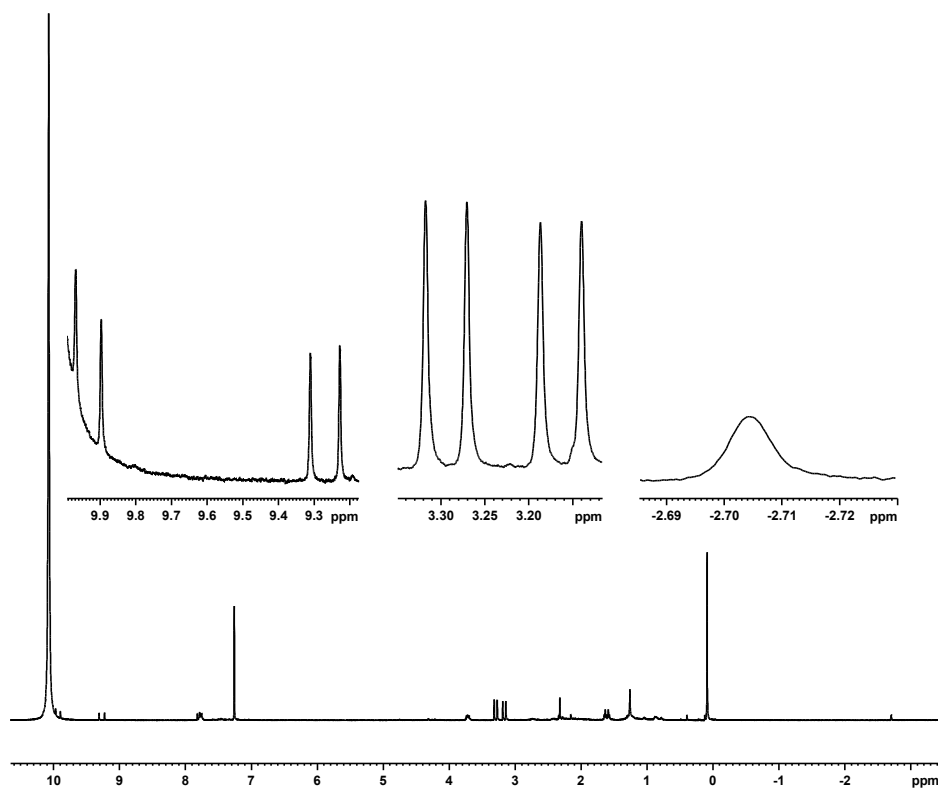


Figure 25: 500 MHz proton NMR spectrum of phenyl neo-confused porphyrin dication $36bH_2^{2+}$ in TFA- $CDCl_3$

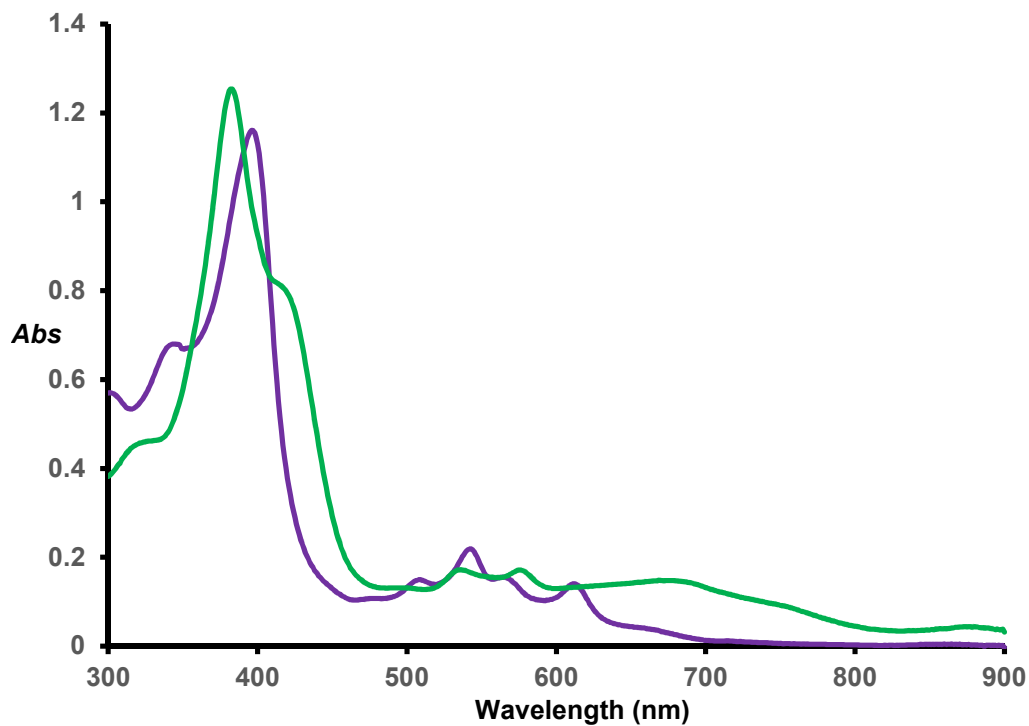
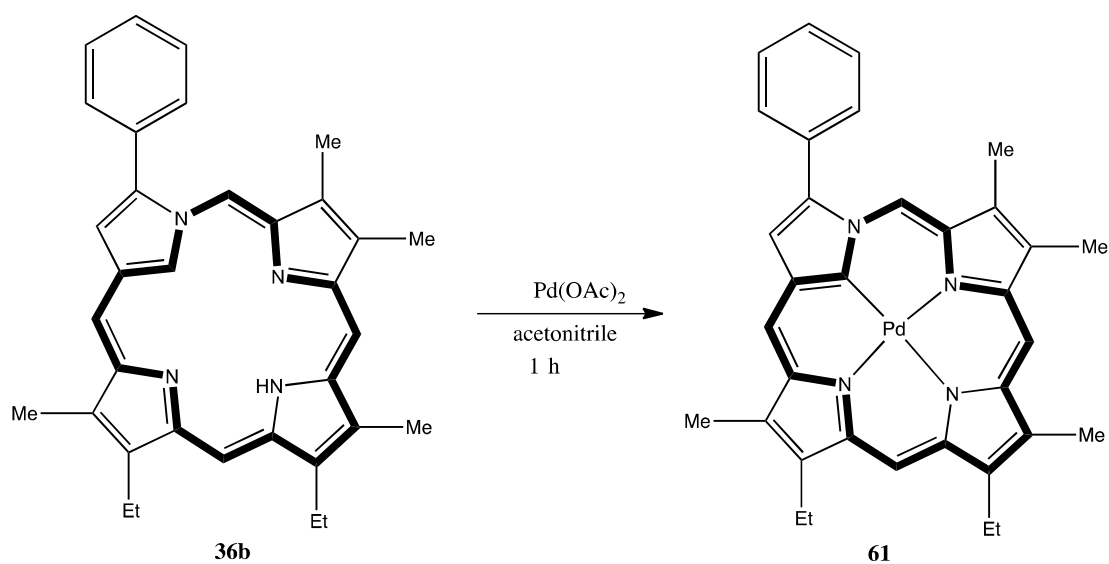


Figure 26: UV-vis spectrum of neo-confused porphyrin **36b** in dichloromethane (purple line) and 2% TFA-CH₂Cl₂ (green line)

The UV-vis spectrum of the phenyl neo-confused porphyrin dication **36b**H₂²⁺ gave a strong Soret band at 382 nm with several Q bands following at higher wavelengths of 536, 576 and 677 nm (Figure 26).

Metalation of phenyl neo-confused porphyrin **36b** was also investigated. Reaction of **36b** with palladium(II) acetate in refluxing acetonitrile for 1 hour afforded the palladium(II) derivative **61** (Scheme 24). The proton NMR spectrum for **61** showed that the metal complex had a slight increase in diatropic character compared to the free base form of neo-confused porphyrin **36b**. The *meso*-protons were shifted slightly downfield. In addition, the external pyrrolic proton showed up as a singlet because there is no longer an internal CH to couple to this unit. As the internal NH and CH units are no longer present, there are no longer any upfield resonances (Figure 27).



Scheme 24: Synthesis of palladium(II) complex **61**

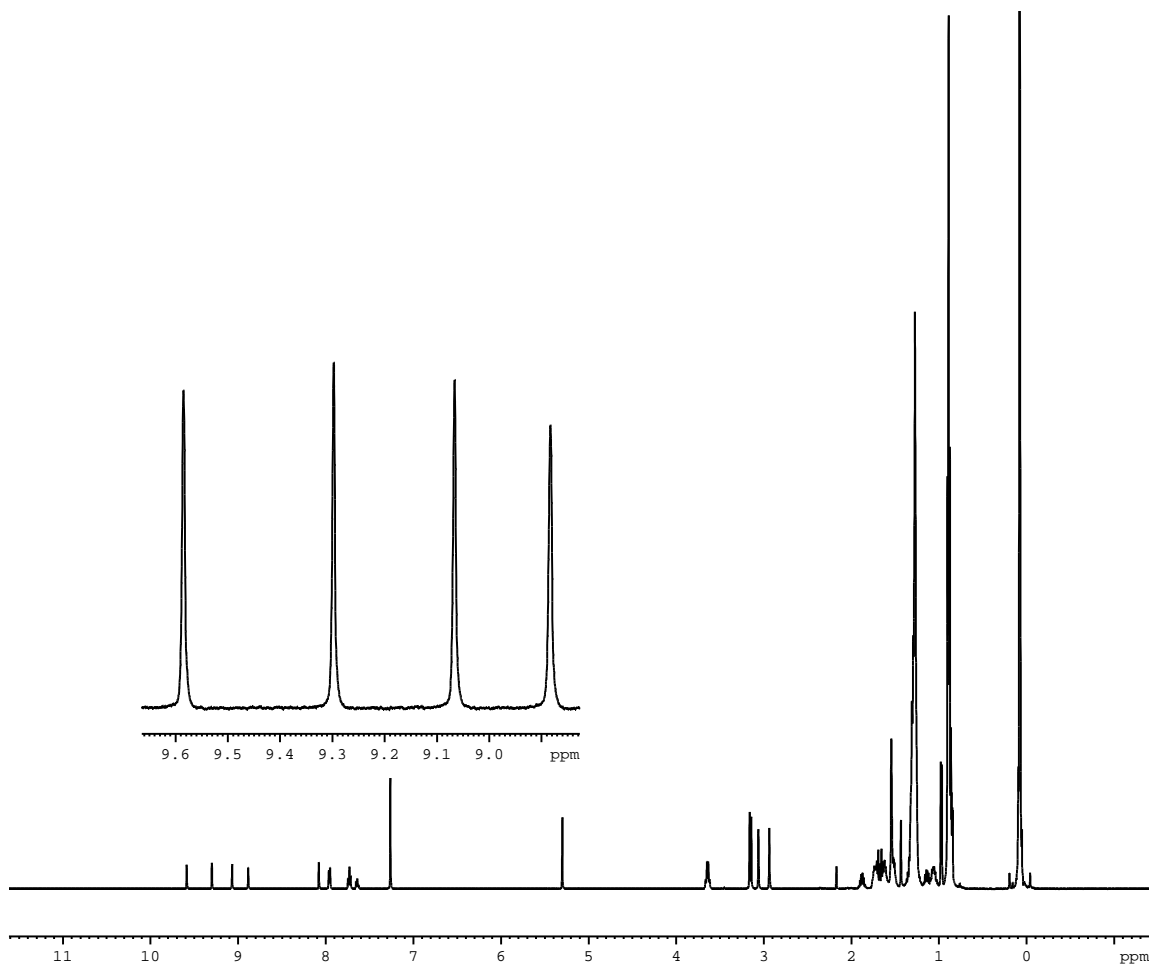
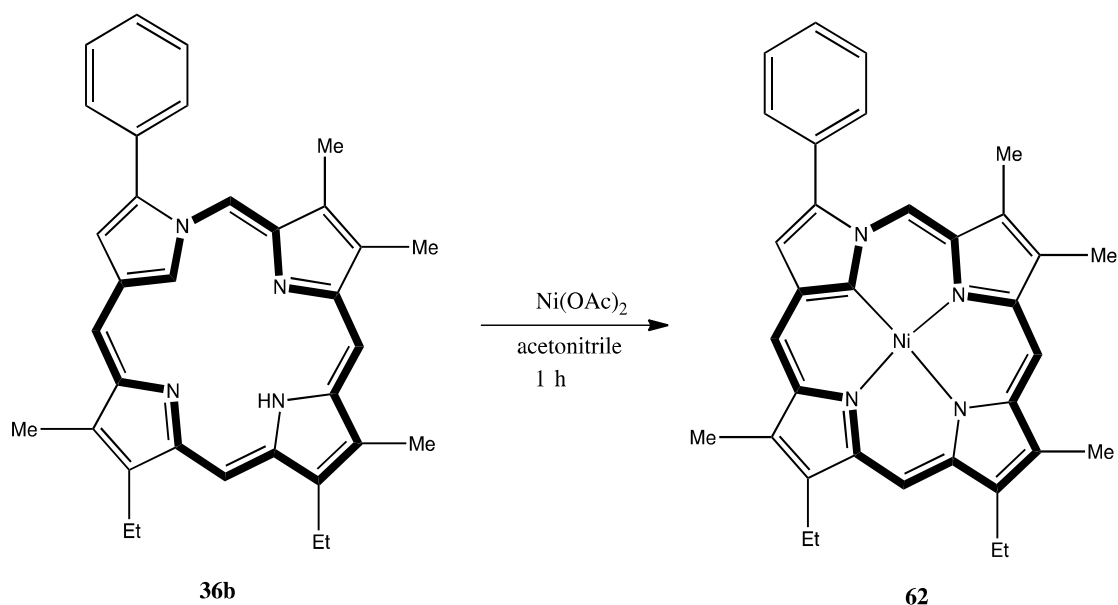


Figure 27: 500 MHz proton NMR spectrum of palladium(II) complex **61** in CDCl_3



Scheme 25: Synthesis of nickel(II) neo-confused porphyrin **62**

The nickel(II) complex of phenyl neo-confused porphyrin **36b** was also investigated. Reaction of **36b** with nickel(II) acetate in refluxing acetonitrile for 1 hour afforded the nickel(II) derivative **62** (Scheme 25). Following purification on an alumina column, the nickel complex **62** was isolated in 60% yield as brown solid. The proton NMR spectrum for **62** showed that the metal complex had similar diatropic character to the free base form of neo-confused porphyrin **36b**, although the *meso*-protons were shifted slightly upfield. In addition, the external pyrrolic proton shows up as a singlet because there is no longer an internal CH to couple to this unit. As the internal NH and CH units are no longer present, there are no longer any upfield resonances (Figure 28).

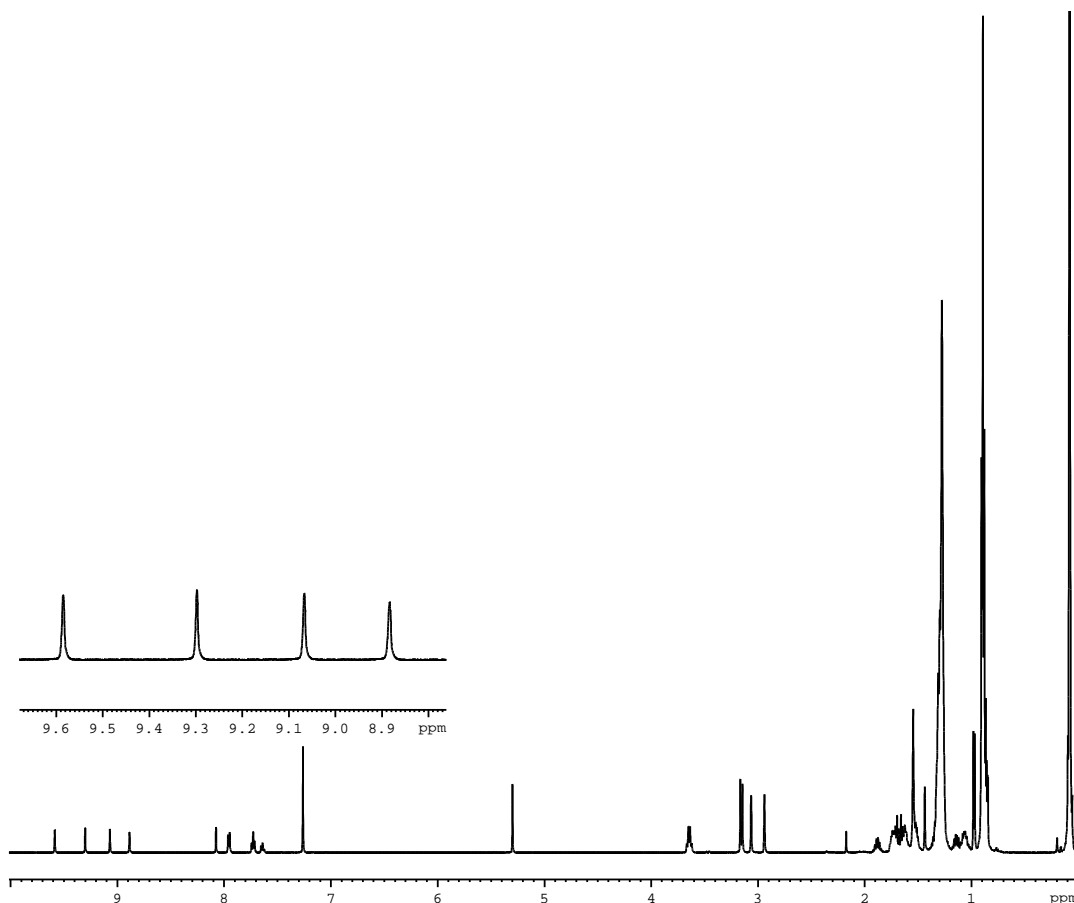
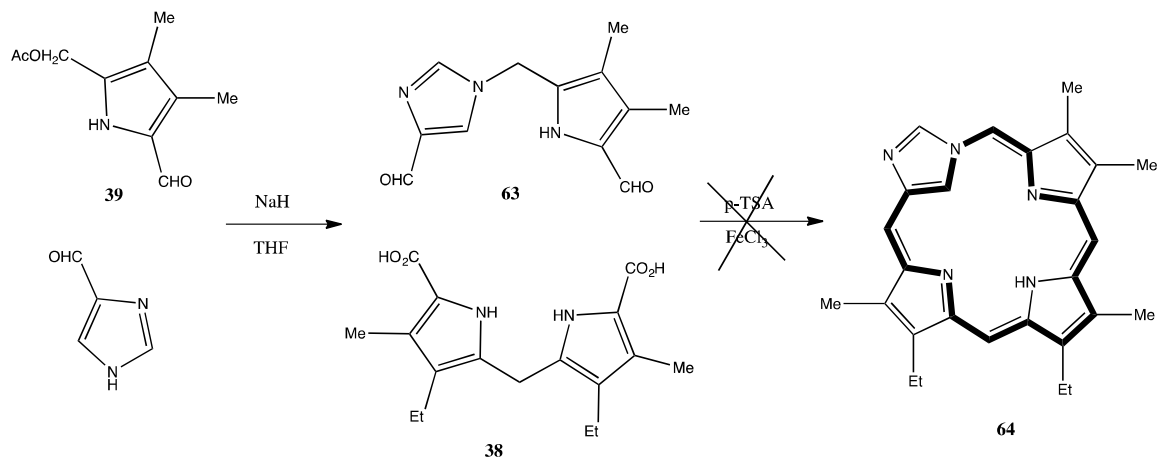


Figure 28: 500 MHz proton NMR spectrum of nickel(II) complex **62** in CDCl_3

The synthesis of an interesting aza-neo-confused system was also targeted (Scheme 26). In this system, the neo-confused pyrrole unit has been replaced by an imidazole moiety. Initially, commercially available imidazole-3-carbaldehyde and acetoxymethylpyrrole aldehyde **39** were reacted with NaH in DMF, but this did not give the desired dipyrroledialdehyde **63**. However, when THF was used as a solvent instead of DMF, pyrrolylmethylimidazoledialdehyde **63** as shown by proton NMR (Figure 29) was isolated in 60% yield. Azadipyrrolymethanedialdehyde **63** was reacted with

dipyrromethanedicarboxylic acid **38** in the presence of *p*-toluenesulfonic acid using MacDonald's "2+2" condensation method, followed by an oxidation step. However, no macrocyclic products could be identified (Scheme 26).



Scheme 26: Attempted synthesis of aza neo-confused porphyrin **64**

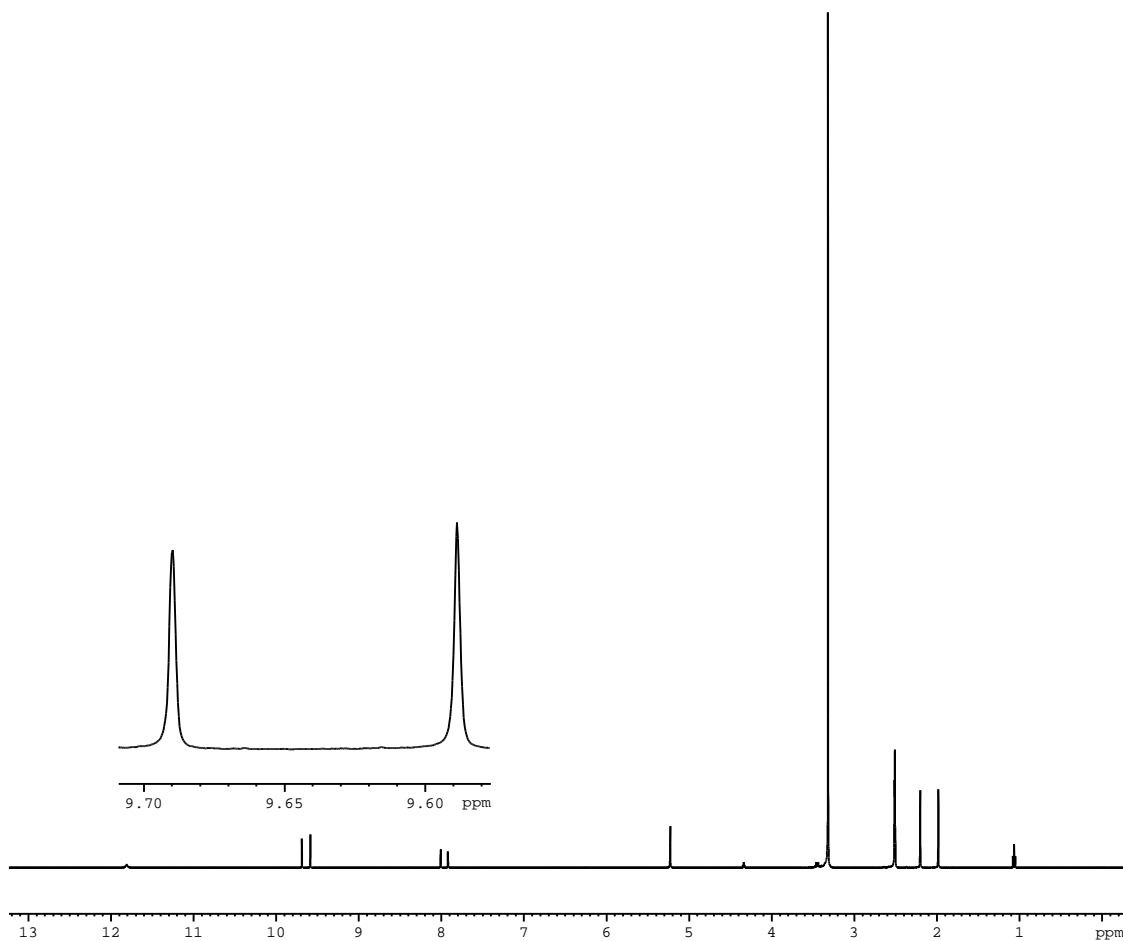
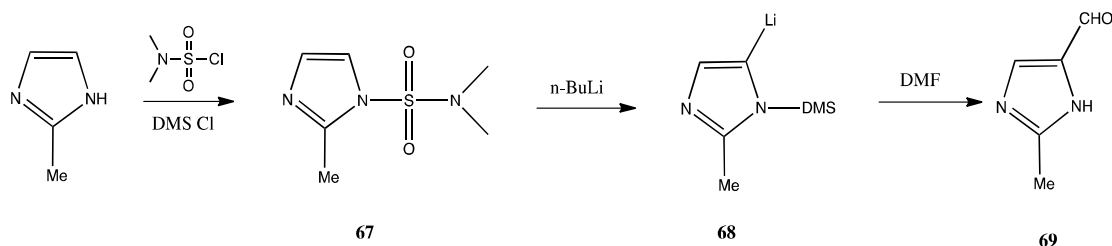


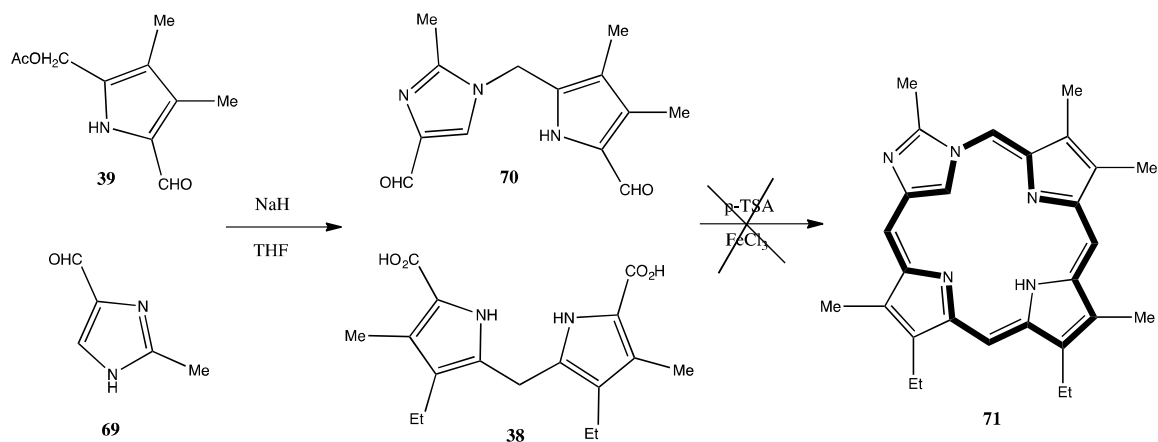
Figure 29: 500 MHz proton NMR spectrum of aza neo-confused dipyrromethane**63** in CDCl₃

In an attempt to increase the reactivity of the aza neo-confused dipyrromethane, a methyl-substituted imidazole aldehyde **69** was also targeted. The synthesis of methyl imidazole aldehyde **69** initially involved a protection step where 2-methyl imidazole was reacted with dimethylsulfamoyl chloride to give **67**. Subsequent treatment with *n*-butyllithium, followed by addition of DMF and hydrolysis, afforded the deprotected aldehyde **69** (Scheme 27).²⁶



Scheme 27: Synthesis of methyl formyl imidazole **69**

Aldehyde **69** was reacted with acetoxyethylpyrrolealdehyde³⁹ and NaH in THF, which successfully gave the methyl aza neo-confused dipyrromethane⁷⁰ as shown by NMR in 65% yield (Figure 30). The dialdehyde⁷⁰ and dicarboxylic acid **38** were reacted in the presence of *p*-toluenesulfonic acid, followed by oxidation with FeCl₃ (Scheme 28). Alternative condensation conditions were also investigated. Unfortunately, all attempts to synthesize aza-neo-confused porphyrin **71** were unsuccessful. It is unclear why the problem was encountered, but it may be that aza neo-confused porphyrins are unstable.



Scheme 28: Attempted synthesis of methyl aza neo-confused porphyrin **71**

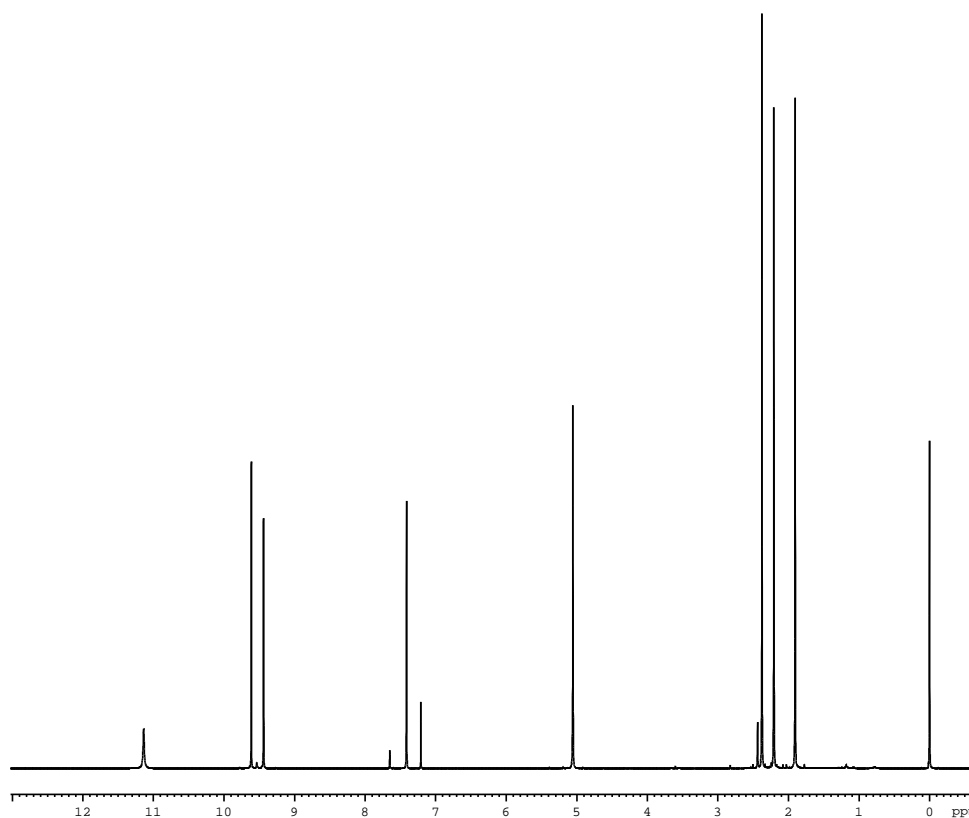


Figure 30: 500 MHz proton NMR spectrum of methyl aza neo-confused dipyrromethane **70** in CDCl₃

Conclusions

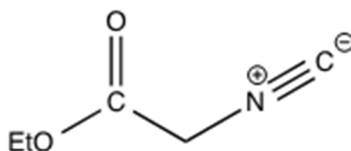
Two examples of neo-confused porphyrins have been synthesized in good yields. These neo-confused porphyrins were shown to retain aromatic character, but this was somewhat reduced compared to benzo-fused neo-confused porphyrins. The observed diatropic character is believed to be due to the presence of a 17-atom 18π electron delocalization pathway. The UV-vis spectra for neo-confused porphyrins also gave porphyrin-like characteristics with a strong Soret band and several Q absorptions. Addition of TFA to solutions of neo-confused porphyrins led to the formation of diprotonated dicationic species that exhibited greatly enhanced diatropicity. Reaction with nickel(II) or palladium(II) acetate gave nickel(II) or palladium(II) organometallic derivatives, and these showed similar diatropic character to free base neo-confused porphyrins. The synthesis of aza neo-confused porphyrins **64** and **71** have also been investigated, but no macrocyclic products could be isolated. It remains to be seen whether this type of neo-confused porphyrin can be accessed by the “2+2” methodology. However, the results from this study demonstrate that neo-confused porphyrins have unique spectroscopic properties. Therefore, this work provides the foundations for further studies into these interesting porphyrin analogues.

CHAPTER III

EXPERIMENTAL

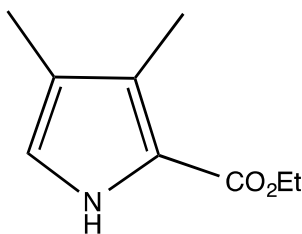
All chemicals were purchased from Acros Organic or Sigma Aldrich. Silica gel and grade III basic alumina were used for column chromatography. All ^1H and ^{13}C NMR spectra were obtained on a BrukerAvance III 400 or 500 MHz NMR spectrometer at 25 °C. Chemical shifts were recorded in parts per million (ppm) relative to CDCl_3 (residual chloroform at δ 7.26 ppm) in proton NMR spectra and the CDCl_3 triplet at δ 77.23 ppm in carbon-13 NMR spectra; for d_6 -DMSO, the proton NMR spectrum was calculated relative to the d_5 -DMSO pentet at 2.51 ppm, while the septet at 39.5 ppm was used as a standard for carbon-13 NMR. UV-Vis spectra were collected on a Cary 100 Bio spectrophotometer. Melting points were collected with a Mel-Temp apparatus. Mass spectrometry data were obtained from the Laboratory for Biological Mass Spectrometry at Texas A&M University.

Ethyl Isocynoacetate(42)



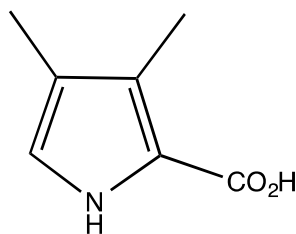
N-Formylglycine ethyl ester (70 g, 0.618 moles), triethylamine (135 g, 1.33 moles), and dichloromethane (550 ml) were placed in 2 L three neck round bottom flask, and was purged with nitrogen and cooled down to 0°C with the aid of a salt-ice bath. Freshly distilled phosphorus oxychloride (81.8 g) was added dropwise to the solution, keeping the temperature at 0-2 °C, and the mixture was stirred for a further 1 h. Sodium carbonate (106 g in 425 ml of water) was added dropwise to the mixture, maintaining the temperature below 25°C. Water was added to bring the total aqueous layer to a volume of 1 L, and two layers separated. The aqueous layer was back extracted with dichloromethane (2 × 250 ml). The combined organic layers were washed twice with brine and dried over potassium carbonate. The solvent was removed under vacuum and the residue was vacuum distilled to yield ethyl isocynoacetate (36.50 g, 0.322 mol, 60.4 %) as a yellow oil, bp 95-100 °C at 20 mmHg; ¹H NMR (500 MHz, CDCl₃): δ 1.28 (3H, t, -CH₂CH₃), 4.15 (2H, s, -CH₂CH₃), 4.25 (2H, q, -OCH₂).

Ethyl 3,4-dimethylpyrrole-2-carboxylate (44)



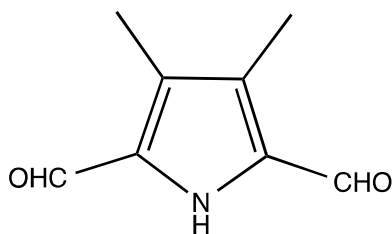
In a round bottom flask was placed ethyl isocyanoacetate (74 g, 0.654 mol), and tetramethylguanidine (150 g, 1.30 mol). After the flask was cooled in an ice-water bath, a solution of 3-acetoxy-2-nitrobutane (100 g, 0.62 mol) in THF (100 ml) and 2-propanol (100 ml) was added dropwise over 30 min at 0°C. The mixture was stirred at room temperature for 20 h. The solvent was removed under reduced pressure. The residue was taken up by dichloromethane (1250 ml) and washed with water (3× 200 ml), 5% HCl (3× 200 ml), water (200 ml), saturated sodium bicarbonate (200 ml) and saturated sodium chloride (200 ml). After drying over sodium sulfate and evaporating the solvent under vacuum, the residue was crystallized from dichloroethane/hexane to afford the pyrrole (50.82 g, 0.303 mol, 49%) as a white solid, mp 93-95 °C (lit. mp 94-95 °C). ¹H NMR (500 MHz, CDCl₃): δ 1.36 (t, 3H, *J* = 7.4 Hz), 2.01 (s, 3 H), 2.27 (s, 3H), 4.33 (q, *J* = 7.4 Hz), 6.65 (d, *J* = 2.91 Hz), 8.73 (s, NH) ppm.

3,4-Dimethylpyrrole-2-carboxylic acid (45)



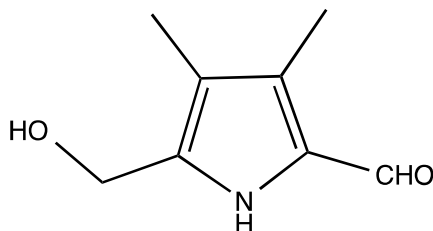
Ethyl 3,4-dimethylpyrrole-2-carboxylate (3.6 g, 0.02 mol) was suspended in 2 ml of 95% ethanol, then a 30% solution of potassium hydroxide (400 ml) was added. The mixture was stirred at reflux for 2 h, and then cooled down to room temperature and placed in ice-water bath. To the resulting brown solution, concentrated HCl was added dropwise, keeping the temperature below 10°C, to give white precipitate. After filtration, the white solid was washed with water ($\times 10$) to remove all traces of acid. The white solid was vacuum dried to give the carboxylic acid (2.99 g, 0.021 mol, 96%). ^1H NMR (500 MHz, acetone- d_6): δ 1.95 (s, 3H), 2.11 (s, 3H), 6.61 (d, 1H, $J = 3.0$ Hz), 10.06 (s, 1H) ppm.

3,4-Dimethyl-2,5-pyrroledicarbaldehyde (46)



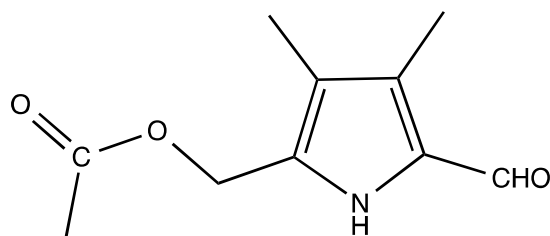
3,4-Dimethylpyrrole-2-carboxylic acid (2.00 g, 0.014 mol) was dissolved in THF (30 ml) and purged with N₂ for 5 min in the dark while cooling the flask in a salt-ice bath. When the solution reached -5°C, triethylorthoformate (32 ml) was added quickly, keeping the temperature below 10°C. After the mixture stirred at 10°C for 1 h, the mixture was poured into water (100 ml). The solution was neutralized by the addition of sodium hydroxide (20 g in 80 ml water). The mixture was extracted with dichloromethane (×4) and the combined organic layers were washed with brine and dried over magnesium sulfate. The solvent was removed under reduced pressure, and residue was recrystallized from chloroform/hexanes to afford the dialdehyde (1.95 g, 12.9 mmol, 97.3%) as a brown solid, mp 157-159°C (lit. mp²¹ 157-158 °C). ¹H NMR (500 MHz, CDCl₃): δ 2.24 (6H, s), 9.41 (2H, s), 9.86 (1H, br) ppm.

5-Hydroxymethyl-3,4-dimethylpyrrole-2-carbaldehyde (47)



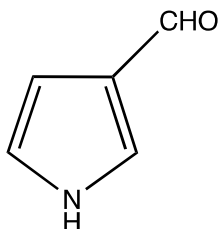
A solution of 3,4-dimethylpyrrole-2,5-dicarbaldehyde (564 mg, 3.73 mmol) in methanol (18 ml) was cooled to 0°C in an ice-salt bath. Sodium borohydride (36 mg, 0.93 mmol) was added and the mixture was allowed to stir for 10 min. Brine (21 ml) was added and the mixture stirred for 15 min. The mixture was extracted with ethyl acetate (×5), and the combined organic layers were dried over MgSO₄. After filtration and evaporation of the solvent, the residue was recrystallized from chloroform/hexanes to give the carbinol (560 mg, 3.66 mmol, 98%), mp 125-126 °C; ¹H NMR (500 MHz, CDCl₃): δ 1.89 (3H, s), 2.19 (3H, s), 3.43 (1H, br), 4.66 (2H, s), 9.38 (1H, s), 10.08 (1H, br) ppm.

5-Acetoxymethyl-3,4-dimethylpyrrole-2-carbaldehyde (39)



Acetic anhydride (7.5 mL) was added to a solution of the foregoing pyrrole carbinol (350 mg, 2.28 mmol) in pyridine (7.5 mL) at -3°C using a salt-ice bath, and the mixture was stirred for 1 h. The mixture was dispersed between dichloromethane and water, and the organic layer was separated. The aqueous layer was further extracted with dichloromethane (x 3) and the combined organic solutions were dried over sodium sulfate. The solvent was removed under reduced pressure and the dark brown residue was recrystallized from chloroform-hexane to give the acetoxymethylpyrrole (380 mg, 1.94 mmol, 85% yield) as a brown solid, mp $123\text{-}124^{\circ}\text{C}$; $^1\text{H NMR}$ (500 MHz, CDCl_3): δ 1.95 (3H, s), 2.01 (3H, s), 2.19 (3H, s), 4.98 (2H, s), 9.14 (1H, br), 9.54 (1H, s) ppm.

Pyrrole-3-carboxaldehyde (49)

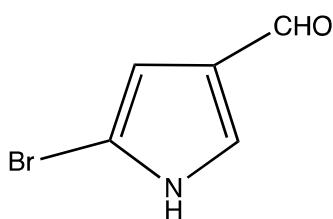


To a suspension of sodium hydride (60% in mineral oil, 13.7g, 285 mmol) in THF (450 ml) was slowly added pyrrole (17.4 g, 259 mmol) at 0° C. The mixture was stirred at the same temperature for 1.5 h. Triisopropylsilylchloride (50 g, 259 mmol) was added to the mixture slowly at 0° C. The mixture was then stirred for another 1.5 h. Ice water (20 ml) was added, and the mixture was extracted with diethyl ether. The extract was washed with water, dried over anhydrous sodium sulfate and concentrated under reduced pressure to give 1-(triisopropylsilyl)pyrroles (57 g, 0.255 mol, quantitative yield).

A solution of 1-(triisopropylsilyl)pyrrole (25.0 g, 112 mmol) in dichloromethane (20 ml) was added to a stirred mixture of DMF (10 ml, 129 mmol) and oxalyl chloride (10.0 ml, 118 mmol) in dichloromethane (510 ml) at 0 °C. The mixture then was placed in an oil bath preheated to 60° C. The solid dissolved for a moment then formed again. The mixture was refluxed for 30 min, then cooled to 0° C, and the resulting precipitate was collected by filtration. The solid was washed with dry ether several times, then vacuum dried to give N,N-dimethylpyrrole-3-formiminium chloride as a white powder (17.0 g, 97%). This material was taken on to the next step without further purification. N,N-dimethylpyrrole-3-formiminium chloride (2.10 g, 13.2 mmol) was added to a 5% sodium hydroxide solution (200 ml) and the mixture stirred at room temperature for 4 h. The solution was extracted with dichloromethane, dried over potassium carbonate and

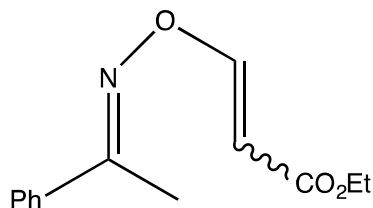
concentrated under reduced pressure. The residue was purified by flash chromatography on silica gel, using hexanes/ethyl acetate (3:1 to 1:1) as the eluent, to yield pyrrole-3-carboxaldehyde (9.4 g, 0.099 mol, 38%) as a brown solid, mp 62-64° C (lit. mp²⁴ 60-61 °C). ¹H NMR □□6.61 (1H, m), 6.78 (1H, m), 6.93 (1H, dd), 9.59 (1H, br), 9.74 (1H, s) ppm.

5-Bromopyrrole-3-carbaldehyde (40a)



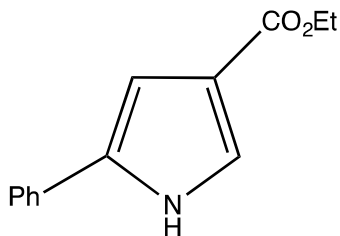
To a solution of pyrrole-3-carboxaldehyde (0.88 g, 9.25 mmol) in THF (13.82 ml) was slowly added a solution of NBS (1.64 g) in DMF (4.60 ml) while maintaining the temperature at -70 °C with the aid of a dry ice-acetone bath, and the mixture was stirred at the same temperature for 1 h and then allowed to warm to -10 °C over 2 h. After the mixture was stirred at the same temperature for 30 min, ice-water was added and the mixture was extracted with ethyl acetate. The extract was washed with an aqueous citric acid solution (10%), sodium bicarbonate (6%) and brine, dried over anhydrous sodium sulfate, and the solvent removed under reduced pressure. The residue was washed with diisopropyl ether (20 ml) to give the bromo pyrrole (0.81 g, 4.6 mmol, 51%) as pale brown solid, mp 124-126°C (lit mp²⁴ 125-128°C). ¹H NMR (500 MHz, CDCl₃) δ 6.59(1H, s), 7.32 (1H, s), 8.94 (1H, br), 9.64 (1H, s) ppm.

Ethyl 3-(1-phenylethylideneaminoxy)acrylate(57)



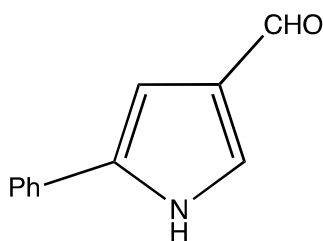
Acetophenoneoxime (800 mg, 5.9 mmol) and 1,4-diazabicyclooctane (72 mg) were dissolved in dichloromethane (16 ml) and stirred to -10°C . At the same temperature, a mixture of ethyl proiolate (0.56 ml) in dichloromethane was added dropwise over 10 min. The reaction was warmed to room temperature and stirred for 20 h. The mixture was concentrated down under reduced pressure and purified by flash chromatography on silica gel using 9:1 petroleum ether/ethyl acetate to give the product (11.04 g, 47.34 mmol, 72%) as a colorless oil. $^1\text{H NMR}$ (500 MHz, CDCl_3) δ 7.69-7.72 (2H, m), 7.40-7.51 (3H, m), 5.71 (1H, d, $J = 12.5$ Hz), 4.23 (2H, q), 2.37 (3H, s), 1.30 (3H, t) ppm.

Ethyl 5-phenylpyrrole-3-carboxylate (58)



A solution of ethyl 3-(1-phenylethylideneaminoxy) acrylate (300 mg, 1.28 mmol) in toluene (7.5 ml) was heated to 175 °C for 2 h under microwave irradiation. The solution was then concentrated down and purified over silica gel (3:1 petroleum ether/ethyl acetate) to yield the pyrrole ester (216 mg, 1.003 mmol, 84%) as an orange oil. ¹H NMR δ 8.83 (1H, br s), 7.47-7.50 (3H, m), 7.37-7.40 (2H, m), 7.24-7.27 (1H, m), 6.91-6.92 (1H, m), 4.31 (2H, q, $J = 7.1$ Hz), 1.38 (3H, t, $J = 7.1$ Hz) ppm.

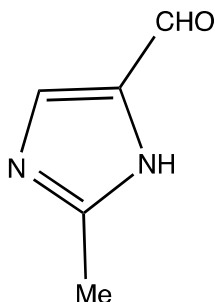
5-Phenylpyrrole-3-carbaldehyde (40b)



To a solution of ethyl 5-phenylpyrrole-3-carboxylate (2.16 g, 10.03 mmol) in THF (100 ml) was added dropwise a 1.0 M solution of DIBAL-H in toluene (24 ml) over 10 min while maintaining the temperature at -78°C , and the mixture was stirred for 1h. After warming the solution to room temperature over 1 h, water (1.4 ml) was added dropwise over 2 min, and stirring was continued for a further 1 h. Celite and magnesium sulfate were added to the mixture, then filtered off and filtrate was evaporated down under reduced pressure to give 5-phenylpyrrole-3-ylmethanol (1.05 g, 6.06 mmol, 85%) as an orange oil. ^1H NMR (500 MHz, DMSO- d_6) δ 4.35 (2H, d, $J = 5.3$ Hz), 4.59 (1H, t, $J = 5.3$ Hz), 6.45-6.46 (1H, m), 6.74-6.75 (1H, br m), 7.11-7.15 (1H, m), 7.31-7.35 (2H, m), 7.57-7.59 (2H, m), 11.04 (1H, brs) ppm. To a solution of foregoing carbinol (1.05 g, 6.06 mmol) in acetonitrile (23.3 ml) was added tetra-*n*-propylammonium perruthenate (0.32 g), *N*-methylmorpholine *N*-oxide (1.64 g), and 4 $^{\circ}\text{A}$ molecular sieves (3.3 g), and the mixture was stirred for 1.5 h. The mixture was filtered off through Celite, and the solvent was evaporated under reduced pressure. The residue was purified on a silica gel column (hexanes/ethyl acetate 4:1) to give the aldehyde (0.60 g, 3.5 mmol, 60%) as a pale yellow solid, mp $138-140^{\circ}\text{C}$ (lit mp²⁴ $137-139^{\circ}\text{C}$). ^1H NMR (CDCl_3) δ 6.88 (1H,

m), 7.21-7.25 (1H, m), 7.33-7.37 (2H, m), 7.40-7.44(3H, m), 8.85 (1H, br), 9.78(1H, s) ppm.

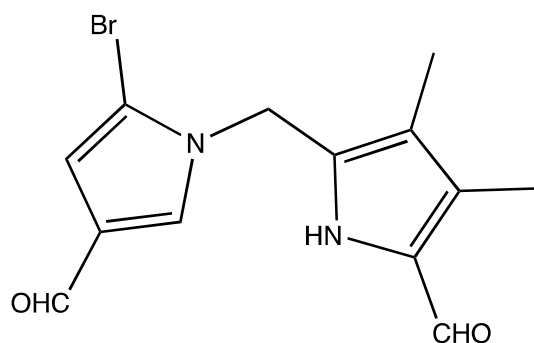
4(5)-Formyl-2-methylimidazole (69)



To a solution of 2-methylimidazole (5.0 g, 0.045 moles) in dichloroethane (70 ml) was added N,N-dimethylsulfamoyl chloride (13 ml) and Et₃N (70 ml), and the mixture was stirred at room temperature for 20 h. After filtration, the solid was washed with dichloroethane, and the combined organic solutions were washed with saturated sodium carbonate, dried over magnesium sulfate, and evaporated down. Distillation (95-110 °C) afforded 2-methyl-1-1-(N,N-dimethylsulfamoyl)imidazole (10.0 g, 52.84 mmol, 90%) as a colorless oil. A solution of the foregoing intermediate (5.5 g) in THF (200 ml) was cooled to -76 °C, *n*-butyllithium (30 ml, 1.6 M in hexanes) was added while keeping the temperature at -76° C. The mixture was stirred at the same temperature for a further 30 min. DMF (21 ml) was added dropwise and the mixture stirred at -78° C for 1 h. The mixture was allowed to warm up to room temperature over 1 h and stirred for 30 min. The pH was adjusted to 1 with concentrated hydrochloric acid, and the resulting mixture was stirred for 2 h. The pH was then adjusted to 8 with saturated NaHCO₃, and the THF

was removed under reduced pressure. The residue was extracted with ethyl acetate (3× 150 ml), the combined organic layers dried over magnesium sulfate, and the solvent evaporated to give the aldehyde (2.6 g, 23.61mmol, 82%) as a faint yellow solid. ¹H NMR (500 Hz, DMSO-d₆) δ 12.06 (1H, br), 9.66 (1H, s), 7.99 (1H, s), 2.54 (3H, s) ppm.

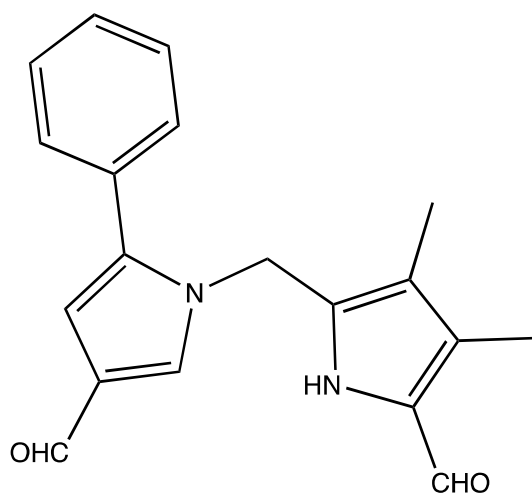
2-Bromo-3',4'-dimethyl-1,2'-dipyrrylmethane-4,5'-dicarbaldehyde (37a)



Sodium hydride (60% in mineral oil, 48 mg, 0.5 mmol) was added to a solution of 5-bromo-3-pyrrolecarbaldehyde (144 mg, 0.827 mmol) in DMF (30 ml) and the mixture was stirred for 30 min at room temperature. To the mixture, a solution of acetoxymethylpyrrole aldehyde³⁹ (171 mg, 0.875 mmol) in DMF (15 ml) was added dropwise over 10 min, and the mixture was stirred for 18 h at 30°C. The mixture was then diluted with ether and washed with water. The aqueous phase was back extracted with ether (x3) and the combined organic layers dried over sodium sulfate. After suction filtration, the solvent was evaporated down under reduced pressure. Recrystallization from ethanol gave the dipyrrolylmethane (190 mg, 0.615 mmol, 65%) as a pale brown solid. mp 196-198° C; ¹H NMR (500 Hz, CDCl₃) δ 1.95 (3H, s), 2.21 (3H, s), 5.01 (2H,

s), 6.63 (1H, d, $J = 1.9$ Hz), 7.15 (1H, d, $J = 1.9$ Hz), 8.98 (1H, br), 9.53 (1H, s), 9.56 (1H, s) ppm. ^{13}C NMR (CDCl_3): δ 8.50, 8.81, 43.88, 105.72, 111.0, 120.34, 126.96, 128.84, 129.50, 130.04, 131.94, 177.65, 184.15 ppm.

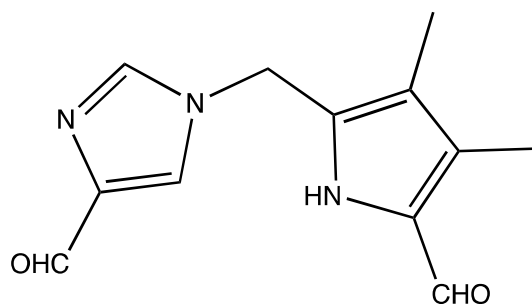
2-Phenyl-3',4'-dimethyl-1,2'-dipyrrylmethane-4,5'-dicarbaldehyde (37b)



Sodium hydride (60% in mineral oil, 44 mg) was added to a solution of 5-phenyl-3-pyrrolicarbaldehyde (147 mg, 0.479 mmol) in DMF (27.55 ml) and the mixture was stirred for 30 min at room temperature. To the mixture, a solution of acetoxymethylpyrrole aldehyde (156 mg, 0.799 mmol) in DMF (13.8 ml) was added dropwise over 10 min, and the mixture was stirred for 18 h at 30°C. The mixture was then diluted with ether and washed with water. The aqueous phase was back extracted with ether (x3) and the combined organic layers dried over sodium sulfate. After suction filtration, the solvent was evaporated down under reduced pressure. Recrystallization from ethanol gave the dipyrrylmethane (185 mg, 0.603 mmol, 60%) as a brown

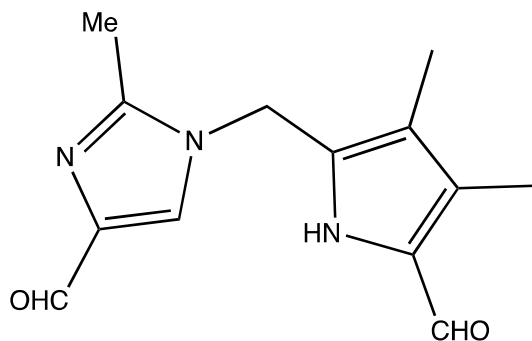
solid, mp 202-204 °C; ¹H NMR (500 Hz, CDCl₃) δ 1.79 (3H, s), 2.15 (3H, s), 5.00 (2H, s), 6.61 (1H, d, *J* = 1.7 Hz), 7.19 (1H, d, *J* = 1.7 Hz), 7.24-7.27 (2H, m), 7.35-7.38 (3H, m), 8.57 (1H, br), 9.47 (1H, s), 9.69 (1H, s) ppm.

1(5-Formyl-3',4'-dimethyl-2-pyrrolylmethyl)imidazole-4-carbaldehyde (63)



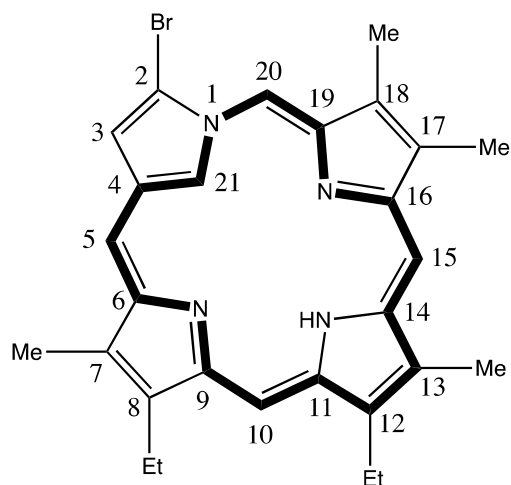
Sodium hydride (60% in mineral oil, 26 mg) was added to a solution of formyl imidazole (87 mg, 0.905 mmol) in THF (16.3 ml) and the mixture was stirred for 30 min at room temperature. To the mixture, a solution of acetoxymethylpyrrole aldehyde (92 mg, 0.471 mmol) in THF (8.2 ml) was added dropwise over 10 min, and the mixture was stirred for 18 h at 30 °C. The mixture was then diluted with ether and washed with water. The aqueous phase was back extracted with ether (x3) and the combined organic layers dried over sodium sulfate. After suction filtration, the solvent was evaporated down under reduced pressure. Recrystallization from ethanol gave the dipyrrolylmethane (109 mg, 0.471 mmol, 60%) as a brown solid, mp 198-200 °C; ¹H NMR (500 Hz, DMSO-d₆) δ 1.98 (3H, s), 2.20 (3H, s), 5.23 (2H, s), 7.92 (1H, s), 8.01 (1H, s), 9.58 (1H, s), 9.69 (1H, s), 11.83 (1H, br) ppm.

1(5-Formyl-3',4'-dimethyl-2-pyrrolylmethyl)2-methylimidazole-4-carbaldehyde (70)



Sodium hydride (60% in mineral oil, 48 mg) was added to a solution of 4(5)-formyl-2-methylimidazole (104 mg, 0.944 mmol) in THF (21.5 ml) and the mixture was stirred for 30 min at room temperature. To the mixture, a solution of acetoxymethylpyrrole aldehyde **39** (122 mg, 0.624 mmol) in THF (10.72 ml) was added dropwise over 10 min, and the mixture was stirred for 18 h at 30°C. The mixture was then diluted with ether and washed with water. The aqueous phase was back extracted with ether (x3) and the combined organic layers dried over sodium sulfate. After suction filtration, the solvent was evaporated down under reduced pressure. Recrystallization from ethanol gave the dipyrrolylmethane (78 mg, 0.320 mmol, 60%) as a brown solid, mp 200-202 °C; ¹H NMR (500 Hz, DMSO-d₆) δ 1.90 (3H, s), 2.20 (3H, s), 2.37 (3H, s), 5.05 (2H, s), 7.20 (1H, s), 7.64 (1H, s), 9.43 (1H, s), 9.60 (1H, s), 11.15 (1H, br) ppm. ¹³C NMR (DMSO-d₆): δ 8.50, 8.91, 13.38, 41.73, 120.25, 126.62, 129.54, 130.50, 140.06, 147.23, 177.96, 185.25.

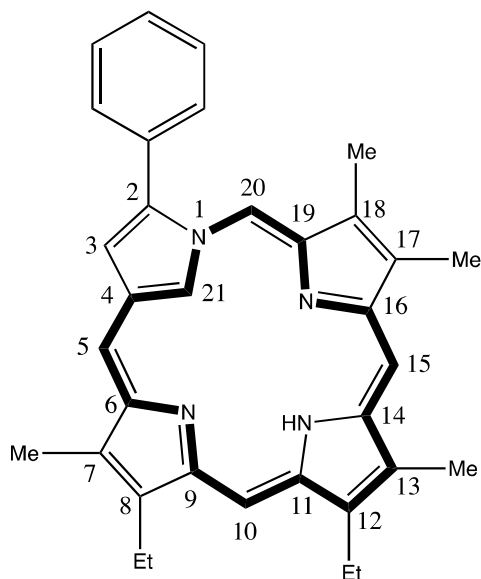
2-Bromo-8,12-diethyl-7,13,17,18-tetramethylneo-confused porphyrin (36a)



p-Toluenesulfonic acid (56 mg) in methanol (6 mL) was added dropwise to a stirred mixture of dialdehyde **37a** (31 mg, 0.10 mmol) and dipyrromethanedicarboxylic acid **38** (32 mg, 0.10 mmol) in dichloromethane (50 mL) and methanol (6 mL). The resulting mixture was allowed to stir for 16 h at room temperature. The solution was shaken with a 0.2% aqueous ferric chloride solution for 1 h to oxidize the phlorin intermediate. The organic phase was separated and the aqueous solution back extracted with dichloromethane. The combined organic solutions were washed with water and 5% aqueous sodium bicarbonate solution, and the solvent was removed under reduced pressure. The residue was purified by column chromatography on grade 3 alumina

eluting with hexanes and dichloromethane (3:1). The neo-confused porphyrin was collected as a pink-purple fraction. Recrystallization from chloroform-hexane gave the neo-confused porphyrin **36a** (20.4 mg, 0.040 mmol, 45%) as a purple powder, mp>300 °C. UV-vis (1% Et₃N-CH₂Cl₂): ϵ_{\max} (log ϵ) 338 (sh, 4.53), 392 (4.81), 508 (3.82), 542 (4.03), 564 (3.74), 613 (3.66), 682 nm (3.75); UV-vis (2% TFA-CH₂Cl₂): ϵ_{\max} (log ϵ) 377 (4.74), 403 (4.75), 533 (3.73), 576 (3.78), 664 nm (3.86). ¹H NMR (500 Hz, CDCl₃) δ 1.25 (1H, s), 1.60 (3H, t, *J* = 7.8 Hz), 1.66 (3H, t, *J* = 7.8 Hz), 2.17 (1H, s), 2.97 (3H, s), 3.00 (3H, s), 3.02 (3H, s), 3.14 (3H, s), 3.47 (2H, q, *J* = 7.8 Hz), 3.64 (2H, q, *J* = 7.8 Hz), 7.91 (1H, d, *J* = 1.6 Hz), 8.46 (1H, s), 8.54 (1H, s), 8.90 (1H, s), 9.46 (1H, s) ppm. ¹H NMR (dication **36a**H₂²⁺, 500 MHz, TFA-CDCl₃) δ -2.28 (1H, s), 1.47 (3H, t, *J* = 7.9 Hz), 1.52 (3H, t, *J* = 7.9 Hz), 3.08 (3H, s), 3.12 (3H, s), 3.15 (3H, s), 3.20 (3H, s), 3.52-3.60 (4H, overlapping quartets), 7.68 (1H, s), 9.00 (1H, s), 9.08 (1H, s), 9.64 (1H, s), 10.03 (1H, s) ppm. ¹³C NMR (500 Hz, CDCl₃) δ 10.82, 16.48, 16.65, 19.14, 93.29, 93.90, 108.91, 110.16, 112.80, 118.57, 119.55, 122.70, 134.80, 135.44, 140.04, 140.78, 141.61, 141.74, 143.10, 161.00 ppm. ¹³C NMR (500 Hz, TFA-CDCl₃) δ 10.76, 11.04, 11.21, 11.60, 15.49, 19.17, 19.47, 94.43, 96.16, 108.81, 114.44, 118.71, 126.01, 132.83, 136.70, 140.07, 142.20, 142.51, 144.16, 146.12, 147.69, 150.68, 154.45 ppm.

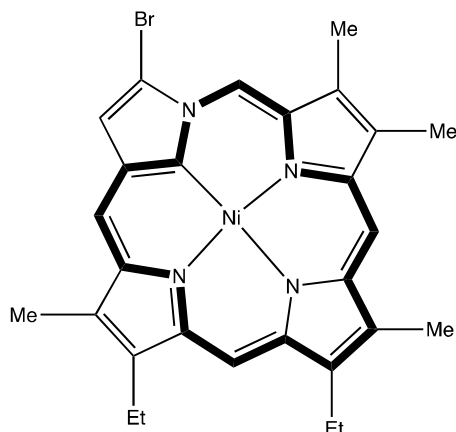
2-Phenyl-8,12-diethyl-7,13,17,18-tetramethylneo-confused porphyrin (36b)



p-Toluenesulfonic acid (56 mg) in methanol (6 mL) was added dropwise to a stirred mixture of dialdehyde **36b** (29 mg, 0.946 mmol) and dipyrromethanedicarboxylic acid **38** (30 mg, 0.942 mmol) in dichloromethane (50 mL) and methanol (6 mL). The resulting mixture was allowed to stir for 16 h at room temperature. The solution was stirred with a 0.2% aqueous ferric chloride solution for 1 h to oxidize the phlorin intermediate. The organic phase was separated and the aqueous solution back extracted with dichloromethane. The combined organic solutions were washed with water and 5% aqueous sodium bicarbonate solution, and the solvent was removed under reduced

pressure. The residue was purified by column chromatography on grade 3 alumina eluting with hexane and dichloromethane (3:1). The neo-confused porphyrin was collected as a pink-purple fraction. Recrystallization from chloroform-hexane gave the neo-confused porphyrin **36b** (19.5 mg, 0.0391 mmol, 40%) as a purple powder, mp>300°C. UV-vis (1% Et₃N-CH₂Cl₂): λ_{\max} (log ϵ) 344 (4.49), 396 (4.72), 508 (3.83), 542 (3.99), 602 (3.84), 612 nm (3.80); UV-vis (2% TFA-CH₂Cl₂): λ_{\max} (log ϵ) 382 (4.75), 417 (sh, 4.56), 536 (3.89), 576 (3.89), 677 nm (3.82). ¹H NMR (500 MHz, CDCl₃) δ 1.23 (1H, s), 1.61 (3H, t, *J* = 7.4 Hz), 1.67 (3H, t, *J* = 7.4 Hz), 2.14 (1H, br), 2.86 (3H, s), 2.79 (3H, s), 3.04 (3H, s), 3.17 (3H, s), 3.50 (2H, q, *J* = 7.7 Hz), 3.66 (2H, q, *J* = 7.7 Hz), 7.58-7.63 (1H, m), 7.69-7.73 (2H, m), 7.93-7.98 (3H, m), 8.54 (1H, s), 8.63 (1H, s), 9.10 (1H, s), 9.40 (1H, s) ppm. ¹H NMR (dication **36b**H₂²⁺, 500 MHz, TFA-CDCl₃) δ -2.78 (1H, s), 1.60 (3H, t, *J* = 7.8 Hz), 1.65 (3H, t, *J* = 7.8 Hz), 3.13 (3H, s), 3.18 (3H, s), 3.27 (3H, s), 3.31 (3H, s), 3.67-3.75 (4H, 2 overlapping quartets), 7.75-7.80 (5H, m), 7.84 (1H, s), 9.22 (1H, s), 9.30 (1H, s), 9.89 (1H, s), 9.96 (1H, s) ppm. ¹³C NMR (500 MHz, CDCl₃): δ 11.1, 16.58, 16.91, 19.29, 92.66, 93.76, 111.44, 114.02, 117.62, 119.90, 122.69, 128.33, 128.90, 131.32, 132.25, 133.59, 135.20, 139.23, 139.73, 140.52, 140.99, 141.47, 142.25, 143.08, 144.01, 153.86, 159.92, 161.33 ppm. ¹³C NMR (500 MHz, TFA-CDCl₃): δ 10.68, 11.04, 11.17, 11.44, 15.47, 19.25, 19.50, 94.39, 95.89, 107.95, 114.35, 114.93, 119.64, 126.14, 128.44, 129.59, 130.40, 131.90, 132.82, 136.61, 139.95, 141.04, 142.13, 142.54, 145.87, 146.79, 147.37, 149.50, 153.41 ppm.

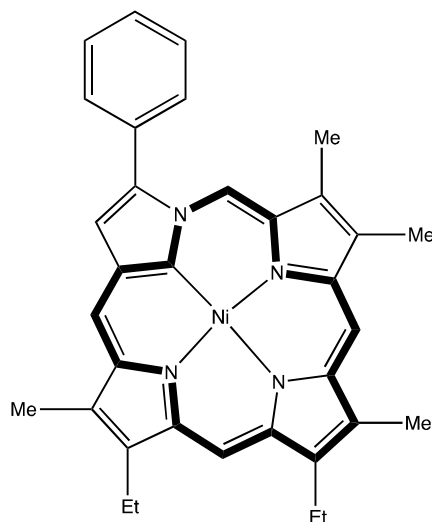
Neo-confused porphyrin nickel complex 53



Neo-confused porphyrin **36a** (15.0 mg, 0.023 mmol) was dissolved in pyridine (15 ml) along with nickel(II) acetate (15.0 mg) and the mixture was stirred under reflux for 1 h. The mixture was diluted with dichloromethane, washed with water and the aqueous solution back extracted with dichloromethane. The combined organic solutions were evaporated under reduced pressure. The residue was purified by column chromatography on grade 3 alumina eluting with 3:1 hexanes/dichloromethane to give the nickel neo-confused porphyrin (10.0 mg, 0.018 mmol, 60%) as a brown powder, mp>300 °C; UV-vis (CH₂Cl₂): λ_{\max} (log ϵ) 334 (4.67), 382 (5.08), 435 (sh, 4.49), 524 (4.03), 629 (3.72), 676 nm (3.69). ¹H NMR (500 Hz, CDCl₃) δ 1.60 (6H, 2 overlapping triplets), 2.91(3H, s),

2.93 (3H, s), 3.01 (3H, s), 3.06 (3H, s), 3.57 (4H, 2 overlapping quartets), 7.81 (1H, s), 8.57 (1H, s), 8.87 (1H, s), 9.43 (1H, s) ppm.

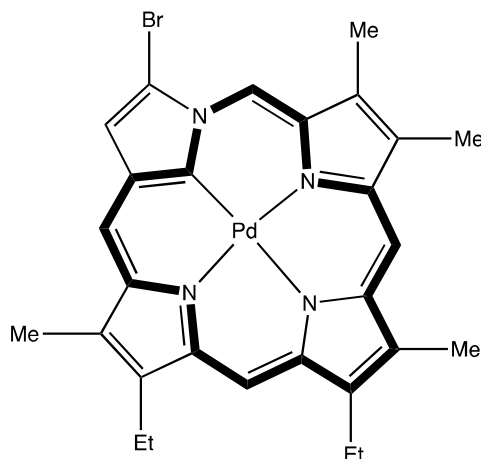
Neo-confused porphyrin nickel complex **62**



Neo-confused porphyrin **36b** (15.0 mg, 0.030 mmol) was dissolved in acetonitrile (15 ml) along with nickel(II) acetate (15.0 mg) and the mixture was stirred under reflux for 1 h. The mixture was diluted with dichloromethane, washed with water and the aqueous solution was back extracted with dichloromethane. The combined dichloromethane solutions was evaporated under reduced pressure, and the residue purified by column chromatography on grade 3 alumina eluting with 3:1 hexanes/dichloromethane to give the nickel neo-confused porphyrin (11 mg, 0.012 mmol, 60%) as a brown powder, mp > 300 °C; ¹H NMR (500 Hz, CDCl₃) δ 1.60 (6H, 2 overlapping triplets), 2.94 (3H, s), 3.06 (3H, s), 3.14 (3H, s), 3.16 (3H, s), 3.64 (4H, q, *J*

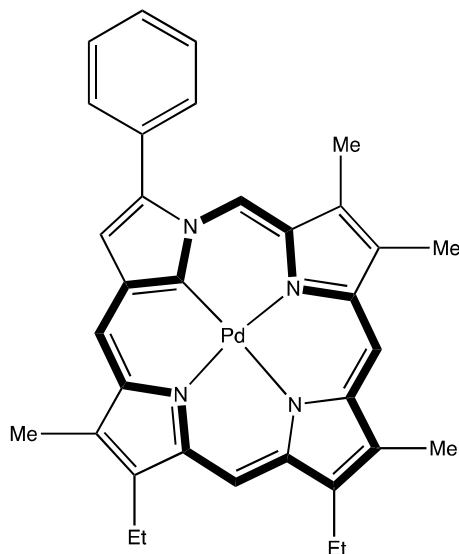
= 7.6 Hz), 7.64 (1H, t, $J = 7.6$ Hz), 7.73 (2H, t, $J = 7.5$ Hz), 7.96 (1H, d, $J = 7.6$ Hz), 8.08 (1H, s), 8.88 (1H, s), 9.06 (1H, s), 9.30 (1H, s), 9.58 (1H, s) ppm.

Neo-confused porphyrin palladium complex⁵⁴



Neo-confused porphyrin **36a** (10.0 mg, 0.019 mmol) was dissolved in acetonitrile (10 ml) along with palladium(II) acetate (10.0 mg) under reflux conditions for 1 h. The mixture was diluted with dichloromethane, and washed with water. The organic solution was evaporated under reduced pressure and the residue was purified by column chromatography on grade 3 alumina eluting with 3:1 hexanes/dichloromethane to give the palladium neo-confused porphyrin (8.0 mg, 0.013 mmol, 80%) as a green solid, mp > 300 °C; UV-vis (CH₂Cl₂): λ_{max} (log ϵ) 370 (4.42), 500 (3.73), 531 (3.72), 602 (3.50), 646 (3.45), 856 nm (3.71). ¹H NMR (500 Hz, CDCl₃) δ 1.60 (6H, 2 overlapping triplets), 2.91 (3H, s), 2.93 (3H, s), 3.01 (3H, s), 3.06 (3H, s), 3.57 (4H, 2 overlapping quartets), 7.81 (1H, s), 8.57 (1H, s), 8.87 (1H, s), 8.98 (1H, s), 9.43 (1H, s) ppm.

Palladium complex of neo-confused porphyrin (61)



Neo-confused porphyrin **36a** (20.0 mg, 0.040 mmol) was dissolved in acetonitrile (10 ml) along with palladium(II) acetate (20 mg) under reflux conditions for 1 h. The mixture was diluted with dichloromethane, and washed with water. The organic solution was evaporated under reduced pressure and the residue was purified by column chromatography on grade 3 alumina eluting with 3:1 hexanes/dichloromethane to give the palladium neo-confused porphyrin (19 mg, 0.0315 mmol, 78%) as a green solid, mp > 300 °C; $^1\text{H NMR}$ (500 Hz, CDCl_3) δ 1.02 (6H, 2 overlapping triplets), 3.03 (3H, s), 3.15 (3H, s), 3.20 (3H, s), 3.25 (3H, s), 3.65-3.74 (4H, 2 overlapping quartets), 7.66 (1H, t, $J = 7.6$ Hz), 7.76 (2H, t, $J = 7.6$ Hz), 8.03 (2H, d, $J = 7.6$ Hz), 8.08 (1H, s), 9.00 (1H, s), 9.16 (1H, s), 9.44 (1H, s), 9.70 (1H, s), 9.89 (1H, s) ppm.

REFERENCES

- [1] Milgrom, L. R. *The Colours of Life*, Oxford University Press: New York; **1997**
- [2] *Porphyrins and Metalloporphyrins*. Smith, K. M., ed.; Elsevier Scientific Pub.Co., **1975**.
- [3] Lash, T. D. *J. Porphyrins Phthalocyanines*.**2011**, 15, 1093-1115.
- [4] Fischer, H.; Klarer, J. Synthese des Ätioporphyrins, Ätiohämins und Ätiophyllins.*Liebigs Ann. Chem.* **1926**,448, 178; Fischer, H.; Zeile, K. Synthese des Hämatoporphyrins, Protoporphyrins und Hämins.*Justus Liebigs Ann. Chem* **1929**,468, 98.
- [5] Wilson B. C. Photodynamic therapy for cancer: principles. *Canadian Journal of Gastroenterology*.**2002**, 16, 393–396.
- [6] Kadish, K. M.; Smith, K. M.; Guillard, R. *The Porphyrin Handbook*, Academic Press: New York, **2000**; Vol. 1-10.
- [7] Adler, A. D.; Longo, F. R.; Shergalis. W. Mechanistic Investigations of Porphyrin Syntheses. I. Preliminary Studies on *ms*-Tetraphenylporphin.*J. Am. Chem Soc.* **1964**,86, 3145; Adler, A. D.; Longo, F. R.; Sklar, L.; Finarelli, J. D.; Finarelli, M. G.Syntheses of *meso*-Substituted Porphodimethenes and Porphyrins with Exocyclic Ring Systems.*J. Heterocyclic Chem.* **1968**,5, 669.

- [8] Rothemund, P. A New Porphyrin Synthesis. The Synthesis of Porphin. *J. Am. Chem. Soc.* **1936**, *58*, 625.
- [9] Lindsey, J. S.; Schreiman, I. C.; Hsu, H. C.; Kearney, P. C.; Marguerettaz, A. M. Rothemund and Adler-Longo reactions revisited: synthesis of tetraphenylporphyrins under equilibrium conditions. *J. Org. Chem.* **1987**, *52*, 827.
- [10] Arsenault, G. P.; Bullock, E.; MacDonald, S. F. Pyrromethanes and Porphyrins Therefrom. *J. Am. Chem. Soc.* **1960**, *82*, 4384.
- [11] Sessler, J. L.; Johnson, M. R.; Lynch, V. Synthesis and crystal structure of a novel tripyrrane-containing porphyrinogen-like macrocycle. *J. Org. Chem.* **1987**, *52*, 4394.
- [12] Lash, T. D. Oxybenzporphyrin, an aromatic semiquinone porphyrin analog with pathways for 18π -electron delocalization. *Angew. Chem. Int. Ed. Engl.* **1995**, *34*, 2533-2535.
- [13] Lash, T. D.; Chaney, S. T.; Richter, D. T. Conjugated macrocycles related to the porphyrins. Part 12. Oxybenzi- and Oxypyriporphyrins: Aromaticity and Conjugation in Highly Modified Porphyrinoid Structures. *J. Org. Chem.* **1998**, *63*, 9076-9088.
- [14] Furuta, H.; Asano, T.; Ogawa, T. N-confused porphyrin - a new isomer of tetraphenylporphyrin. *J. Am. Chem. Soc.* **1994**, *116*, 767-768.
- [15] P. J. Chmielewski, L. Latos-Grazynski, K. Rachlewicz, T. Glowiak, *Angew. Chem., Int. Ed. Engl.* **1994**, *33*, 779-781.
- [16] Furuta, H.; Ishizuka, T.; Osuka, A.; Ogawa, T. *J. Am. Chem. Soc.* **2000**, *122*, 5748-5757.

- [17] Fujino, K.; Hirata, Y.; Kawabe, Y.; Morimoto, T.; Srinivasan, A.; Toganoh, M.; Miseki, A.; Kudo, Y.; Furuta, H. Confusion and Neo-Confusion: Corrole Isomers with an NNNC Core. *Angew. Chem.* **2011**, *123*, 6987–6991.
- [18] Lash, T. D.; Lammer, A. D.; Ferrence, G. M. Neo-Confused Porphyrins, a New Class of Porphyrin Isomers. *Angew. Chem. Int. Ed.* **2011**, *50*, 9718–9721.
- [19] Li, R.; Lammer, A. D.; Ferrence, G. H.; Lash, T. D. Synthesis, Structural Characterization, Aromatic Characteristics, and Metalation of Neo-Confused Porphyrins, a Newly Discovered Class of Porphyrin Isomers. *J. Org. Chem.* **2014**, *79*, 4078–4093.
- [20] AbuSalim, D. I.; Lash, T. D. Aromatic Character and relative stability of neo-confused porphyrin tautomers and related compounds. *Org. Biomol. Chem.* **2013**, *11*, 8306-8323.
- [21] Tardieux, C.; Bolze, F.; Gros, P. C.; Guillard, R. New one-step synthesis of 3,4-disubstituted pyrrole-2,5-dicarbaldehyde, *Synthesis*, **1998**, 267-268.
- [22] Sonnet, P. E. Synthesis of the trail marker of the taxas leaf-cutting ant, *J. Med. Chem.* **1971**, *15*, 97-98.
- [23] Vilsmeier, A.; Haack, A. *Ber. Dtsch. Chem. Ges.* **1927**, *60*, 119.
- [24] Yasuyoshi, A.; Haruyuki, N. Discovery of a Novel Pyrrole Derivative 1-[5-(2-Fluorophenyl)-1-(pyridine-3-ylsulfonyl)-1H-pyrrol-3-yl]-N-methylmethanamine Fumarate (TAK-438) as a Potassium-Competitive Acid Blocker (P-CAB). *J. Med. Chem.* **2012**, *55*, 4446-4456.

[25] Madsen, C.; Jensen, A.; Hansen, C. 5-Substituted Imidazole4-acetic Acid Analogues: Synthesis, Modeling, and Pharmacological Characterization of a Series of Novel γ -Aminobutyric Acid C Receptor Agonists. *J. Med. Chem.* **2007**, *50*, 4147-4161.

APPENDIX
SELECTED NMR SPECTRA

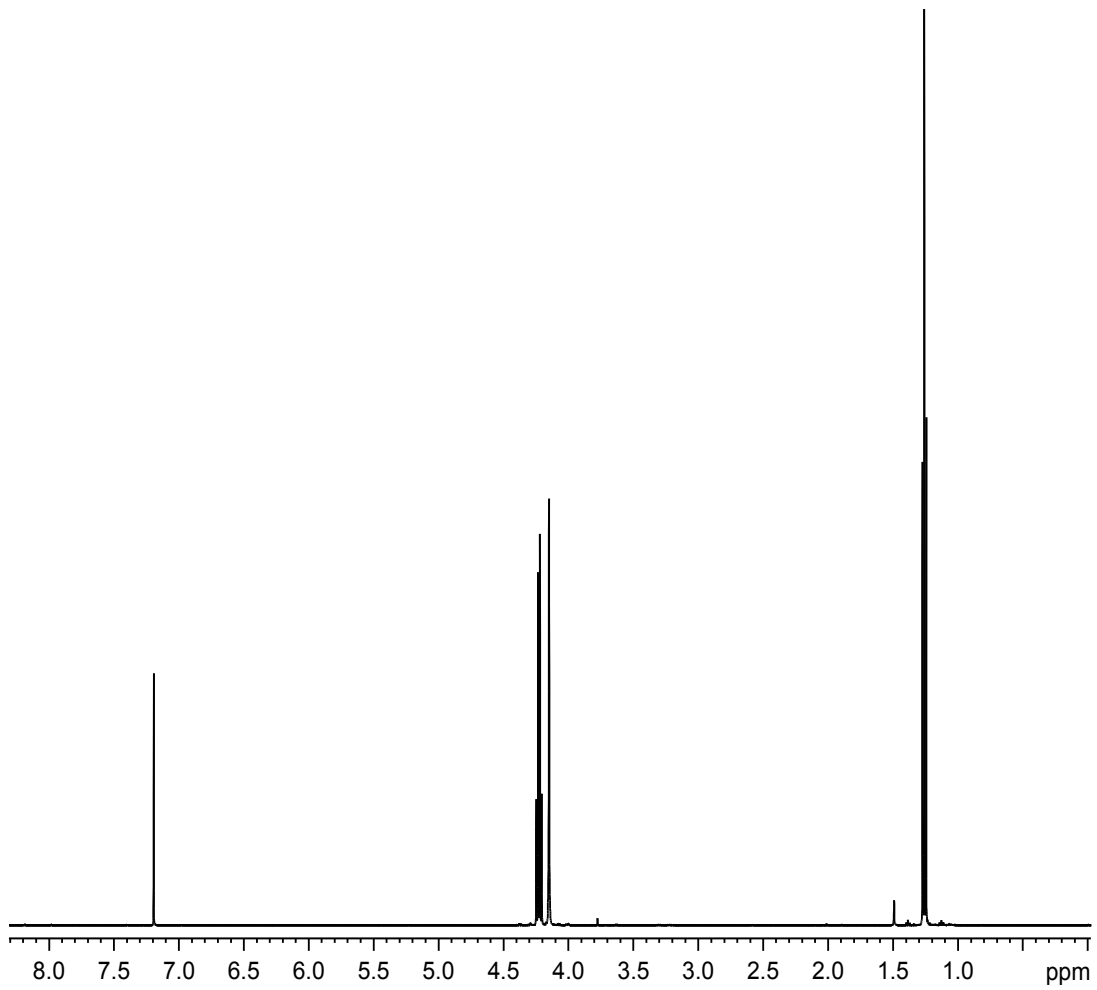


Figure A 1: 500 MHz proton NMR spectrum of ethyl isocyanoacetate⁴² in CDCl₃

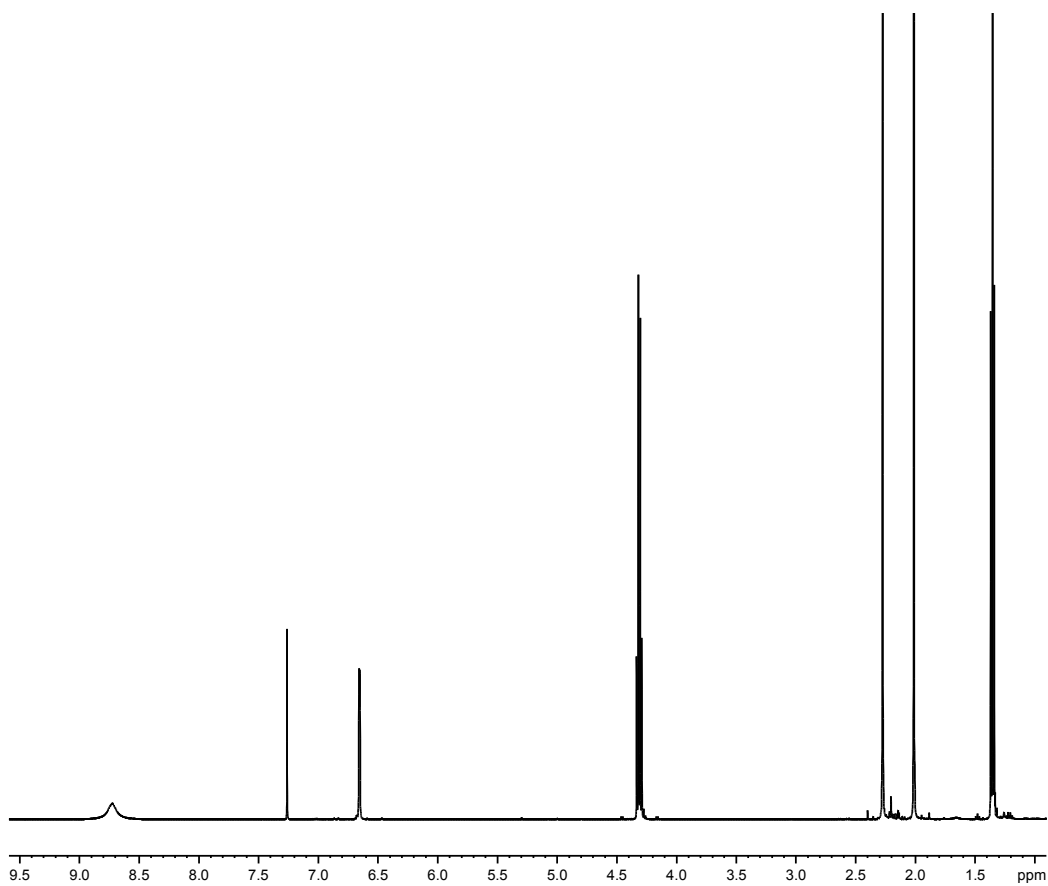


Figure A 2: 500 MHz proton NMR spectrum of ethyl 4-ethyl-3,5-dimethylpyrrole-2-carboxylate **44** in CDCl_3

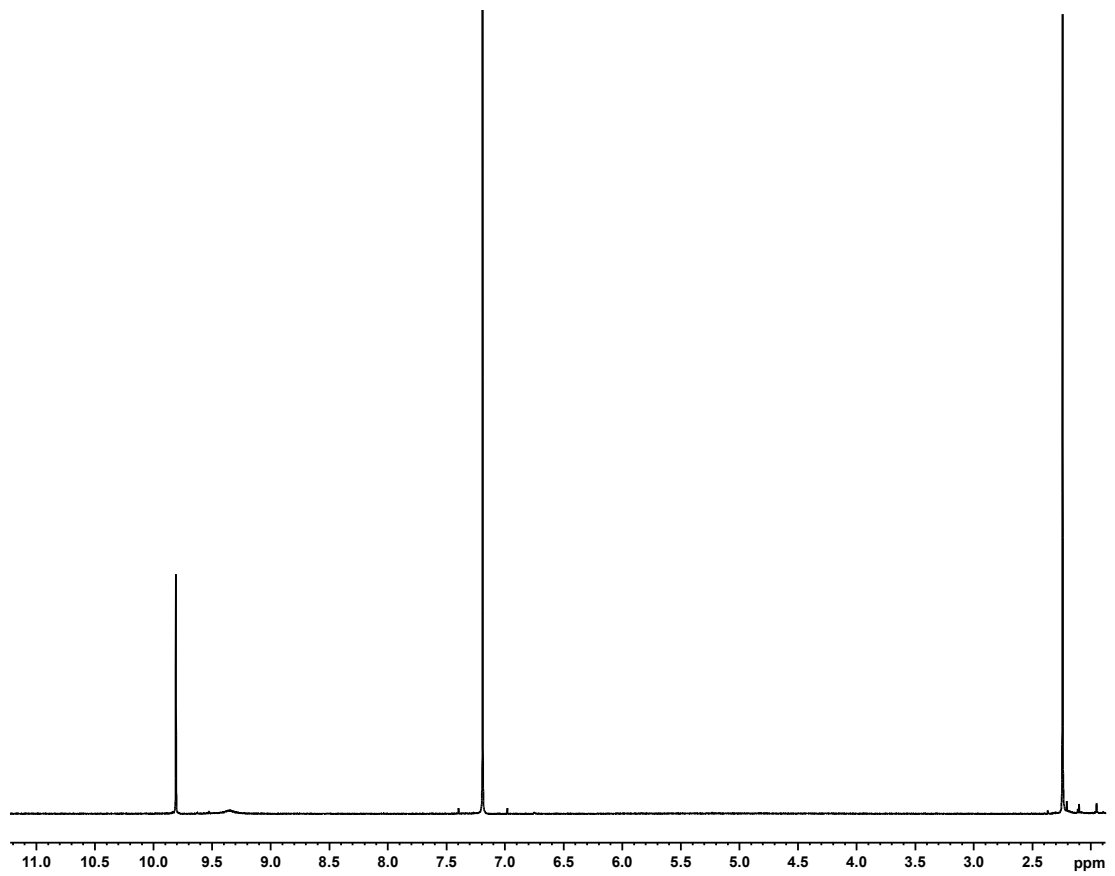


Figure A 3: 500 MHz proton NMR spectrum of 3,4-dimethylpyrrole-2-carboxylic acid in acetone-d₆.

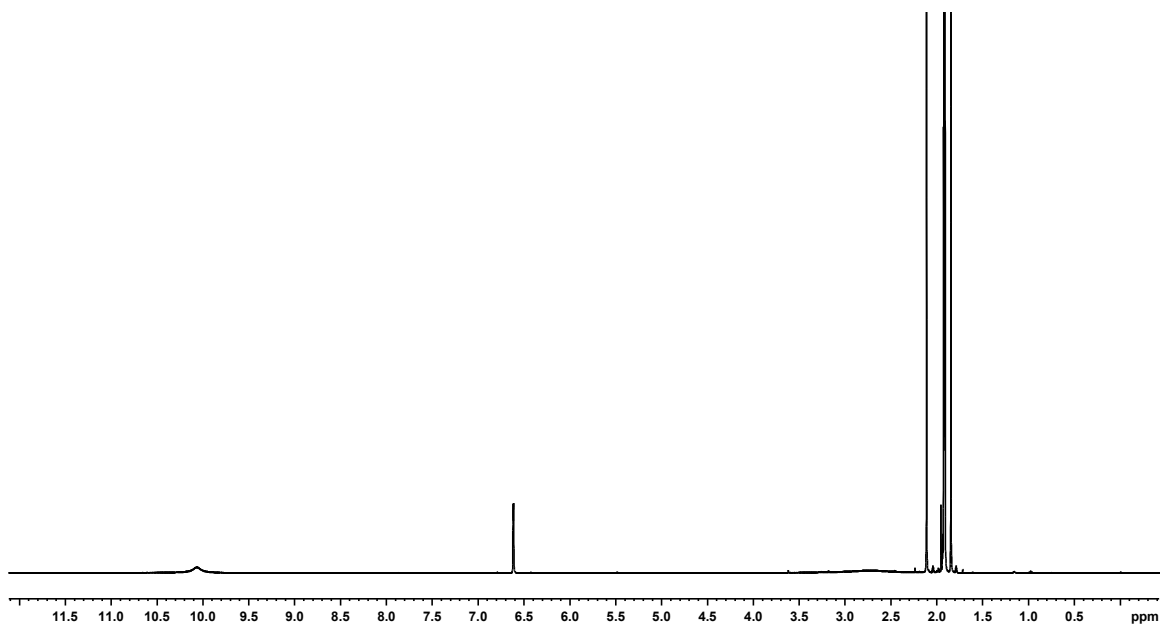


Figure A 4: 500 MHz proton NMR spectrum of 3,4-dimethyl-2,5-pyrroledicarbaldehyde
in CDCl_3

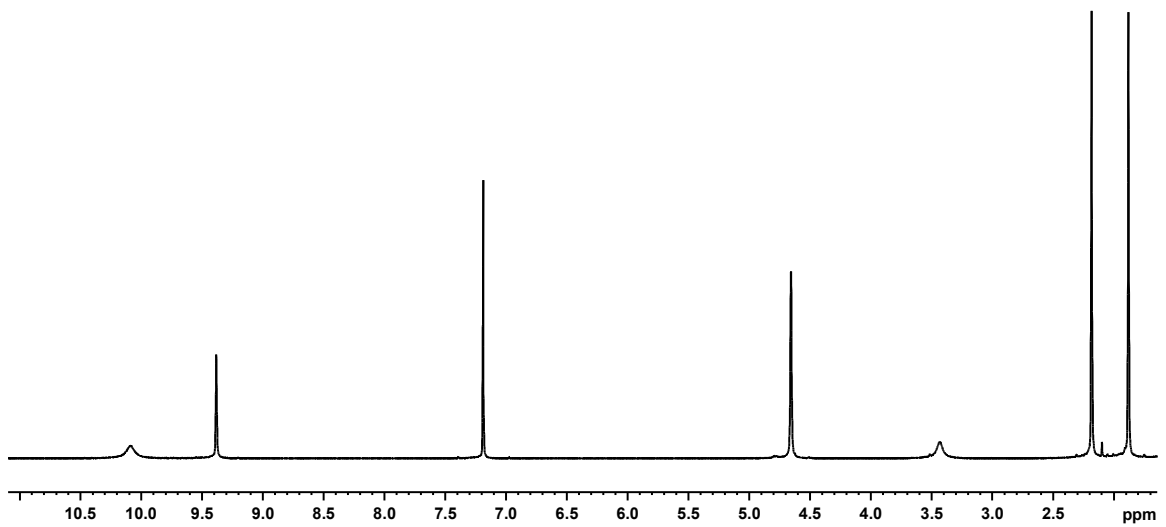


Figure A 5: 500 MHz proton NMR spectrum of 5-hydroxymethyl-3,4-dimethylpyrrole-2-carbaldehyde in CDCl_3

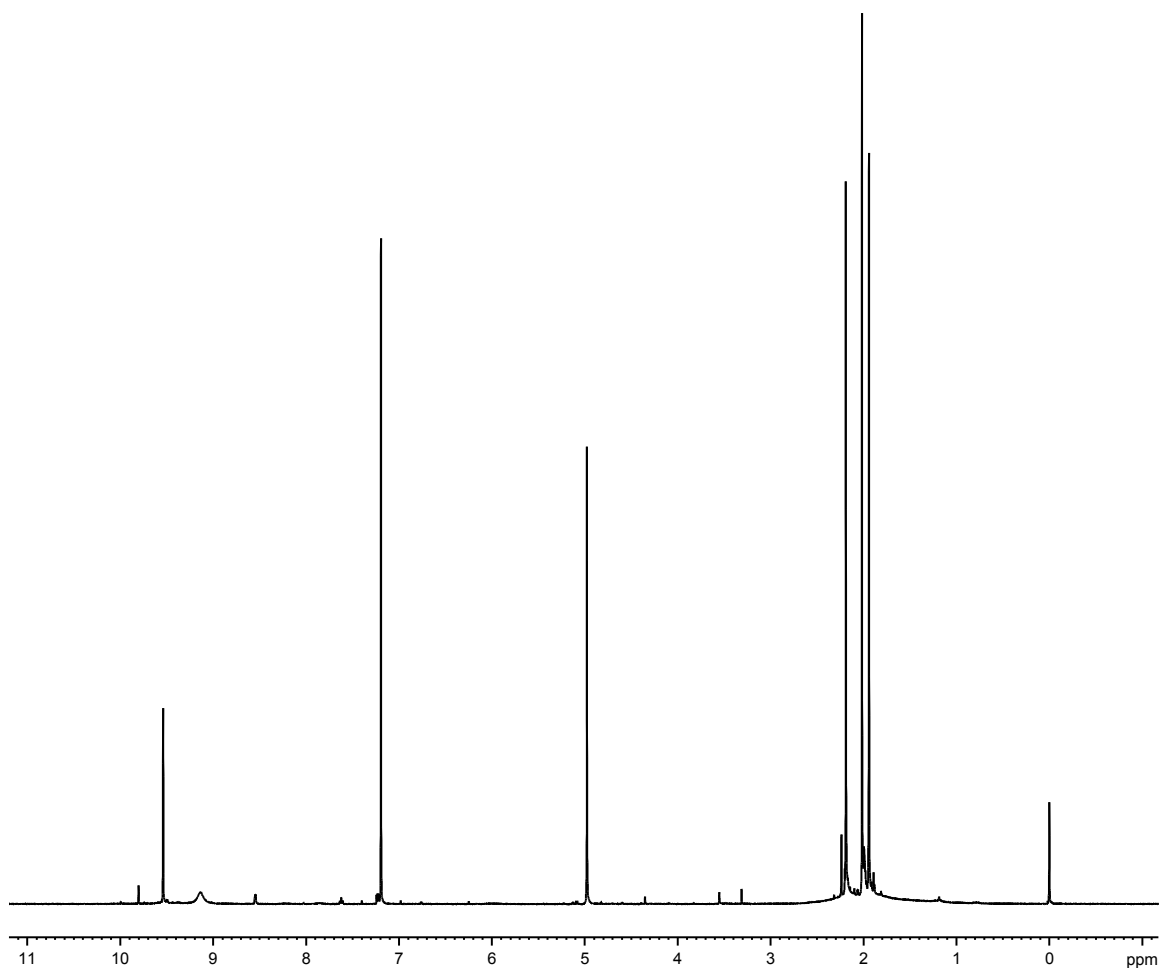


Figure A 6: 500 MHz proton NMR spectrum of 5-acetoxymethyl-3,4-dimethylpyrrole-2-carbaldehyde in CDCl₃.

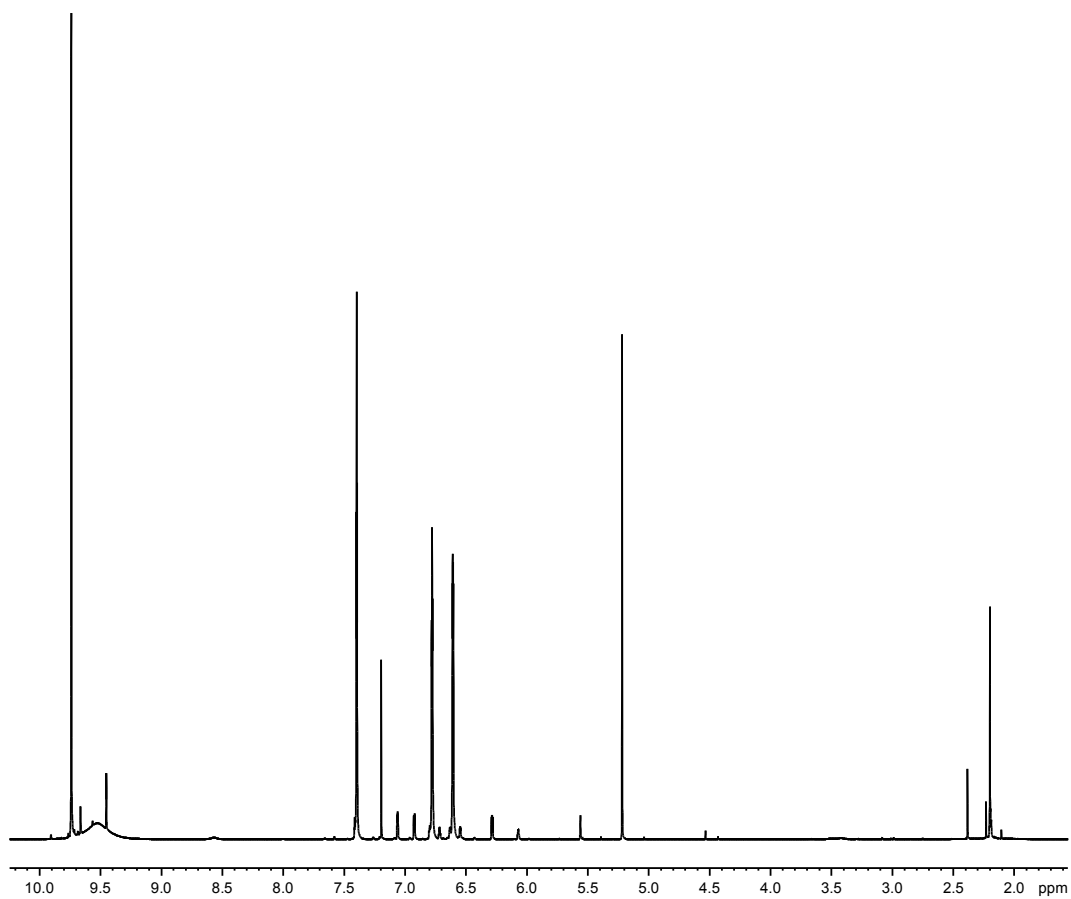


Figure A 7: 500 MHz proton NMR spectrum of pyrrole-3-carboxaldehyde in CDCl_3

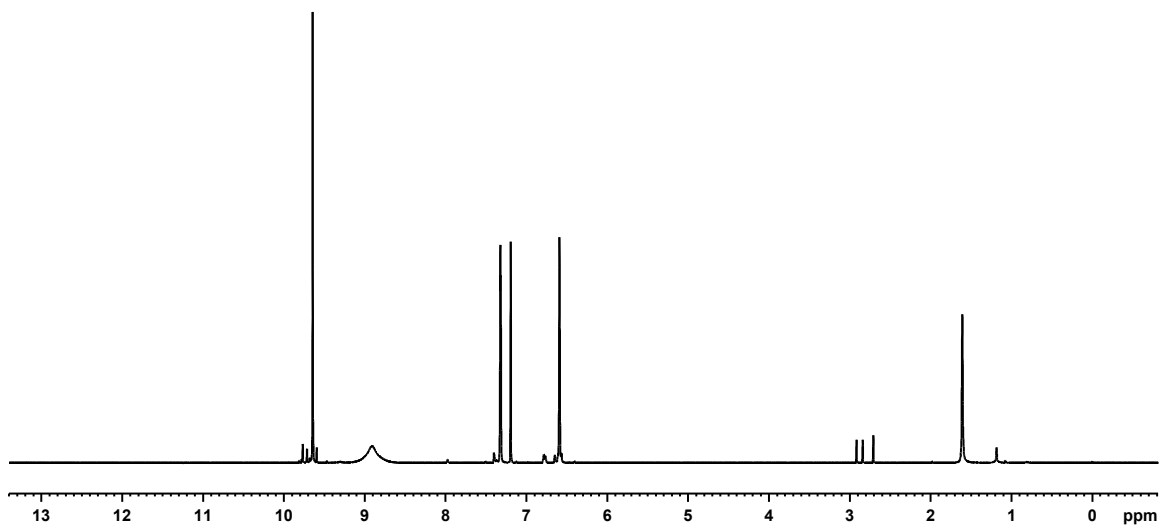


Figure A 8: 500 MHz proton NMR spectrum of 5-bromo-3-pyrrolicarbaldehyde in CDCl_3 .

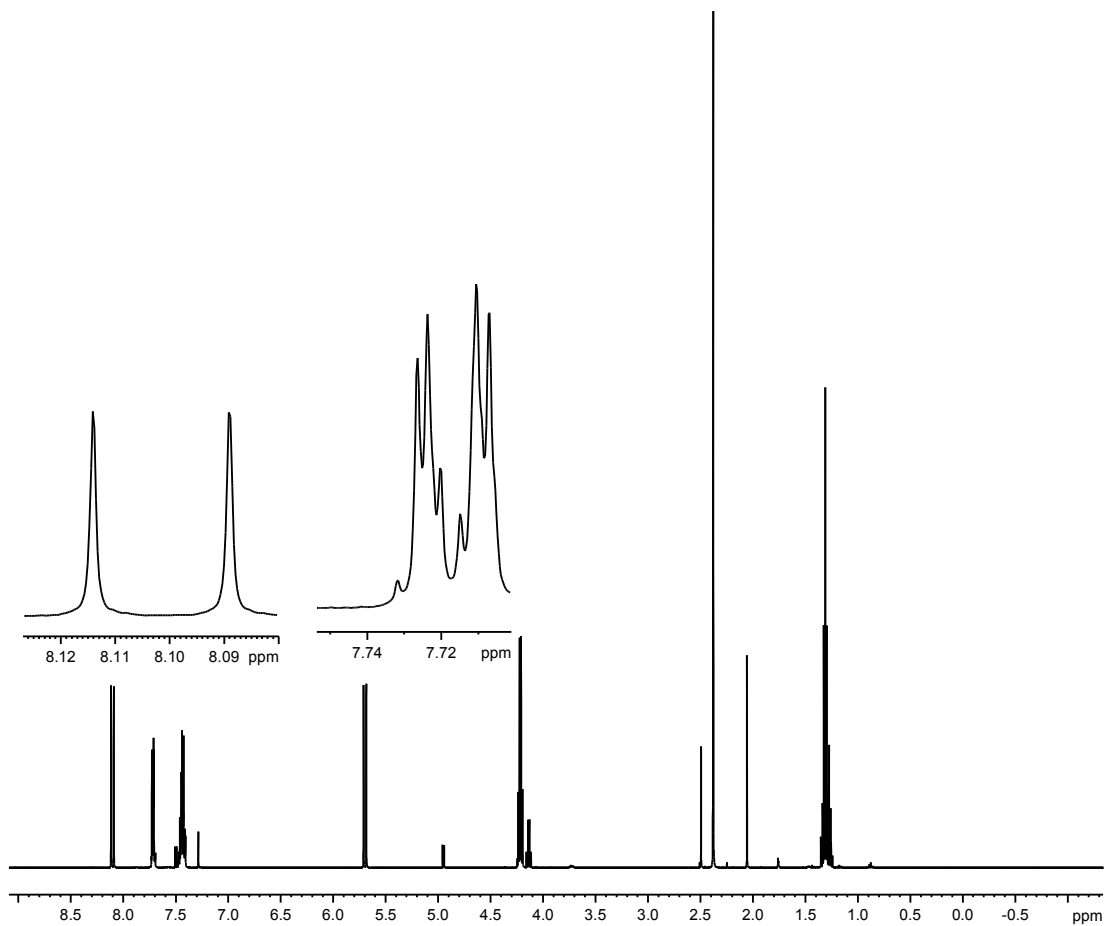


Figure A 9: 500 MHz proton NMR spectrum of acrylate⁵⁷ in CDCl₃

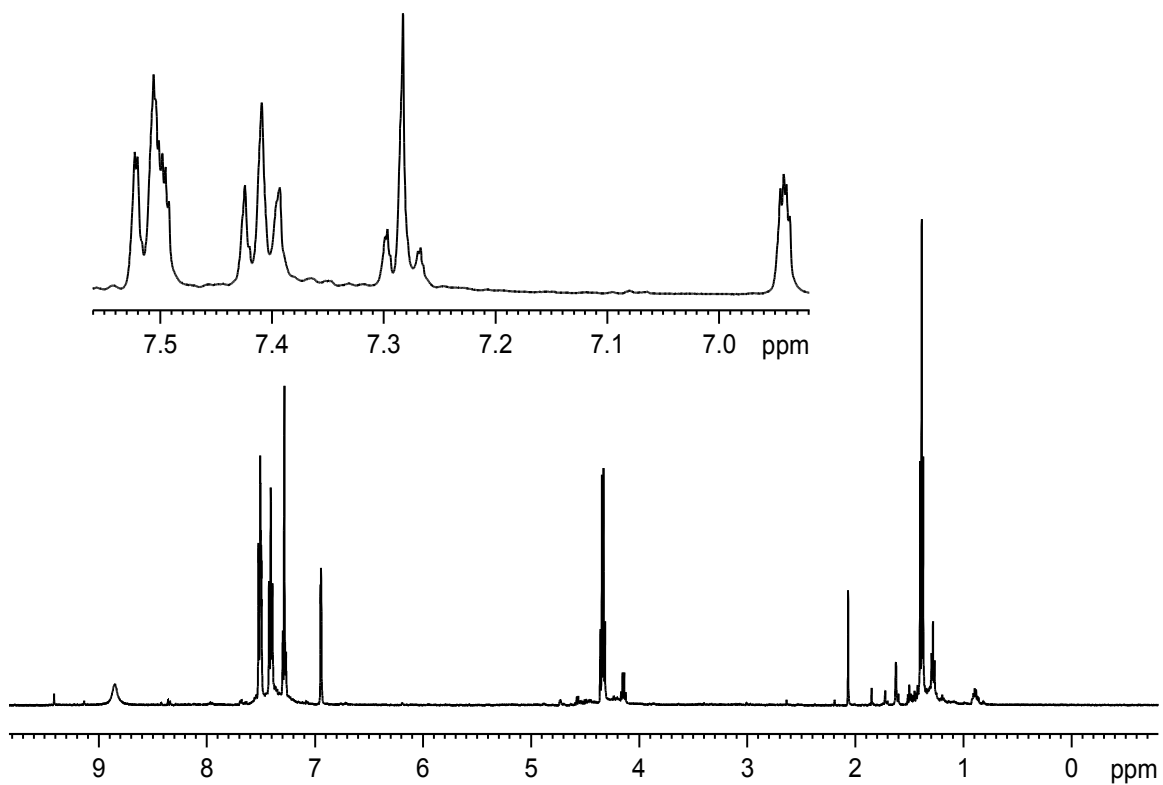


Figure A 10: 500 MHz proton NMR spectrum of ethyl 5-phenyl-3-carboxylate in CDCl₃

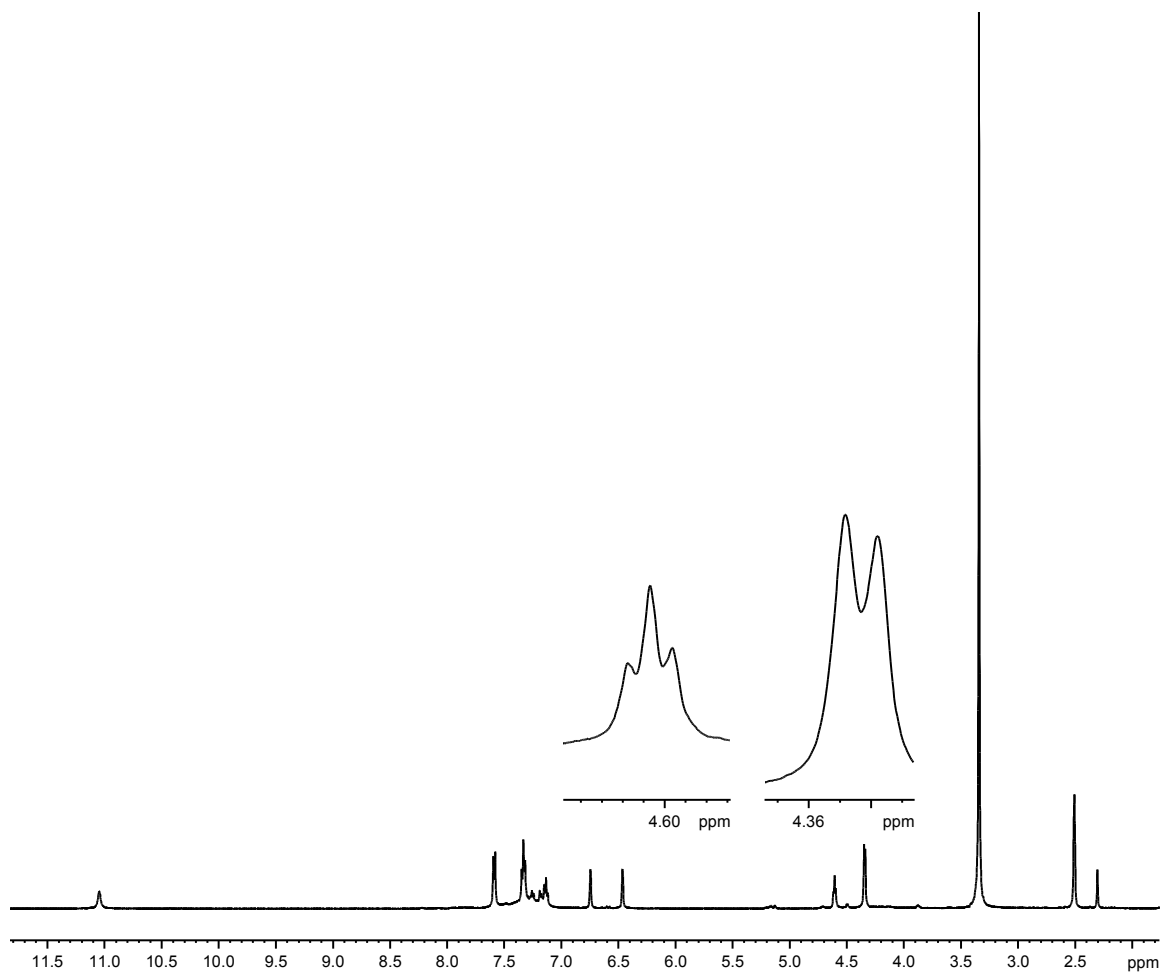


Figure A 11: 500 MHz proton NMR spectrum of phenyl pyrrole carbinol**59** in DMSO-d₆.

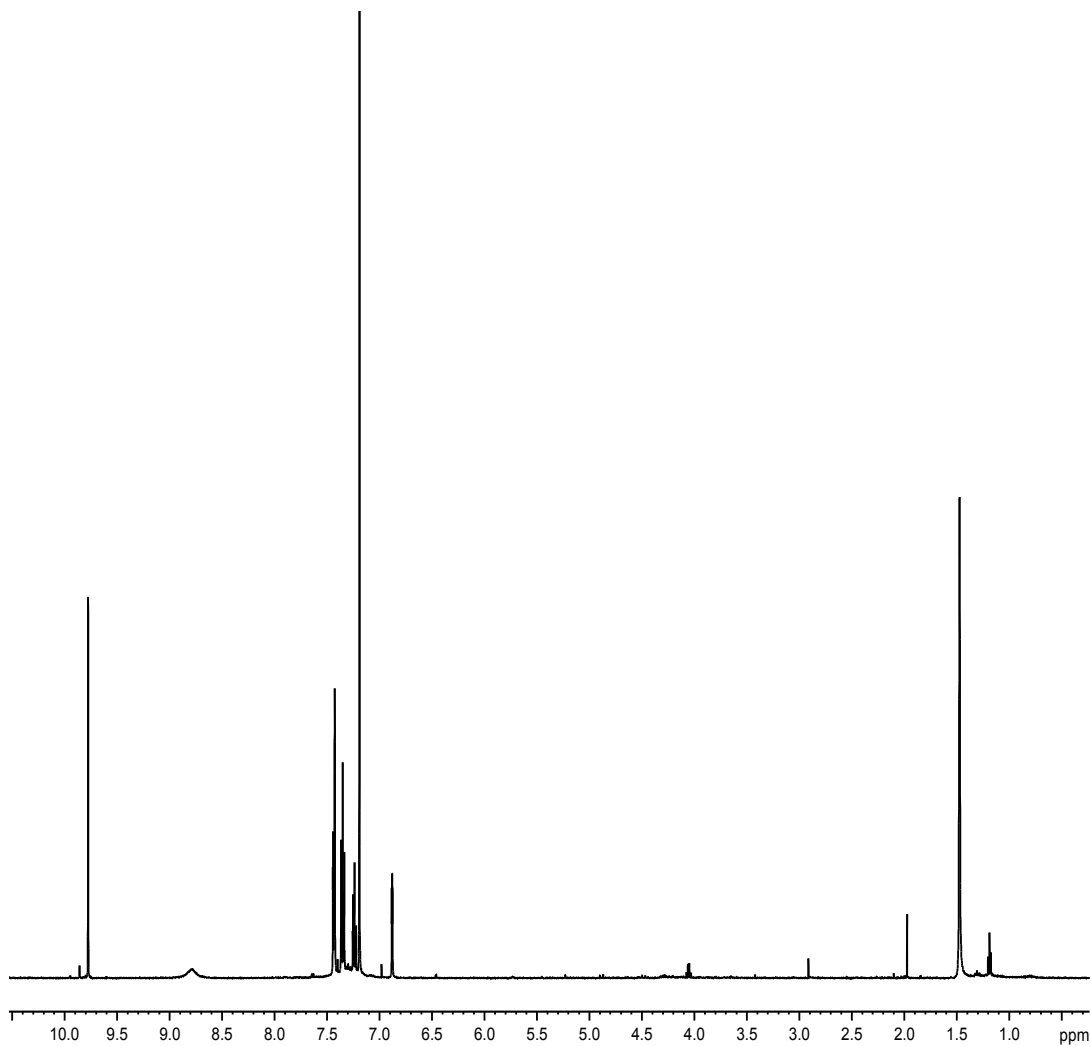


Figure A 12: 500 MHz proton NMR spectrum of phenyl pyrrole aldehyde **40b** in CDCl_3 .

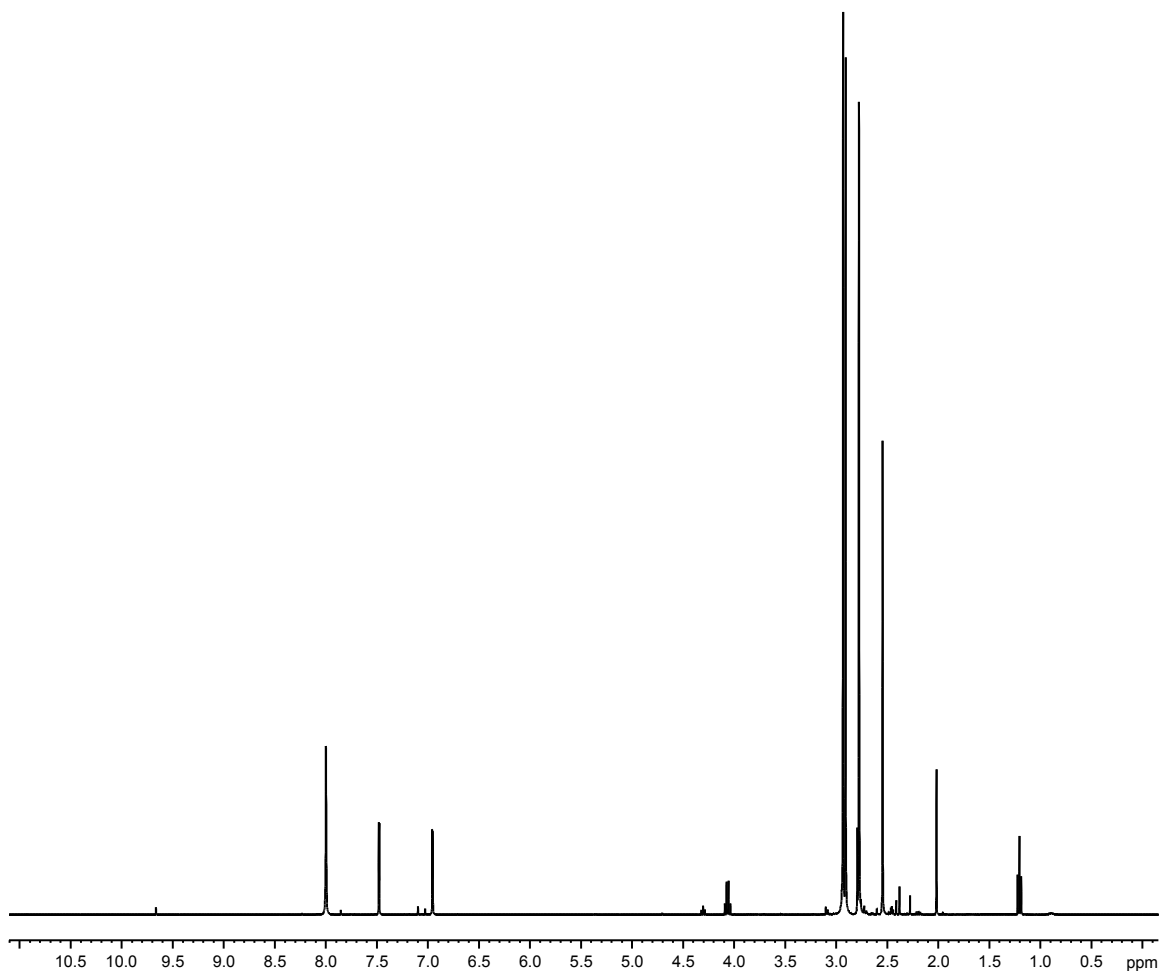


Figure A 13: 500 MHz proton NMR spectrum of 4-formyl-2-methylimidazole in CDCl_3 .

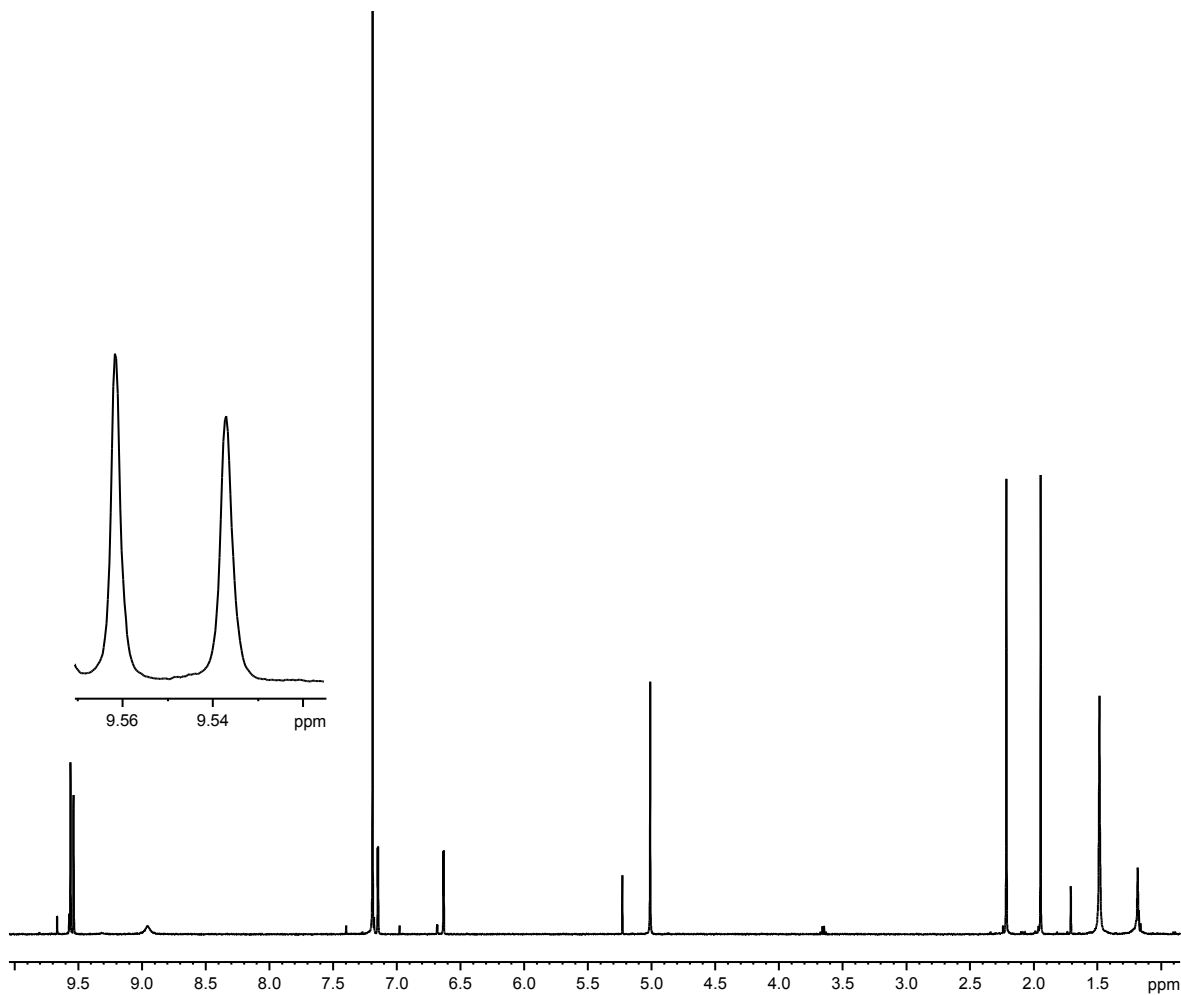


Figure A 14: 500 MHz proton NMR spectrum of bromo neo-confused
dipyrromethane **37a** in CDCl₃.

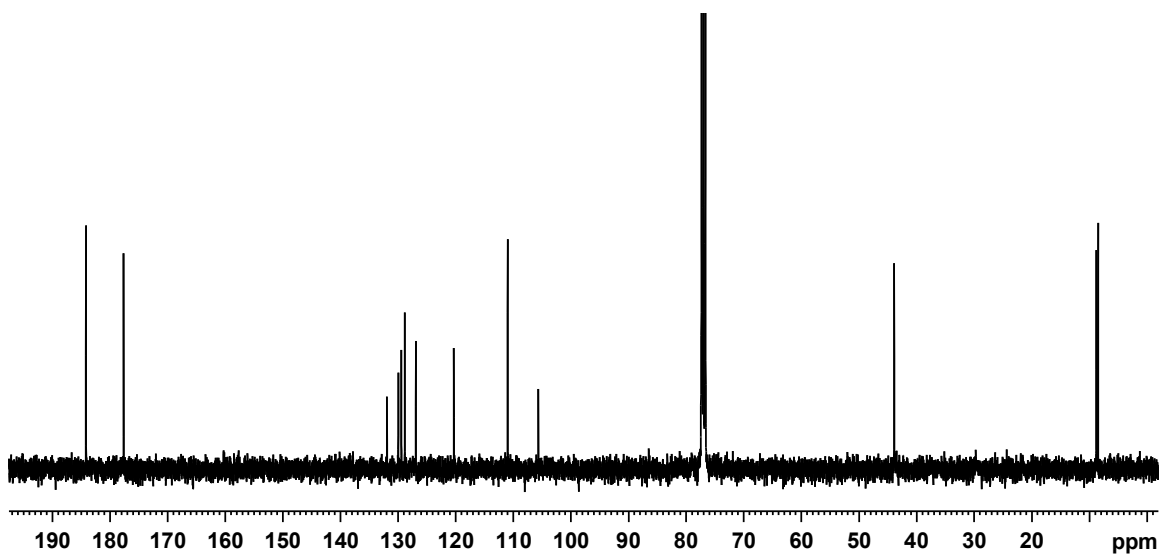


Figure A 15: 125 MHz carbon-13 spectrum of bromo neo-confused dipyrromethane **37a**
in CDCl₃.

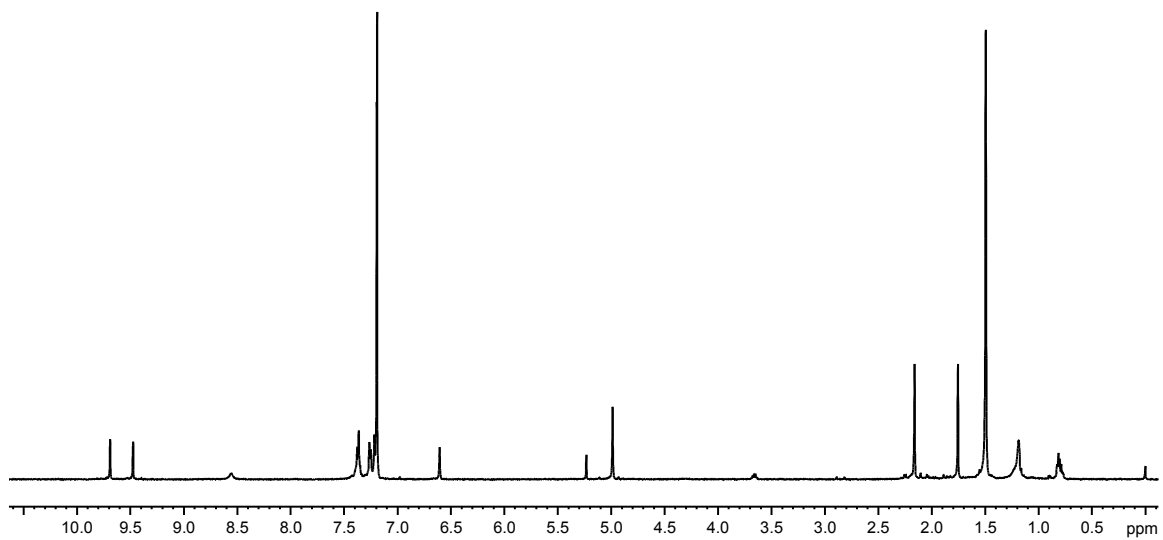


Figure A 16: 500 MHz proton NMR spectrum of phenyl neo-confused dipyrromethane **37b** in CDCl_3 .

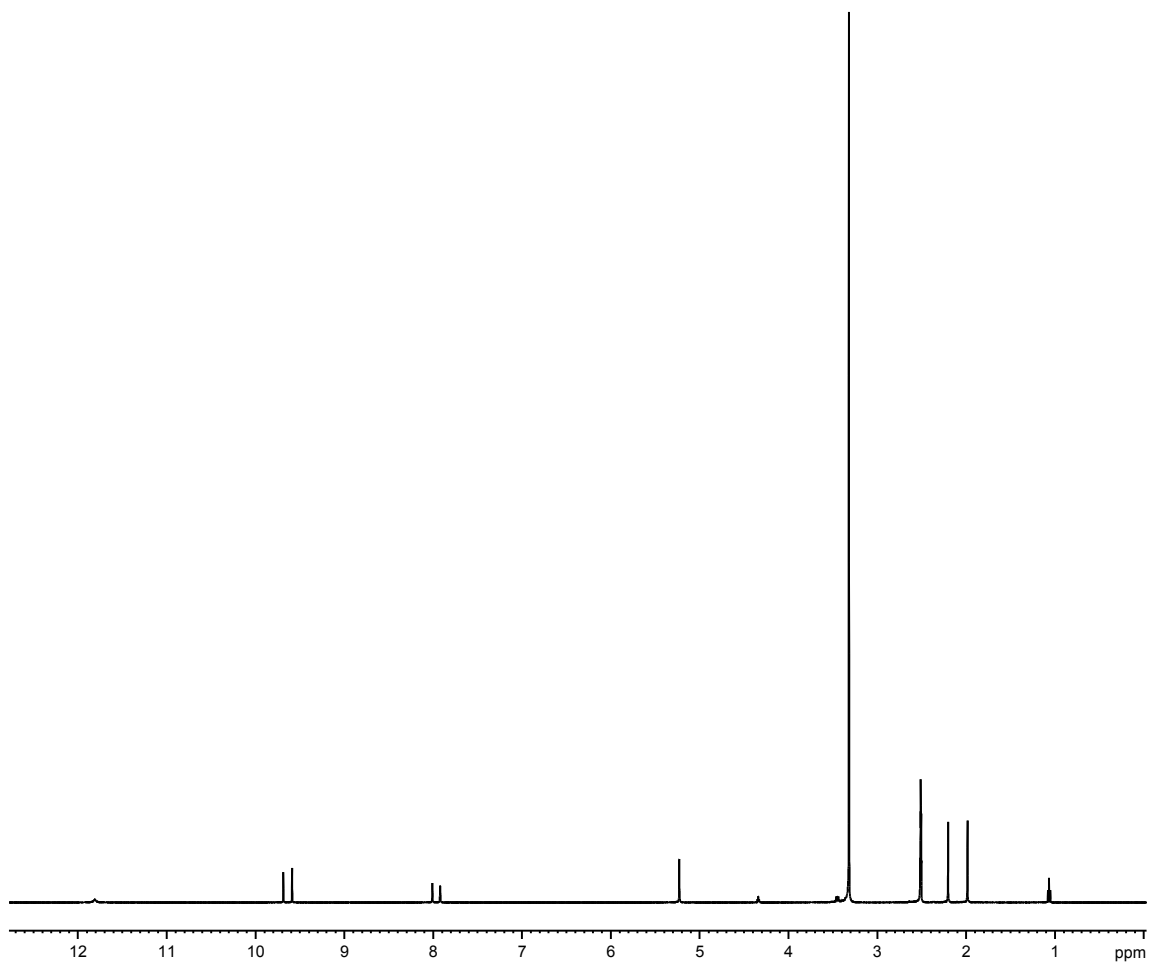


Figure A 17: 500 MHz proton NMR spectrum of formyl imidazole dipyrromethane **63** in DMSO-d₆.

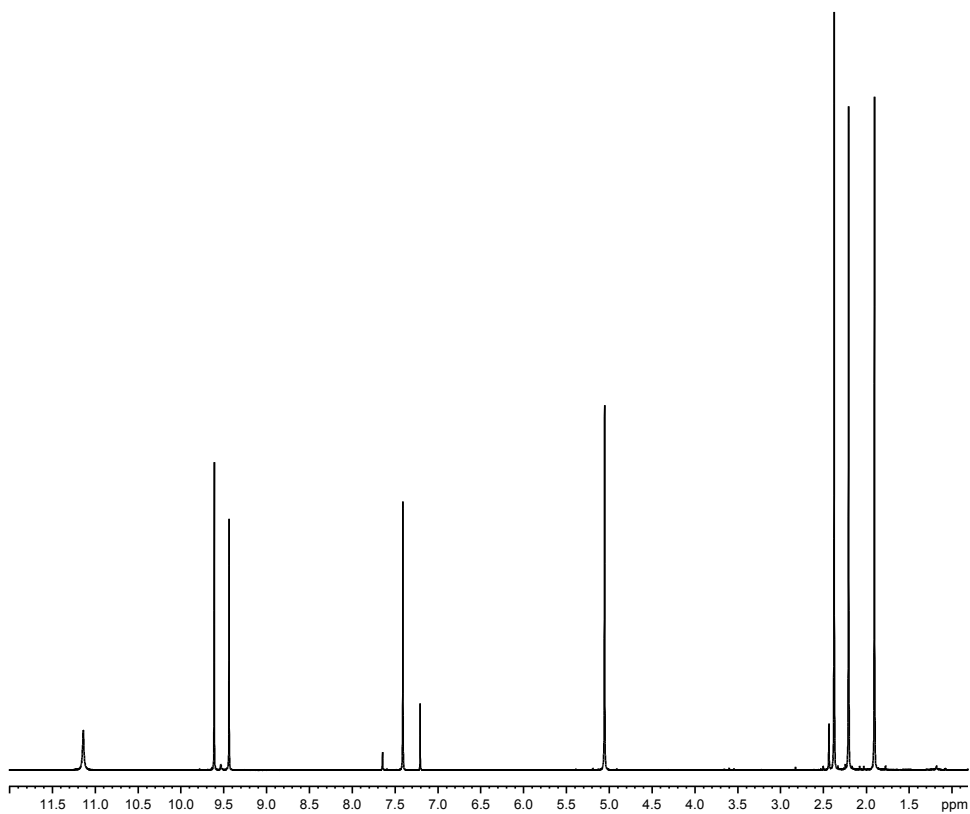


Figure A 18: 500 MHz proton NMR spectrum of methyl formyldipyrromethane **70** in DMSO-d₆.

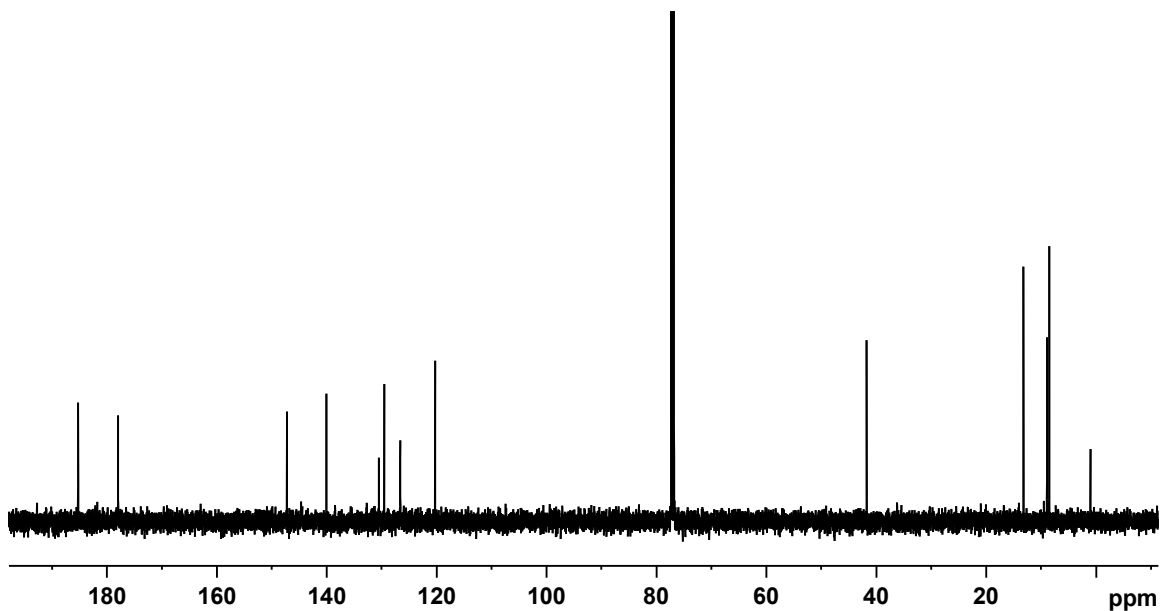


Figure A 19: 125 MHz carbon-13 spectrum of methyl formylimidazoledipyrromethane **70** in DMSO-d₆.

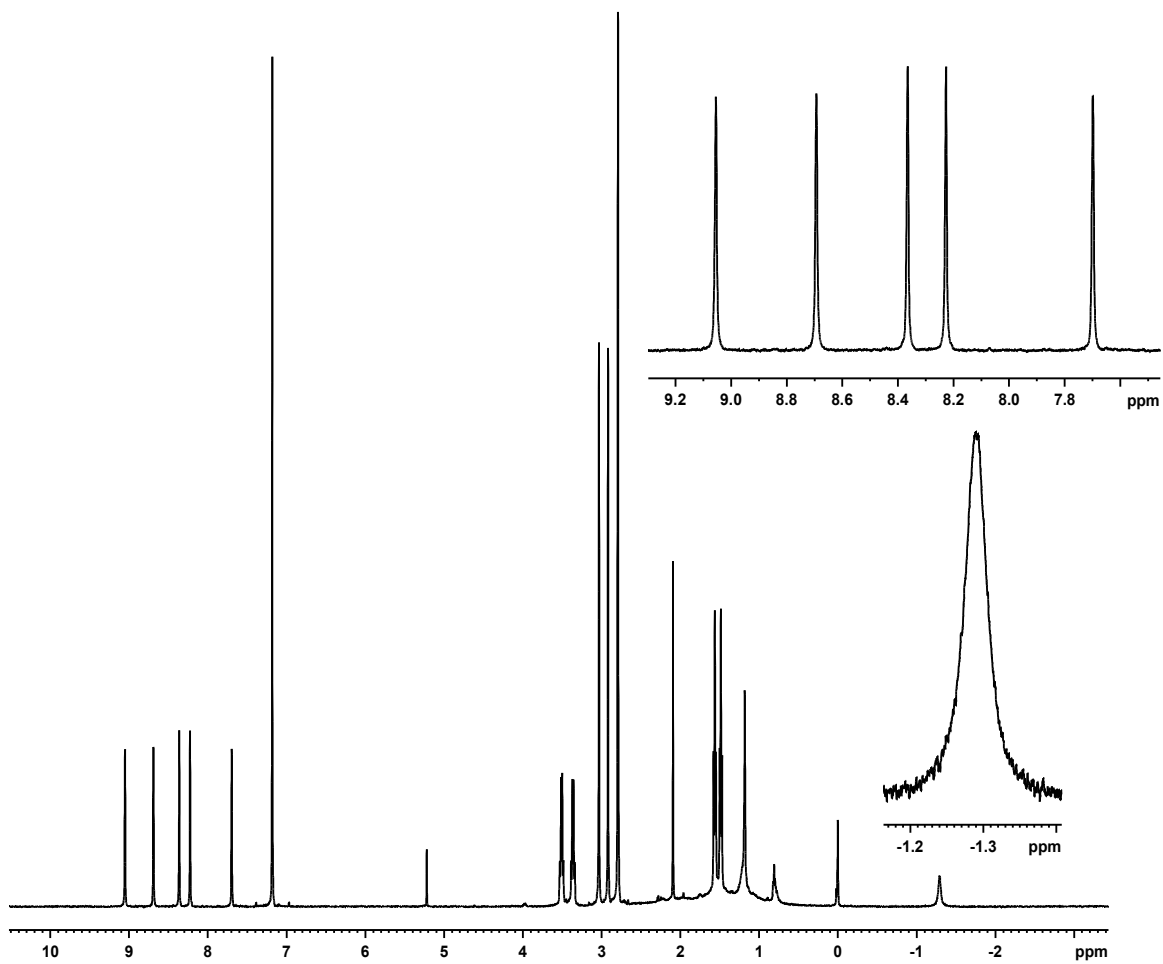


Figure A 20: 500 MHz proton NMR spectrum of neo-confused porphyrin **36a** in CDCl₃.

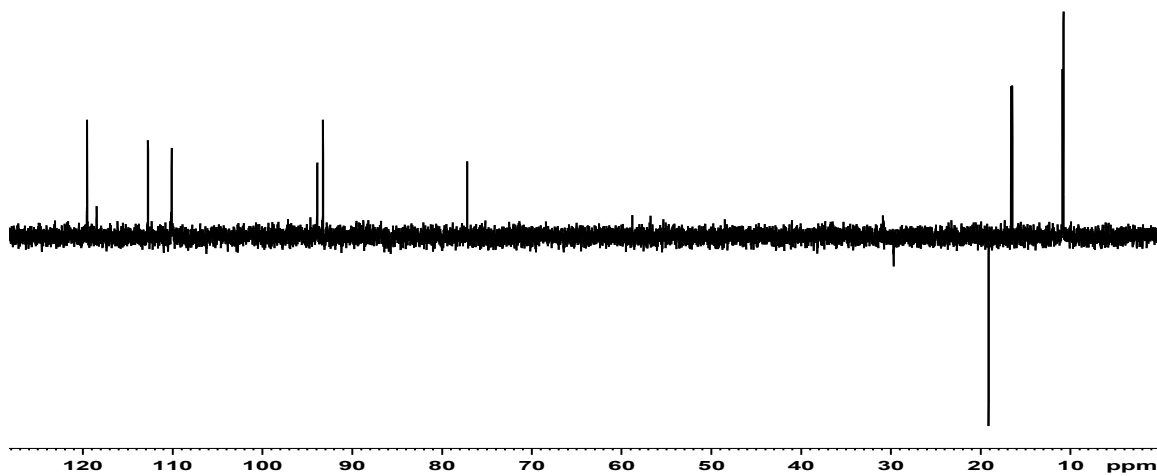


Figure A 21: DEPT-135 NMR spectrum of neo-confused porphyrin **36a** in CDCl_3 .

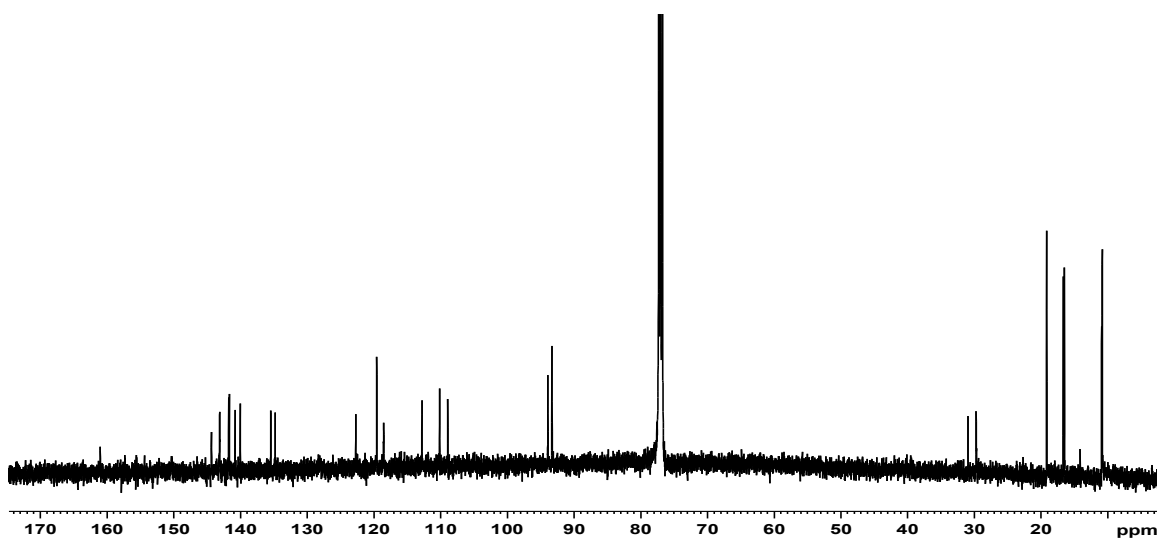


Figure A 22: 125 MHz carbon-13 NMR spectrum of neo-confused porphyrin **36a** in CDCl_3 .

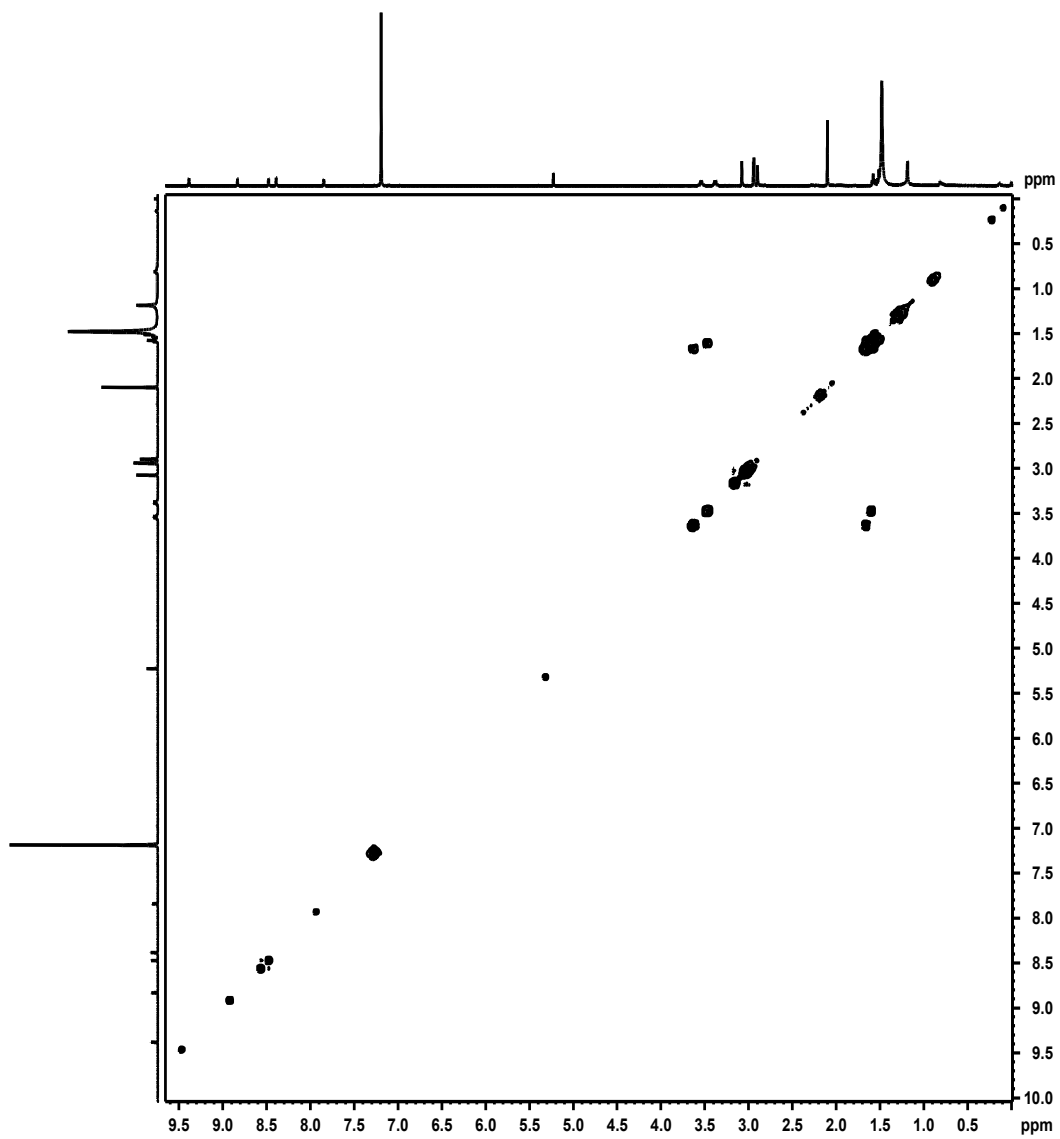


Figure A 23: ^1H - ^1H COSY NMR spectrum of neo-confused porphyrin **36a** in CDCl_3 .

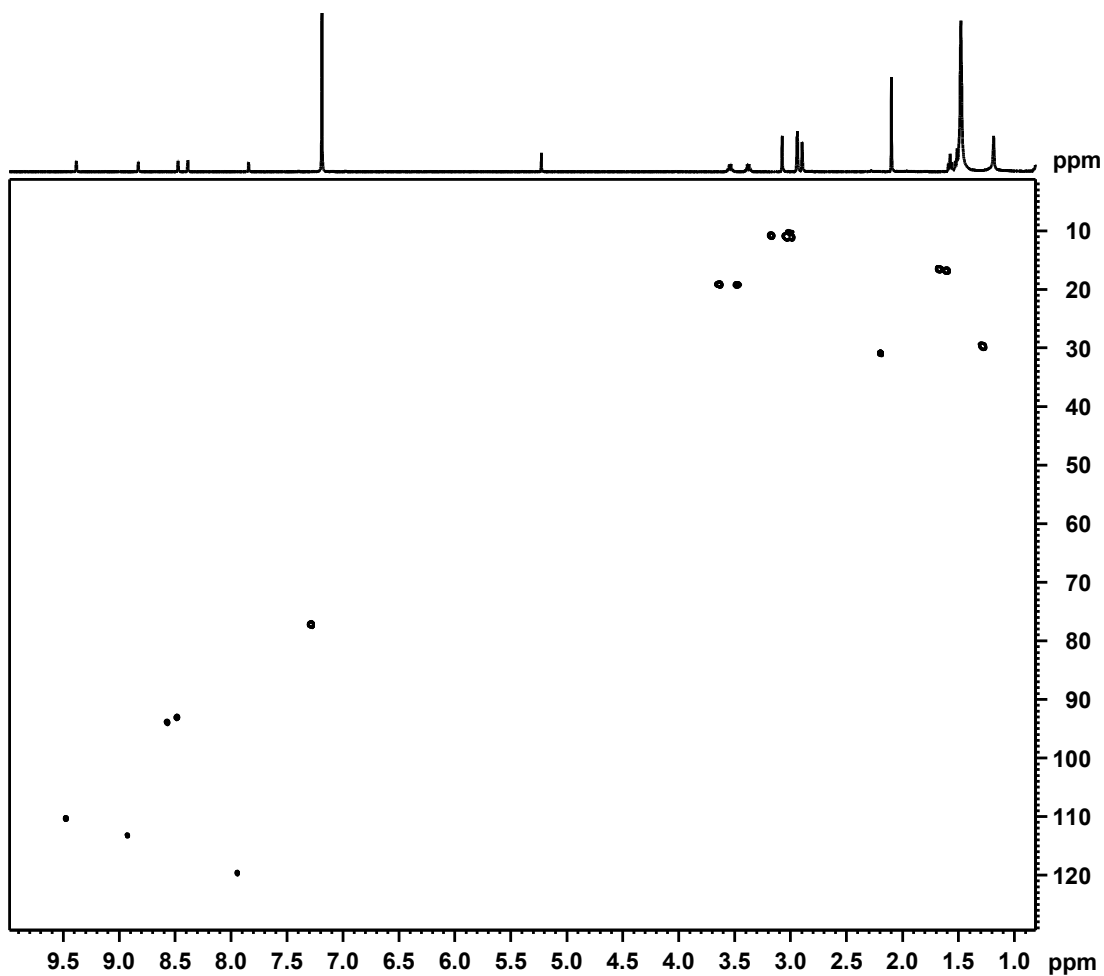


Figure A 24: HSQC NMR spectrum of neo-confused porphyrin **36a** in CDCl₃.

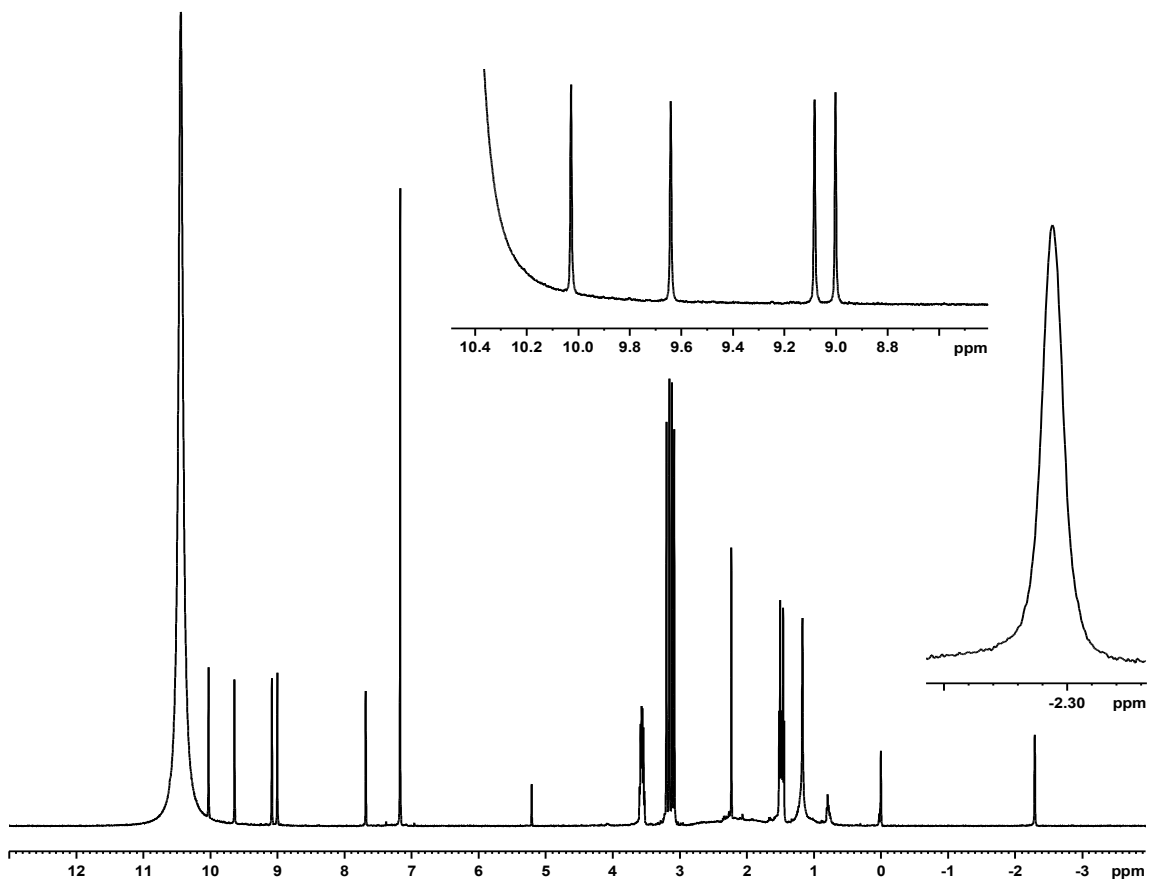


Figure A 25: 500 MHz proton NMR spectrum of neo-confused porphyrin dication $36aH_2^{2+}$ in TFA- $CDCl_3$.

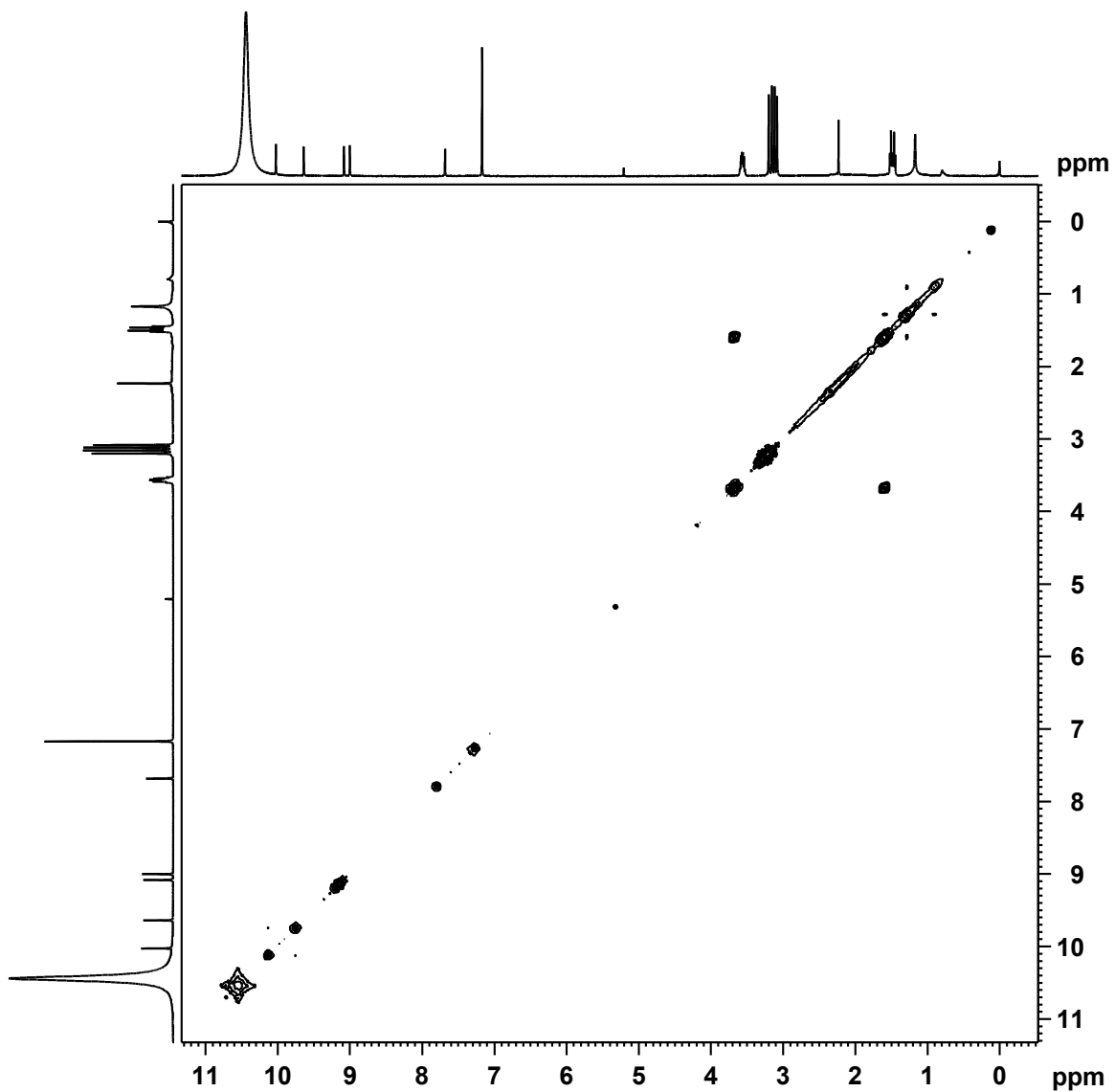


Figure A 26: ^1H - ^1H COSY NMR spectrum of neo-confused porphyrin dication 36aH_2^{2+} in TFA- CDCl_3 .

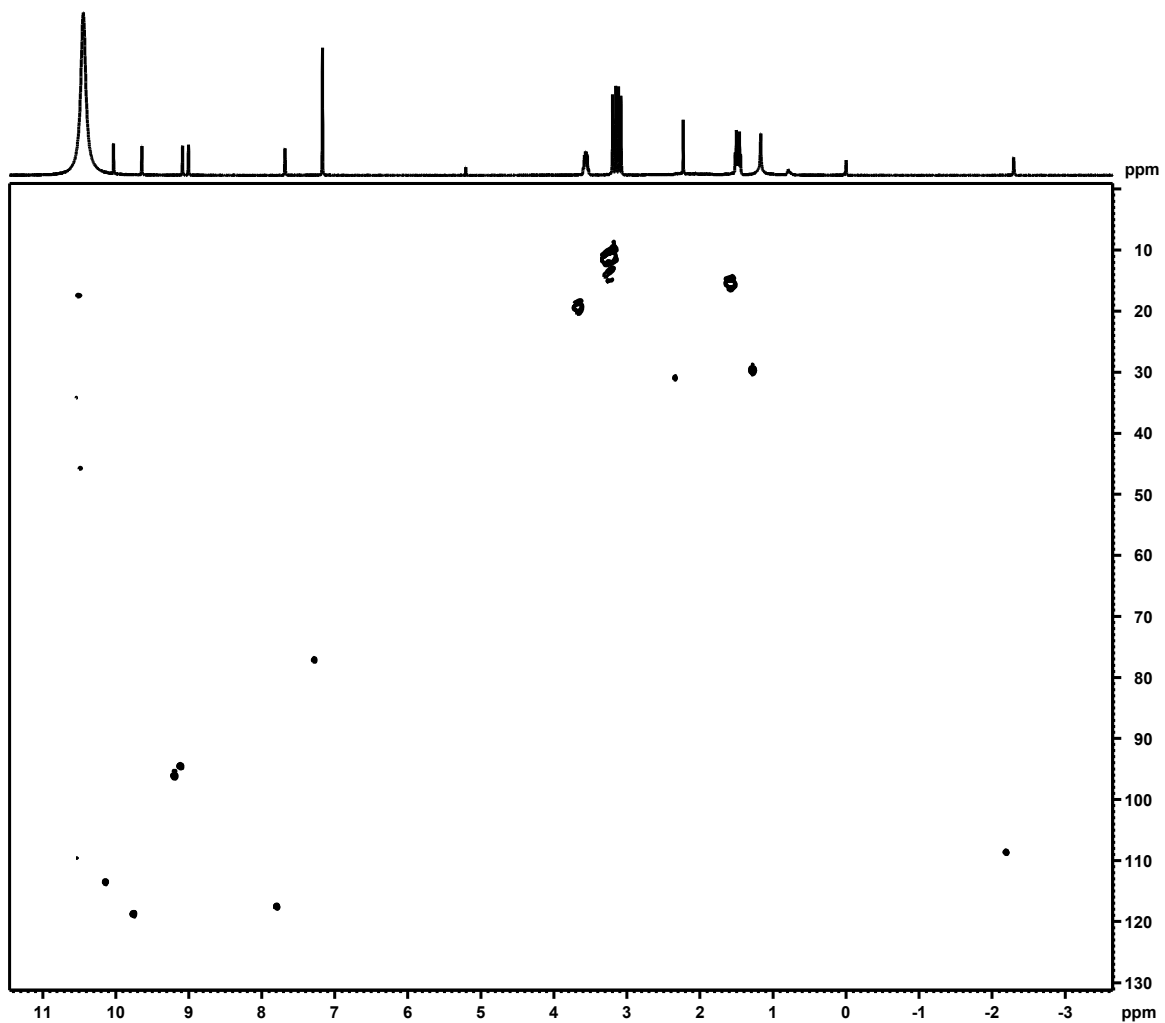


Figure A 27: HSQC NMR spectrum of neo-confused porphyrin **36a**H₂²⁺ in TFA-CDCl₃.

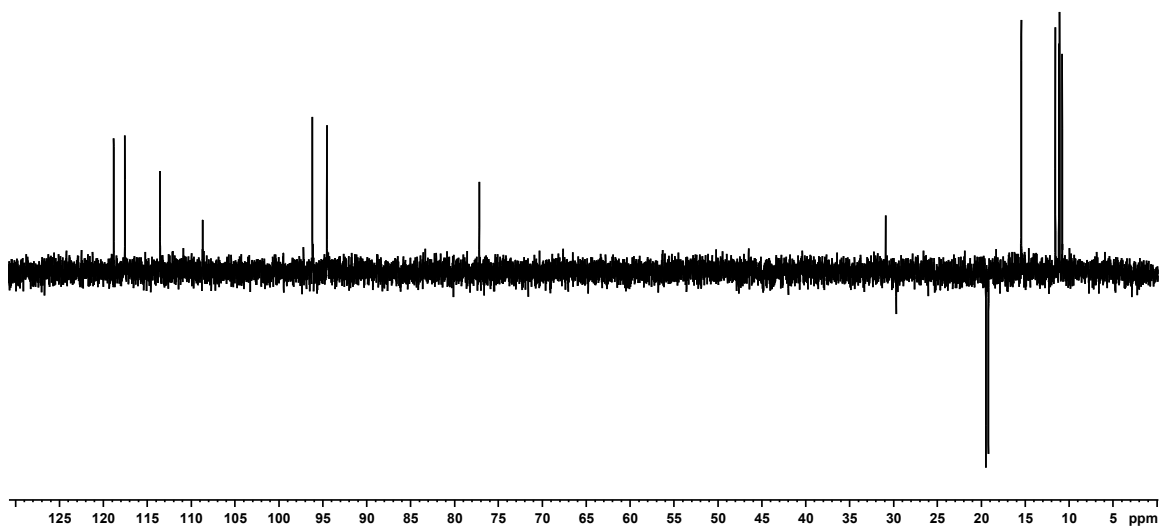


Figure A 28: DEPT-135 NMR spectrum of neo-confused porphyrin **36aH₂²⁺** in TFA-CDCl₃.

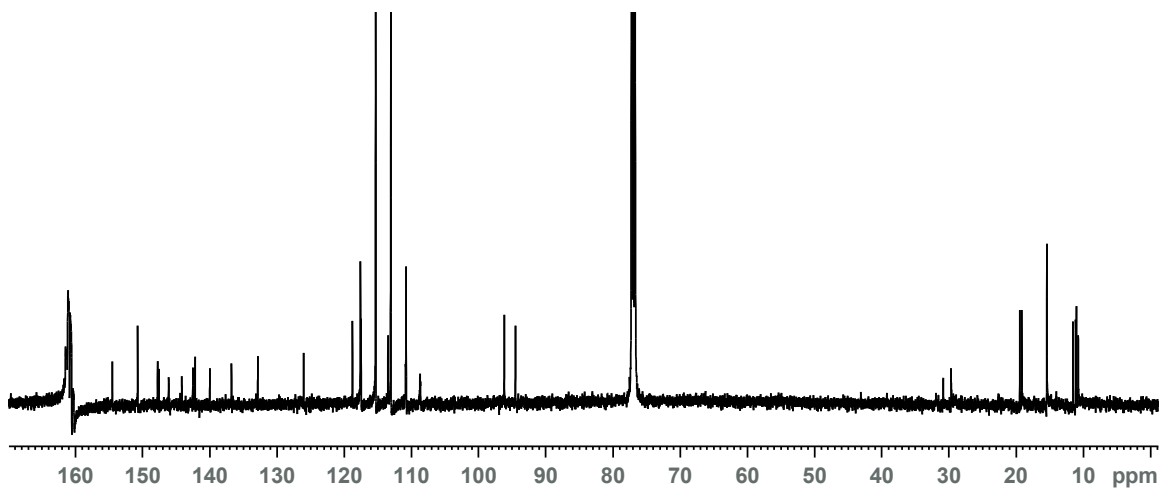


Figure A 29: 125 MHz carbon-13 NMR spectrum of neo-confused porphyrin **36aH₂²⁺** in TFA-CDCl₃.

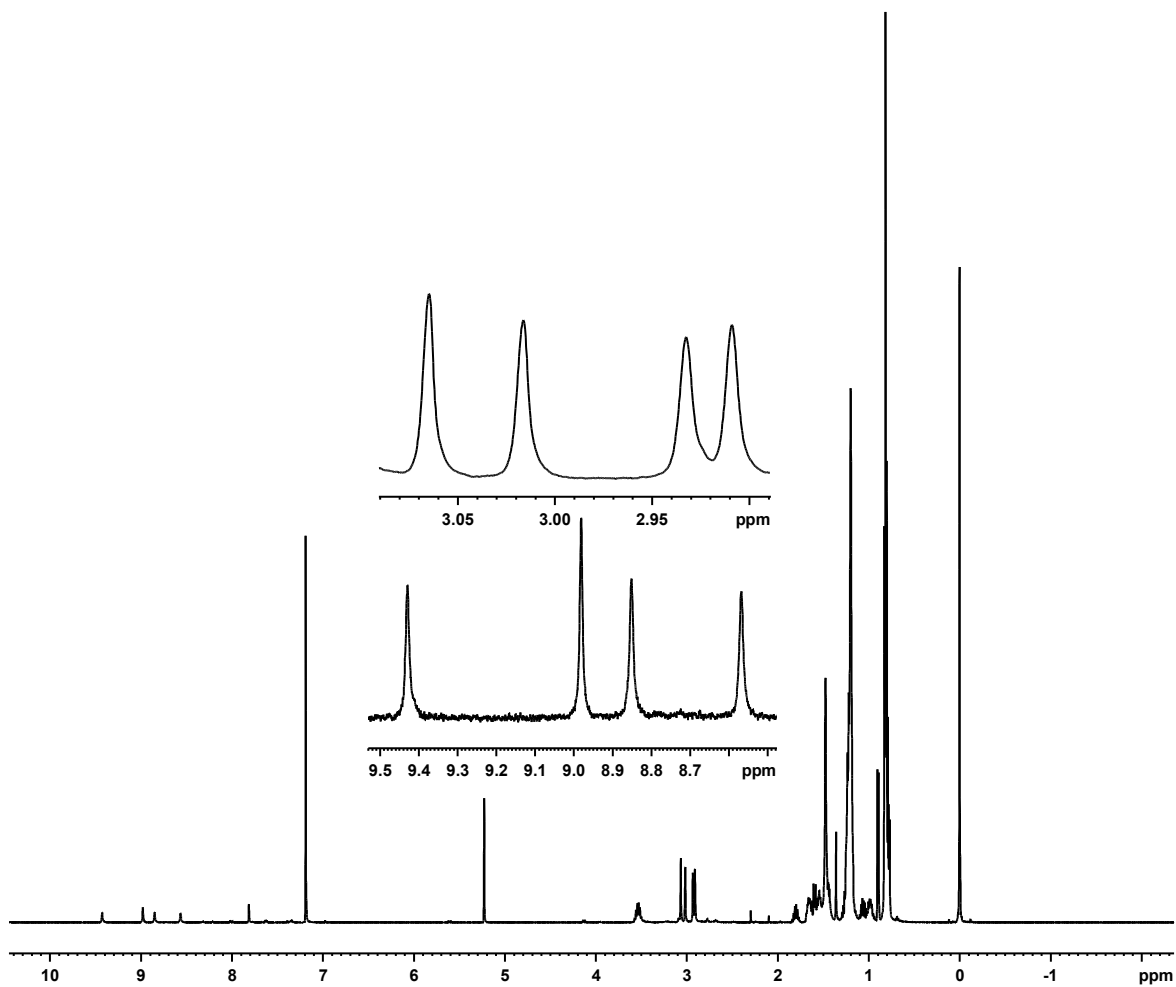


Figure A 30: 500 MHz proton NMR spectrum of palladium complex **54** in CDCl₃.

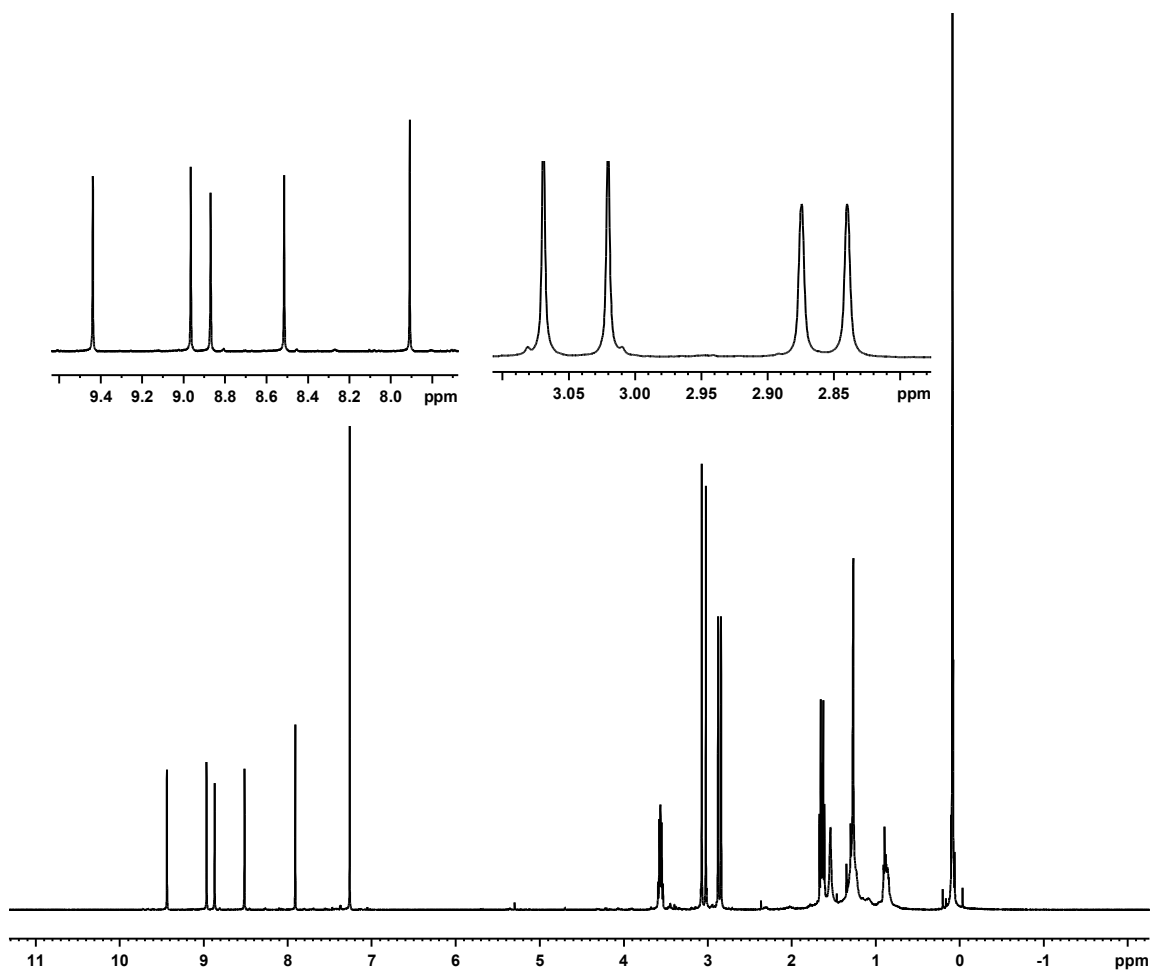


Figure A 31: 500 MHz proton NMR spectrum of nickel complex **53** in CDCl₃.

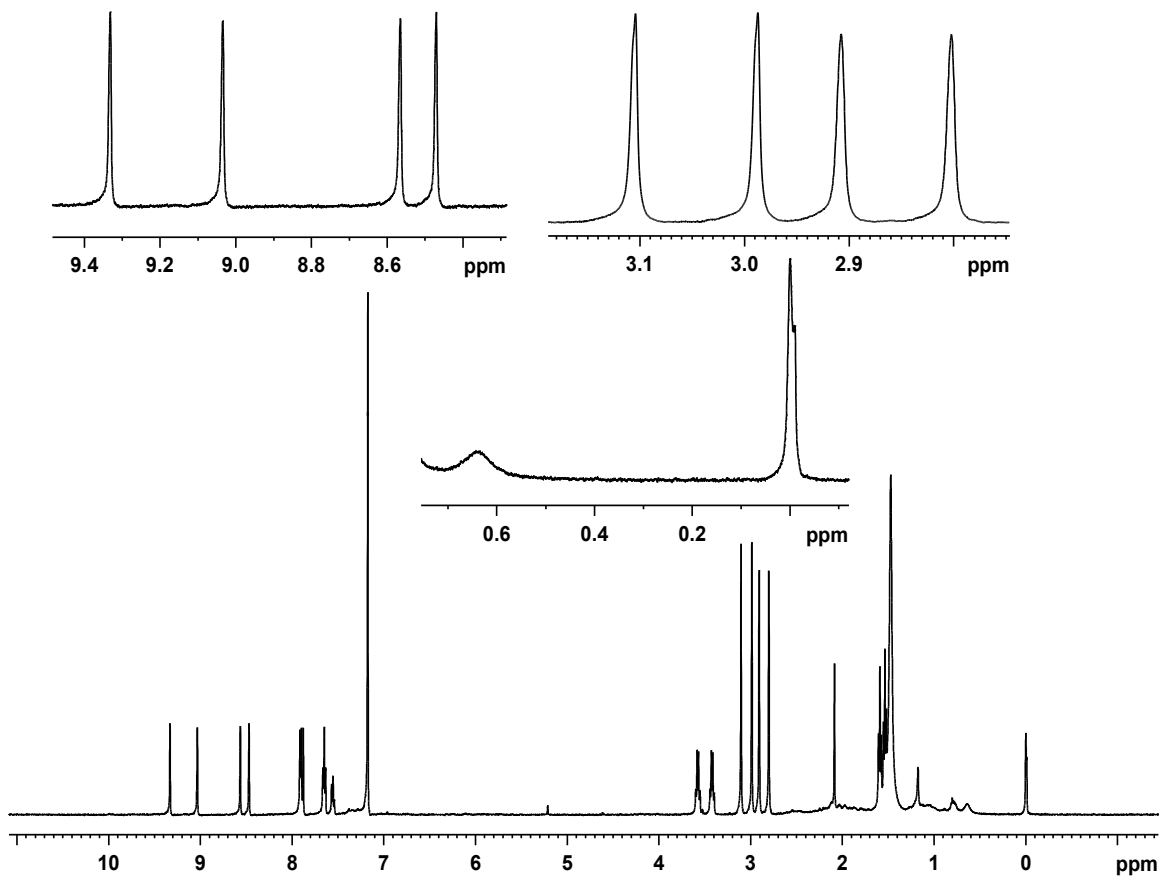


Figure A 32: 500 MHz proton NMR spectrum of neo-confused porphyrin **36b** in CDCl₃.

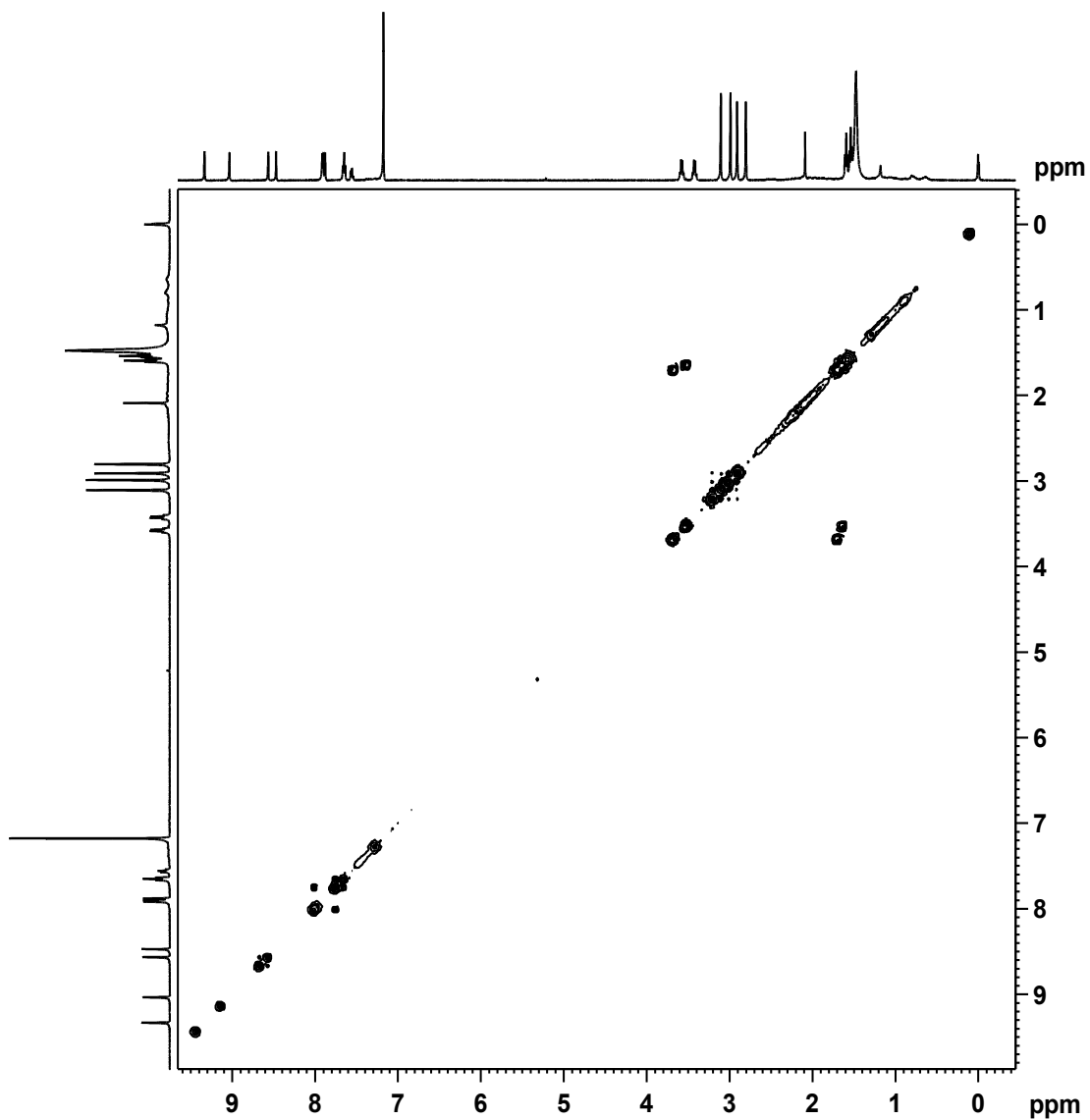


Figure A 33: ^1H - ^1H COSY NMR spectrum of neo-confused porphyrin **36b** in CDCl_3 .

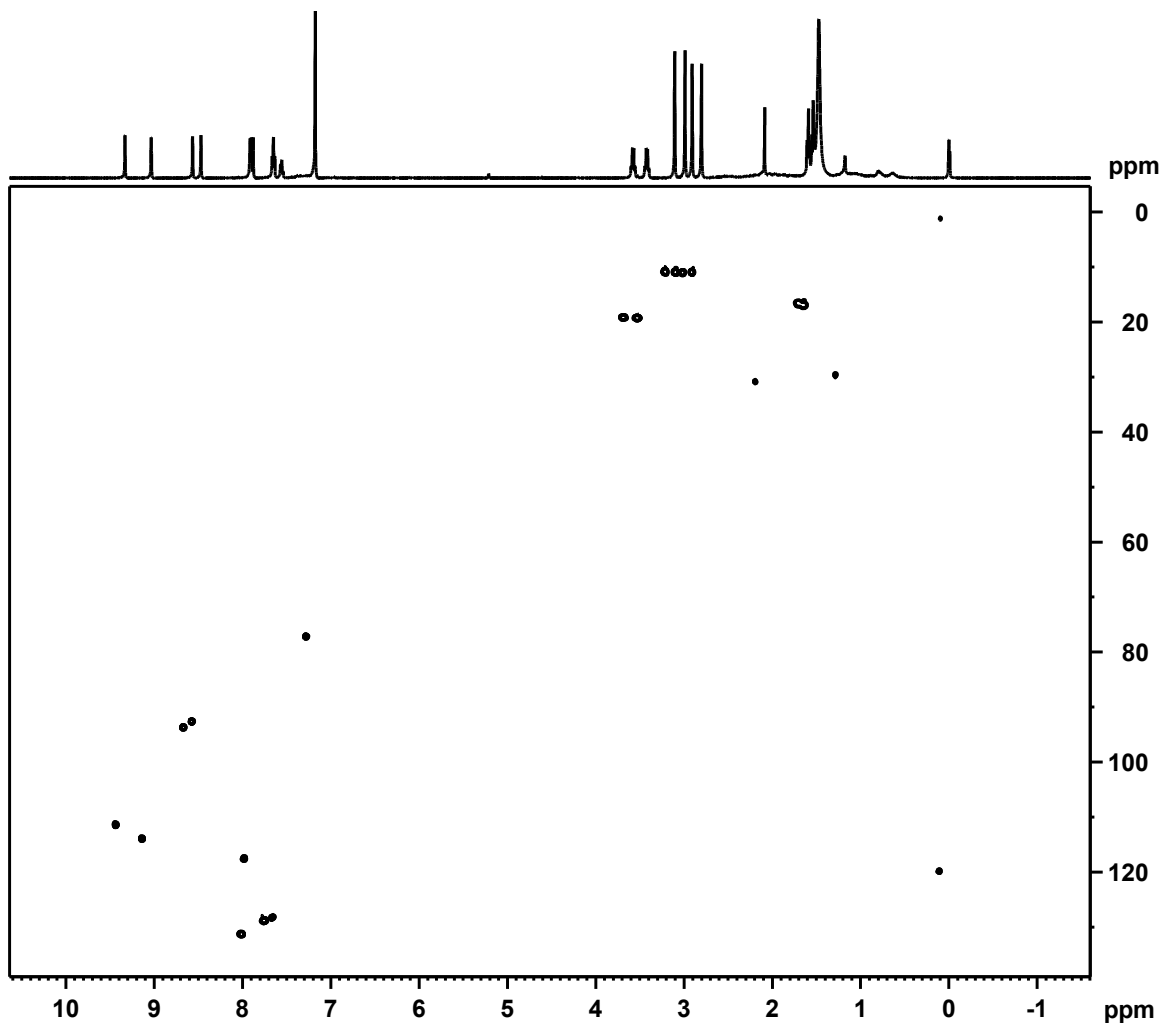


Figure A 34: HSQC NMR spectrum of neo-confused porphyrin **36b** in CDCl_3 .

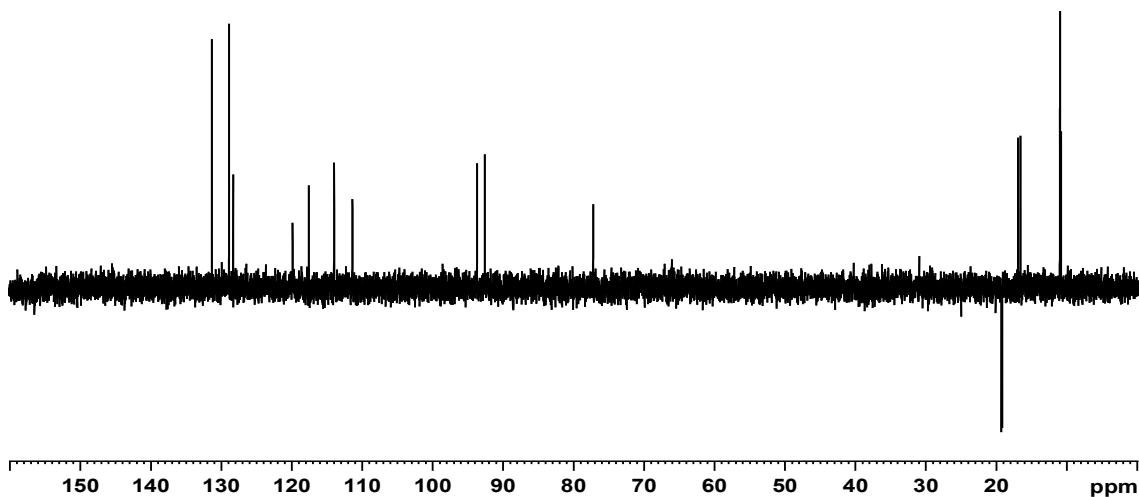


Figure A 35: DEPT-135 NMR spectrum of neo-confused porphyrin **36b** in CDCl_3 .

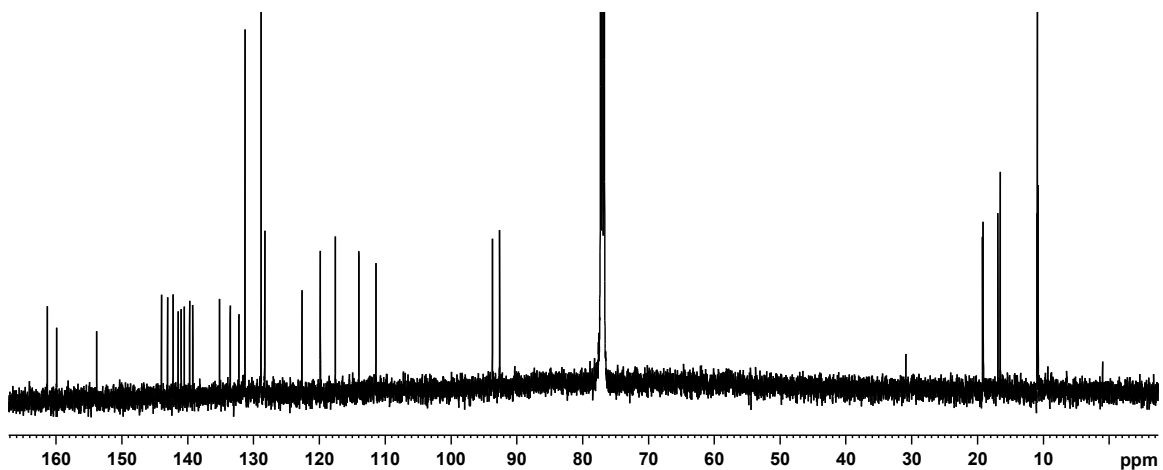


Figure A 36: 125 MHz carbon-13 NMR spectrum of neo-confused porphyrin **36b** in CDCl_3 .

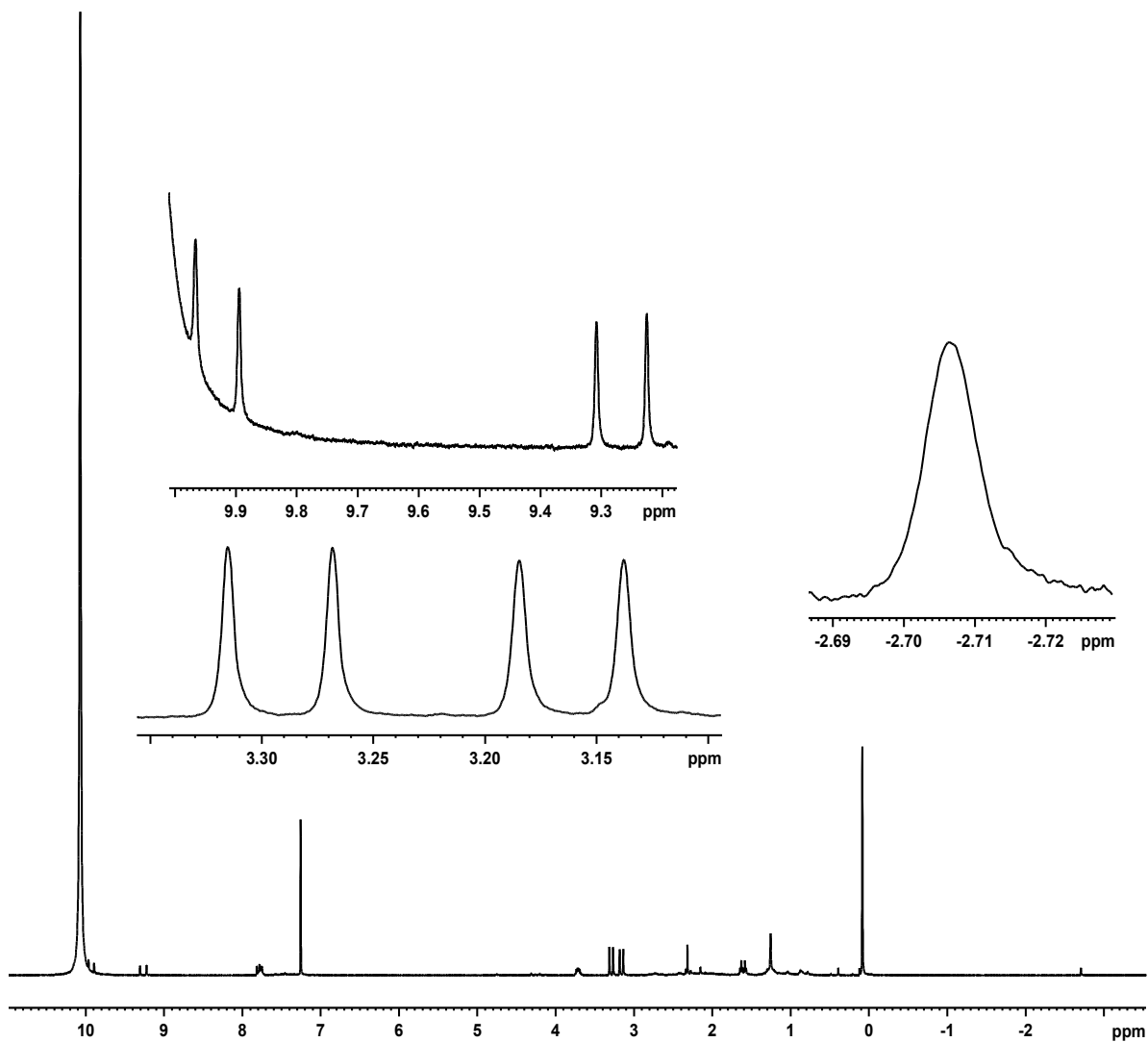


Figure A 37: 500 MHz proton NMR spectrum of neo-confused porphyrin dication $36bH_2^{2+}$ in TFA- $CDCl_3$.

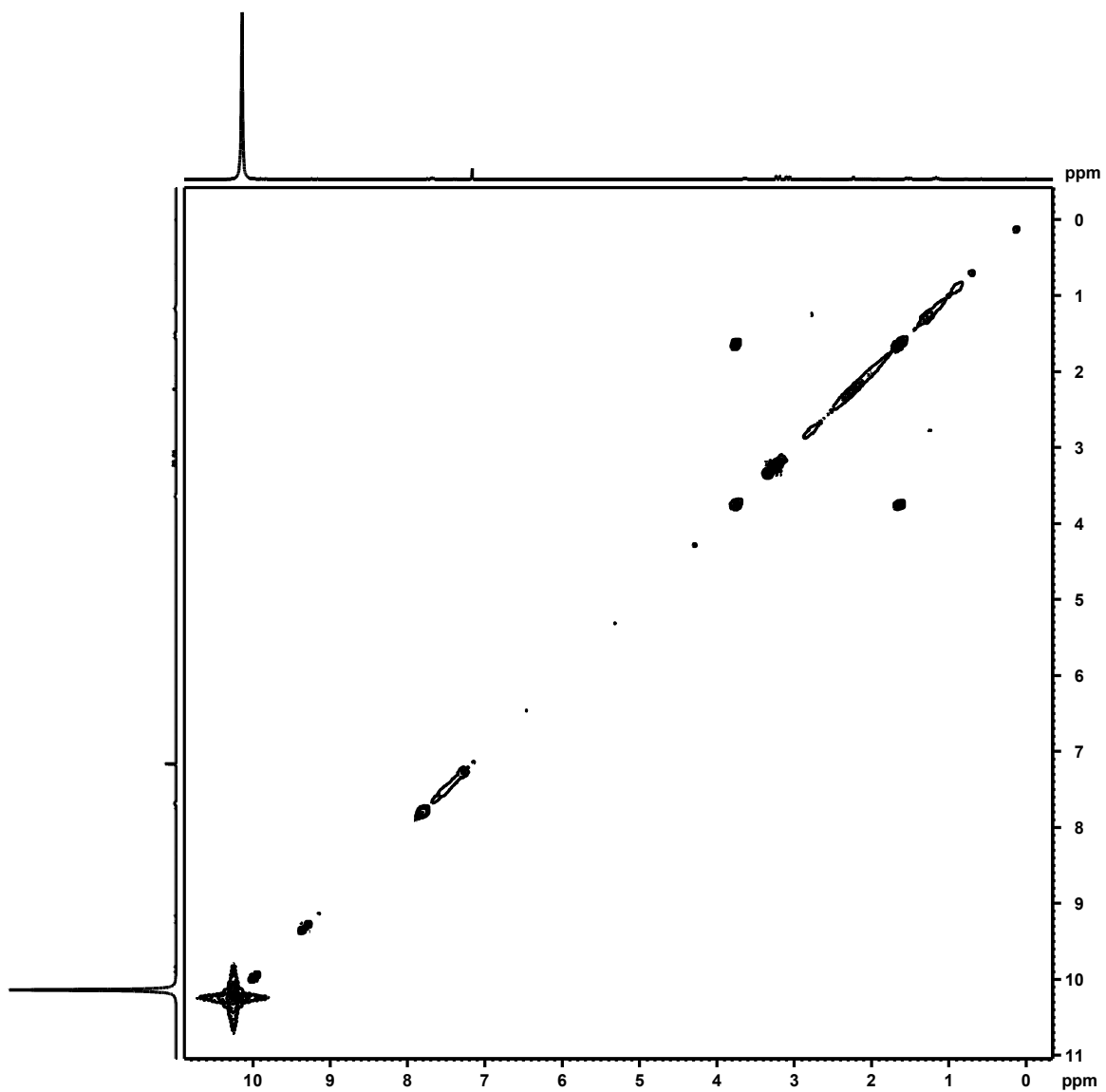


Figure A 38: ¹H-¹H COSY NMR spectrum of phenyl neo-confused porphyrin **36b**H₂²⁺ in TFA-CDCl₃.

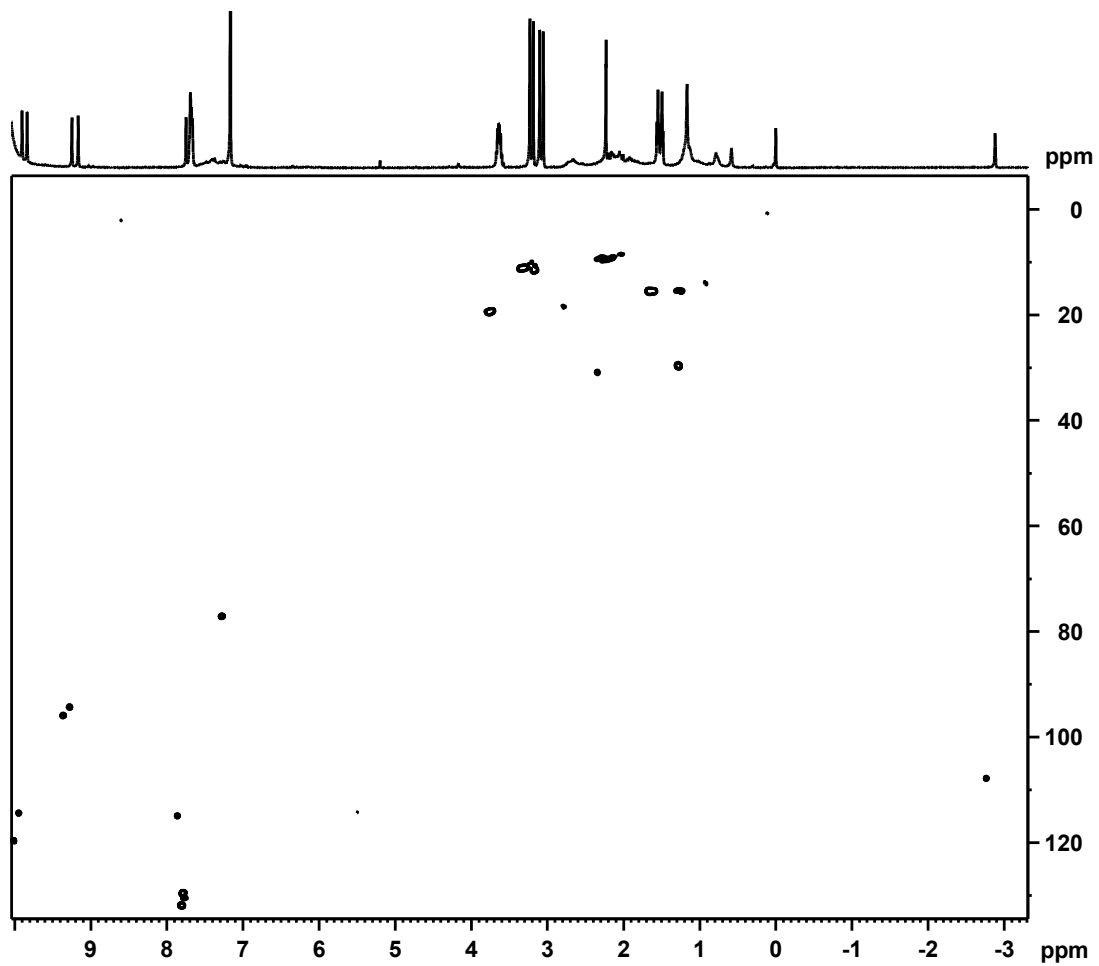


Figure A 39: HSQC NMR spectrum of phenyl neo-confused porphyrin **36b**H₂²⁺ in TFA-CDCl₃.

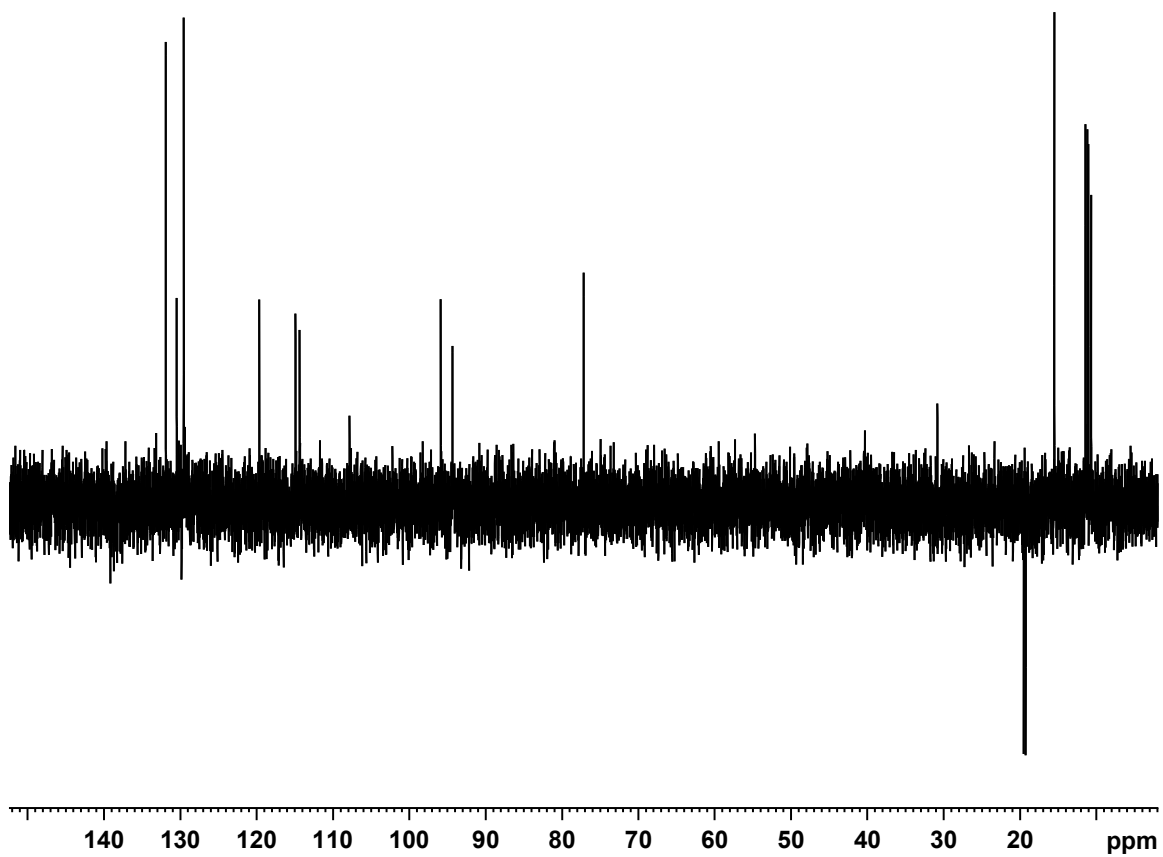


Figure A 40: DEPT-13 NMR spectrum of phenyl neo-confused porphyrin **36b**H₂²⁺ in TFA-CDCl₃.

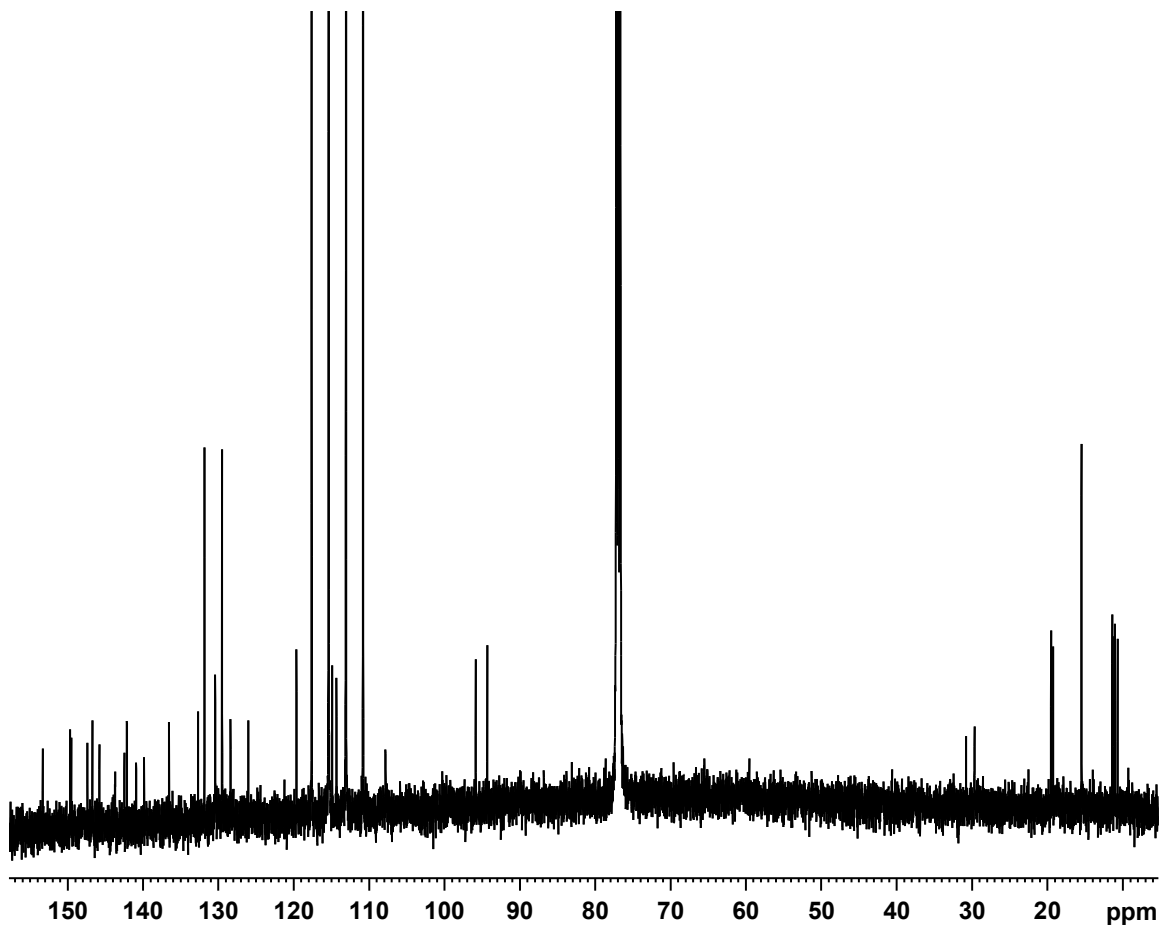


Figure A 41: 125 MHz carbon-13 NMR spectrum of neo-confused porphyrin **36b**H₂²⁺ in TFA-CDCl₃

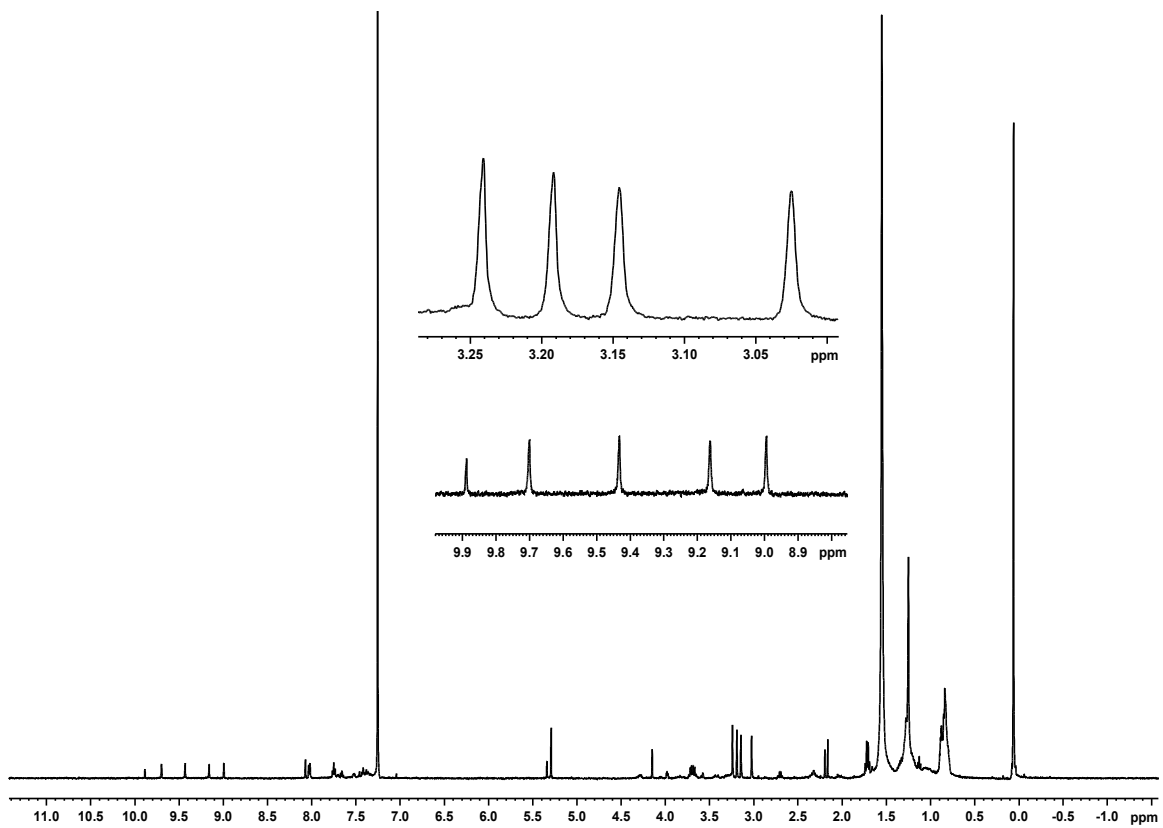


Figure A 42: 500 MHz proton NMR spectrum of palladium complex **61** in CDCl_3 .

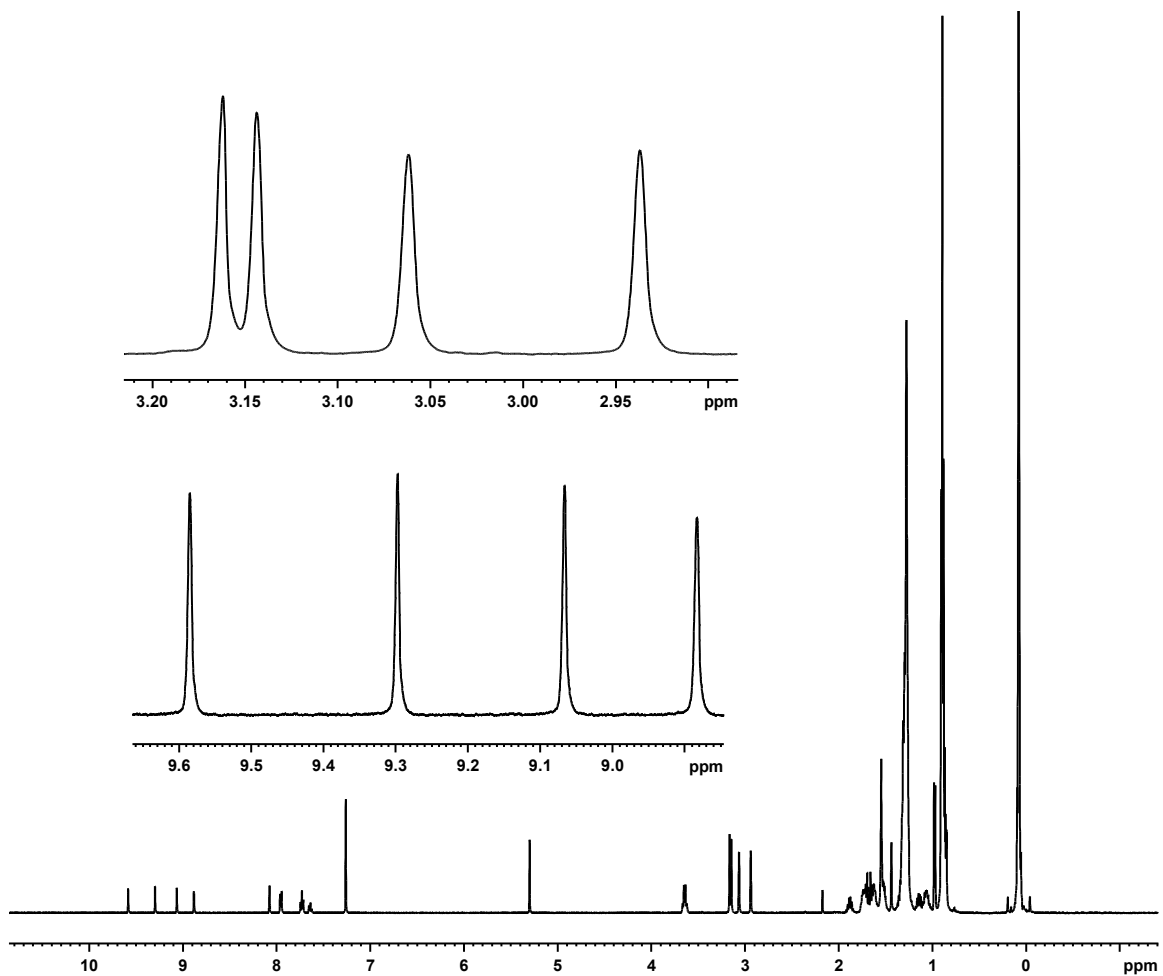


Figure A 43: 500 MHz proton NMR spectrum of nickel complex **62** in CDCl₃